

**UNIVERSITÀ DEGLI STUDI DELLA TUSCIA DI VITERBO**  
**DIPARTIMENTO DI SCIENZE ECOLOGICHE E BIOLOGICHE**

**Corso di Dottorato di Ricerca in**  
Genetica e Biologia Cellulare - XXVII Ciclo

**NEURONAL DIFFERENTIATION PROCESSES: LESSONS FROM**  
**NEUROBLASTOMA MODELS**

**(BIO/11)**

**Tesi di dottorato di:**

Dr. Loredana Guglielmi

**Coordinatore del corso**

Prof. Giorgio Prantera

Firma

**Tutore**

Dr. Armando Felsani

Firma

**8 maggio 2015**

*To my husband, my family and my fellows*

**TABLE OF CONTENTS**

	Pag.
<b>ABSTRACT</b>	IV
<b>RIASSUNTO</b>	V
<b>AIM</b>	VI
<b>Chapter 1 General Introduction</b>	
1. Overview of the nervous system	1
2. Basics of the origin of the nervous system	3
2.1 Neurulation	5
2.1.1 Neural crest cells and the origin of the peripheral nervous system	6
2.2 Proliferation, maturation and migration in the nervous system	7
3. Neuroblastoma cell lines as a valid model to study neuronal differentiation	9
3.1 Retinoids: induction mechanism of neuroblastoma differentiation	10
<b>Chapter 2 MYCN gene expression is required for the onset of the differentiation programme in neuroblastoma cells</b>	
2.1 Summary	13
2.2 Background	14

2.3 Results	16
2.3.1 Retinoic acid (RA) triggers differentiation in the human neuroblastoma LAN-5 cell line	16
2.3.2 N-Myc expression increases during the early phases of RA-induced differentiation in cells of neural origin	18
2.3.3 N-Myc is necessary to activate the differentiation programme in LAN-5 neuroblastoma cells	18
2.3.4 N-Myc overexpression induces differentiation in poorly differentiating neuroblastoma cells	22
2.3.5 MYCN modulation modifies the expression of miRNAs involved in apoptosis preceding neuronal differentiation	25
2.3.6 Inhibition of miR-20a, miR-9 and miR-92a in the wild type SK-N-AS cells restores apoptosis and their differentiation ability	25
2.4 Conclusions	30
2.5 Materials and Methods	34
2.6 Acknowledgements	40
<b>Chapter 3 Massive change of transcription profile following activation of the differentiation programme by choline acetyltransferase forced expression in N18TG2 neuroblastoma cells</b>	
3.1 Summary	41
3.2 Background	42

3.3 Results	44
3.3.1 The transcription profile of the 2/4 clone shows extensive modifications by comparison with the N18TG2 parental cell line	44
3.3.2 ChAT forced exogenous expression modifies cell cycle and neuronal differentiation regulation	46
3.3.3 Lamin A/C is specifically up-regulated after ChAT transfection in 2/4 cells	55
3.3.4 Acetylcholine receptor agonist and antagonist modulates Lmna expression in N18TG2 and 2/4 cells	58
3.3.5 Lamin A/C interactomics network and forced knock-down suggest an involvement of this nuclear envelope protein in ChAT-dependent differentiation cascade	60
3.4 Conclusions	63
3.5 Materials and Methods	67
3.6 Acknowledgements	72
<b>Chapter 4 General Discussion</b>	
4.1 Dying to become a neuron	73
4.2 Neurotransmitters as morphogens	76
<b>REFERENCES</b>	i
<b>APPENDIX</b>	xix

## ABSTRACT

During animal development, a single fertilised egg cell divides and differentiates to produce all of the cells and tissues of the mature organism. Defining the complexity of signals and regulation mechanisms governing the organism's development represents a steep challenge, even nowadays. In this scenario, the nervous system formation and maturation are probably two among the most fascinating fields of developmental biology yet to be completely understood. Fundamental steps of these processes, going from the induction of neural plate to the establishment of rigorous interconnections among billions of nerve cells, are conserved within the Animalia kingdom. In fact, many aspects concerning above all anatomical features of the nervous system development have been clarified thanks to the use of simple model organisms such as, *Drosophila*, *Xenopus* and *C. elegans*. However, many questions remain to be addressed.

A valid replacement of the model organisms, especially for the comprehension of molecular and cellular aspects of the nervous system development, is represented by neuroblastoma cell lines. These systems are extremely suitable to investigate basic, but critical, phases of neuronal differentiation. By treatment with specific substances, able to induce differentiation, neuroblastoma cells display, *in vitro*, typical characteristics of neurons maturation like the up-regulation of differentiation-related genes, the expression of neurofilaments and the outgrowth of dendrites and axons.

In this thesis work four neuroblastoma cell lines have been employed to examine two known, and still debated, phenomena characterising the initial moments of neuronal differentiation: programmed cell death (PCD) and non-synaptic role of the neurotransmitters. The study has revealed new insights in the regulation of these processes, identifying MYCN as a new regulator of PCD at early stages of differentiation and the nucleoskeletal protein Lamin A/C as a possible effector/intermediate of the acetylcholine receptors (AChRs) molecular cascade.

## RIASSUNTO

Durante lo sviluppo animale, una singola cellula uova fecondata é in grado di dividersi e differenziare per produrre tutte le cellule e i tessuti dell'organismo maturo. Definire la complessità dei segnali e dei meccanismi di regolazione che governano lo sviluppo di un organismo rappresenta ancora oggi una sfida di enorme portata. In questo scenario, la formazione e la maturazione del sistema nervoso sono probabilmente due tra i più affascinanti campi della biologia dello sviluppo ancora non completamente chiariti. Momenti fondamentali di questi processi, a partire dall'induzione della placca neurale fino allo stabilirsi di rigorose interconnessioni tra milioni di cellule nervose, sono conservati all'interno del regno animale. Infatti, molti aspetti riguardanti principalmente le caratteristiche anatomiche dello sviluppo del sistema nervoso sono stati messi in luce grazie all'utilizzo di semplici organismi modello quali, *Drosophila*, *Xenopus* e *C. elegans*. Tuttavia, molti quesiti restano da risolvere.

Un valido sostituto degli organismi modello, principalmente per la comprensione degli aspetti molecolari e cellulari dello sviluppo del sistema nervoso, é rappresentato dalle linee cellulari di neuroblastoma. Questi sistemi risultano estremamente utili per studiare fasi basilari, ma allo stesso tempo critiche, del differenziamento. Grazie al trattamento con specifiche sostanze, in grado di indurre il differenziamento, le cellule di neuroblastoma mostrano, *in vitro*, caratteristiche tipiche della maturazione dei neuroni come la up-regolazione di geni coinvolti nel differenziamento, l'espressione dei neurofilamenti e la crescita di dendriti e assoni.

In questa tesi quattro linee di neuroblastoma sono state utilizzate per esaminare due fenomeni noti, ma ancora dibattuti, tipici delle prime fasi del differenziamento neuronale: la morte cellulare programmata (PCD) e il ruolo non-sinaptico dei neurotrasmettitori. Lo studio condotto ha portato a definire nuovi punti riguardanti i due processi, identificando MYCN come nuovo regolatore della morte cellulare programmata durante le fasi precoci del differenziamento e la proteina nucleoscheletrica Lamina A/C come un possibile effettore/intermedio della cascata molecolare attivata dai recettori per l'acetilcolina (AChRs).

## AIM

The aim of this thesis work was to study neuronal differentiation processes using neuroblastoma cell lines as models.

LAN-5 and SK-N-AS cells were used to study the role of the very well-known oncogene MYCN, which is considered a hallmark for neuroblastoma disease, in the onset of neuronal differentiation programme. Multiple evidences demonstrated how MYCN displays an enigmatic behaviour in defining neuroblastoma phenotype. LAN-5 and SK-N-AS cell lines can be described as two opposites as it concerns MYCN. Indeed, LAN-5 are known to be MYCN-amplified, whereas SK-N-AS are MYCN non-amplified, thus representing an extremely suitable system to investigate MYCN amplification effect on neuronal differentiation.

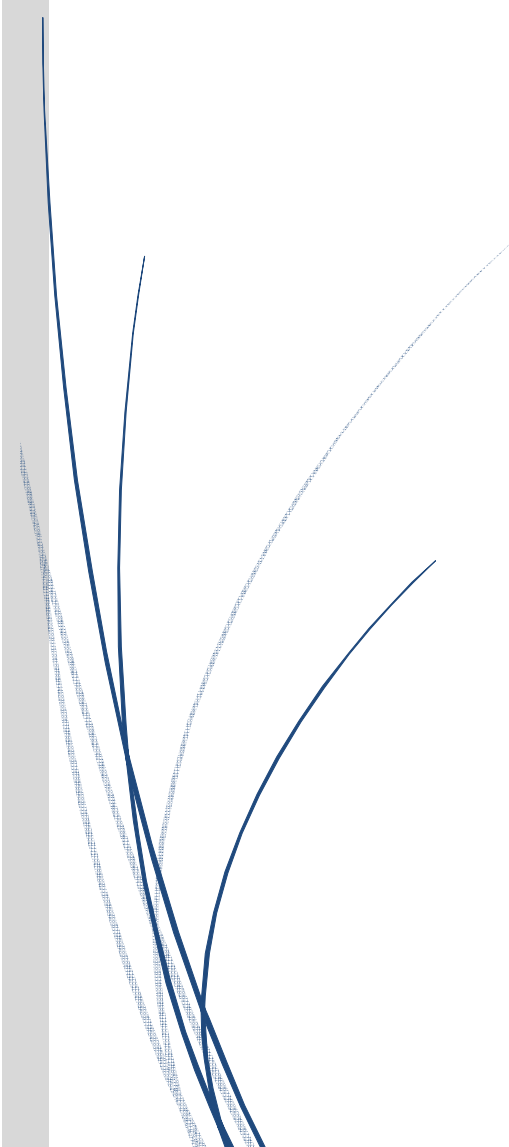
On the other hand, the N18TG2 and 2/4 cells were chosen to analyse the effect of neurotransmitter synthesis on neuronal differentiation. The production of neurotransmitters and the expression of their specific receptors at early stages during nervous system development, before the formation of synaptic contacts, clearly raise the possibility of a non-synaptic role of neurotransmitters. N18TG2 and 2/4 cells were expressly created to address this question: N18TG2 (parental clone) and 2/4 (ChAT-transfected derived clone) are isogenic cell lines which differ only for the presence of the choline acetyl-transferase (ChAT) enzyme which restores the ability of acetylcholine production and as a consequence of differentiation in 2/4 clone. The manipulation simplicity of this model allowed a genome-wide study to decipher the multiple effects of acetylcholine as morphogen prior to the formation of synaptic connections.





# Chapter 1

## General Introduction



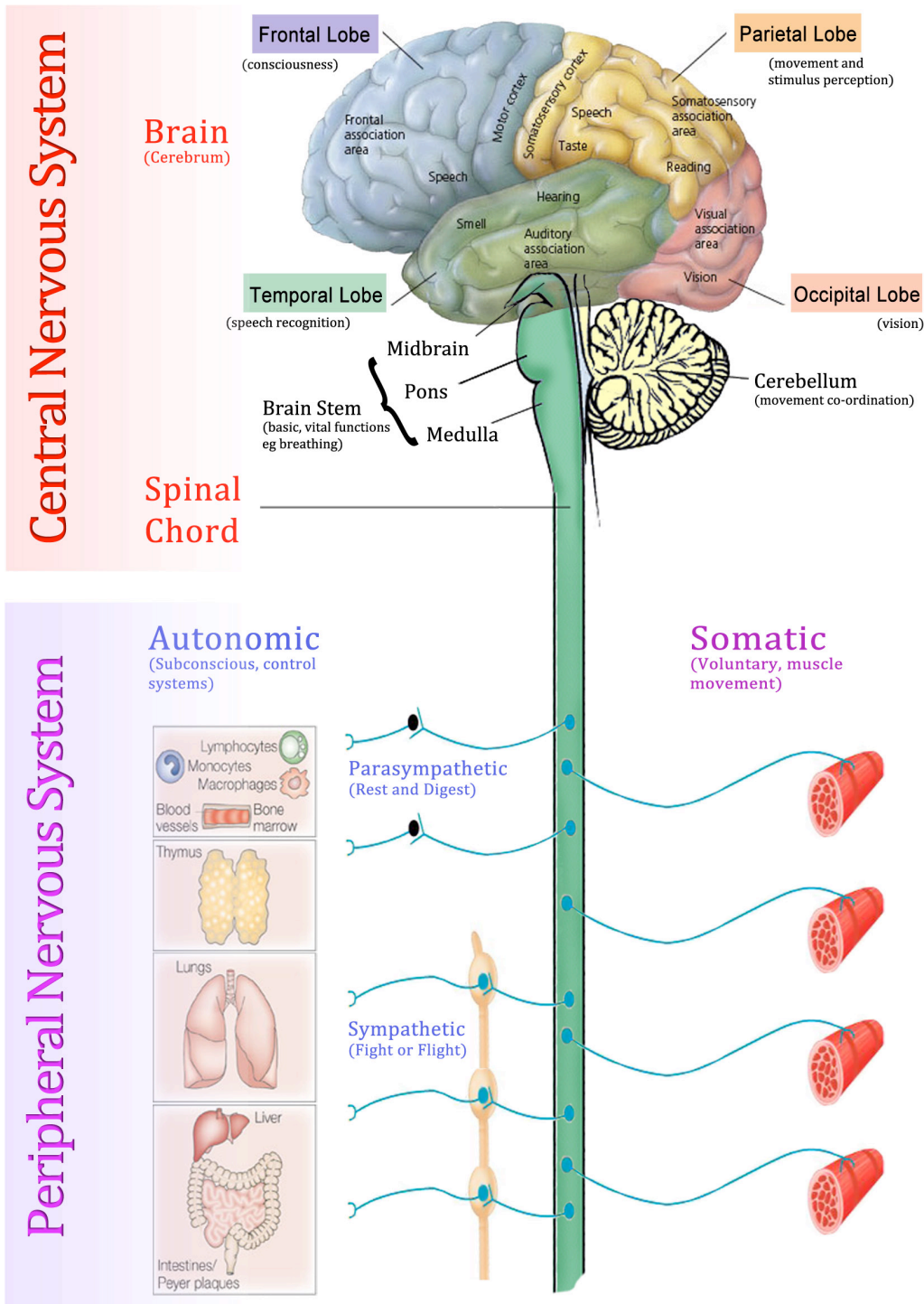
“God may forgive your sins, but your nervous  
system won't”  
**Alfred Korzybski**

## 1. Overview of the nervous system

The nervous system is that part of our body that coordinates both voluntary and involuntary actions thanks to the transmission of specific signals. The nervous system is composed by two main divisions, the Central Nervous System (CNS) and the Peripheral Nervous System (PNS). The brain and the spinal cord are the only components of the CNS, whereas the PNS appears to be more articulated in its structure. Motor nerves and sensory nerves represent the major branches of the PNS; each of these branches is composed by two subgroups, the visceral and the somatic divisions. The first division is associated with involuntary responses, the latter is related to voluntary control of effects. In particular, the involuntary branch of the motor division is known as Autonomic Nervous System (ANS) and is further divided into Sympathetic and Parasympathetic nervous systems. Sympathetic and parasympathetic divisions typically act in opposition to each other. The sympathetic division usually makes the scene when a quick response is required, while the parasympathetic division functions when there is no rush in giving a response. For this reason, the sympathetic system is often referred to as the "fight or flight" system and the parasympathetic system is often considered the "rest and digest" or "feed and breed" system. The nervous system derives its name from nerves, particular fibrous structures innervating every part of our body. Nerves are the constituents of the nervous system and their identification dates back to the ancient Egyptians, Greeks and Romans but their complete structure was not examined in depth until modern time through the use of the microscope (Finger S, 2001). The building blocks of nerves are extremely specialised cells called neurons that form a vast network of billions of units. The typical morphology of a neuron reflects its function: the fibers or dendrites branching from the body of the cell receive "messages" that, after being processed, are transmitted via a long wire-like structure called axon. The nature of these "messages" is essentially electrochemical; electrical signals are converted into chemical ones and vice versa. Neurons communication occurs sequentially from one neuron to the next in charge, like in a domino effect and the junction region between two consecutive neurons is known as synapse. Not all neurons are capable of high-speed transmission signals, only those provided with a proper insulation (myelin) around their axons can reach extreme velocities. Myelin is actually an extension of the cell membrane of a particular type of cells that also populate our nervous system, called glial cells. Glia performs many important tasks within the nervous system; providing nutrients to promote neuron growth, nursing and repairing neurons that are injured and protecting the nervous system from infection. Oligodendrocytes are the glia that

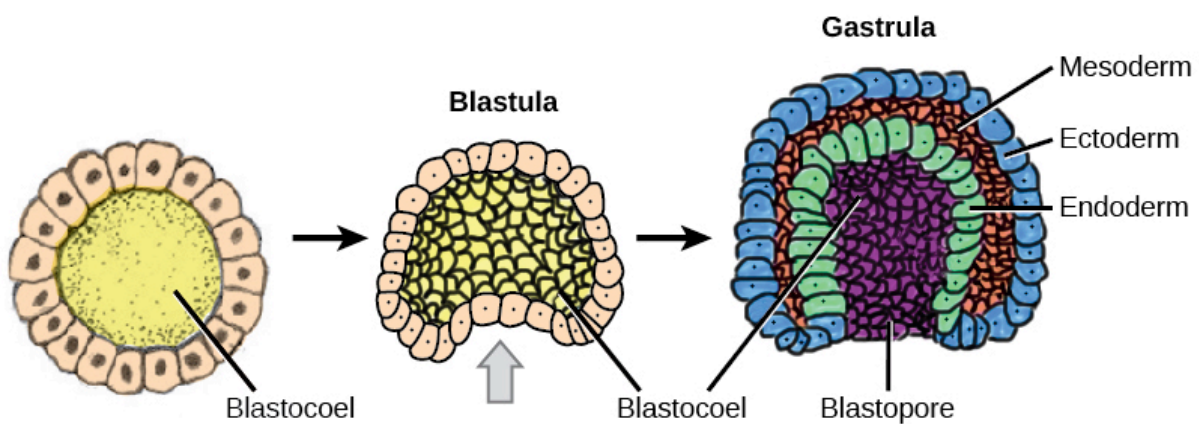
produce myelin in the central nervous system. Glial cells called Schwann cells provide myelin to axons of the peripheral nervous system.

# The Nervous System



## 2. Basics of the origin of the nervous system

Specialised cells, tissues, organs, and interconnected systems all originate from a single fertilised egg. Sequential divisions characterize the first phases of development. After the third cleavage a group of loosely arranged blastomeres (embryonic stem cells) called morula is converted to a mass of flattened and tightly interconnected cells. The blastomeres stand against each other at the surface of the morula, maximizing their contact with one another, and a cavity, called blastocoel, starts to appear within the morula. The appearance of this hollow identifies the entire structure as the blastocyst stage and coincides with the formation of two distinct cell types: an outer mass of trophoblasts and an inner mass of blastomeres. The formation of these two cell types constitutes the first lineage restriction that occurs during development. The trophoblasts develop into the placenta, whereas the blastomeres give rise to the embryo. When the embryo reaches the 64-cell stage the blastocoel has expanded and the embryo starts to acquire a sort of polarity with the inner mass cells falling into two subgroups, those facing the trophoblast side and the others facing the blastocoel side and the trophoblasts also divided into those in contact or not with the inner mass cells. At this point, the critical step to properly proceed is represented by the implantation stage. The trophoblasts and the ovaries both participate with specific signals to prepare the wall of the womb for this event. The implantation consists in the physical attachment of the blastocyst to the womb. As soon as implantation occurs, the initial polarity of the embryo become more evident and the gastrulation stage begins. An additional level of commitment is established during this stage with the formation of a three-layered structure: an outer ectoderm, an inner endoderm and a middle mesoderm.

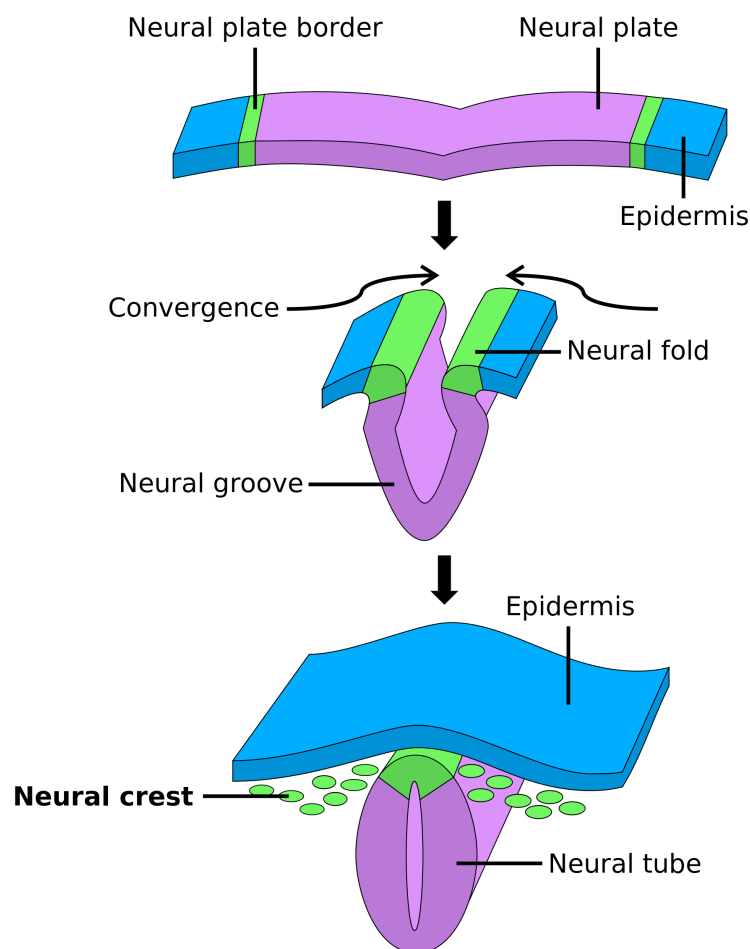


**Early stages of embryo development:** Gastrulation and formation of the three-layered embryo

The ectoderm represents the embryonic tissue that gives rise to the skin and the nervous system. The initial step in the formation of the nervous system is called neural induction. When the process starts the embryo is around 16 days old. For years, the nature of the induction has been one of the main issues to be solved in developmental neurobiology. The controversy was based on whether the induction signal acted vertically from the dorsal mesoderm towards the ectoderm or horizontally within the plane of ectoderm. Experiments conducted during the first 30 years of the 20<sup>th</sup> century by Spemann and Mangold initially proved that the vertical signal was predominating, as the transplant of the dorsal blastopore lip resulted in the formation of a second nervous system in recipient organisms. Interestingly, the duplicated nervous system developed from the ventral region of the recipient's ectoderm and not from the transplanted tissue. The first experiments performed in *Xenopus* embryo were then replicated also for higher vertebrates and the "organizer", i.e. the dorsal blastopore lip, turned out to be able to promote neural induction also across species, suggesting a conserved mechanism in evolution. In 1987, with the discovery of the expression of the N-CAM molecule by the ectoderm cells the alternative explanation of a planar signal was proposed again. Despite all the efforts to find the primitive neural organizer its nature remains elusive still nowadays, but one clear aspect of neural commitment is that neural induction does not depend on signals that promote neural differentiation but on blocking molecules that inhibit neural fate. This fact poses neural commitment as the default state of ectoderm. Every cell that resides in the ectoderm and is not committed to become part of the nervous system has its neural default fate inhibited. Three molecules were isolated from the "organizer" and demonstrated to be the responsible inhibitors of the epidermal-promoting bone morphogenetic proteins (BMPs): noggin, follistatin and chordin. These oversimplified descriptions surely appear slightly more complicated in higher model organisms than in *Xenopus*, where the preliminary experiments were performed. It is now evident that other inhibitors of the BMPs might be present, hence the molecular mechanism of neural induction may definitely turn up to be more complex than that described so far. Studies on other signal cascades paved the way for new insights in the comprehension of neural induction. A direct involvement of the Fibroblast Growth Factors (FGF), Wnts and Insulin-like Growth Factors (IGF) pathways has been proposed, opening a scenario in which the neural fate might not be the default one and active signals may also be required in parallel with BMPs inhibition.

## 2.1 Neurulation

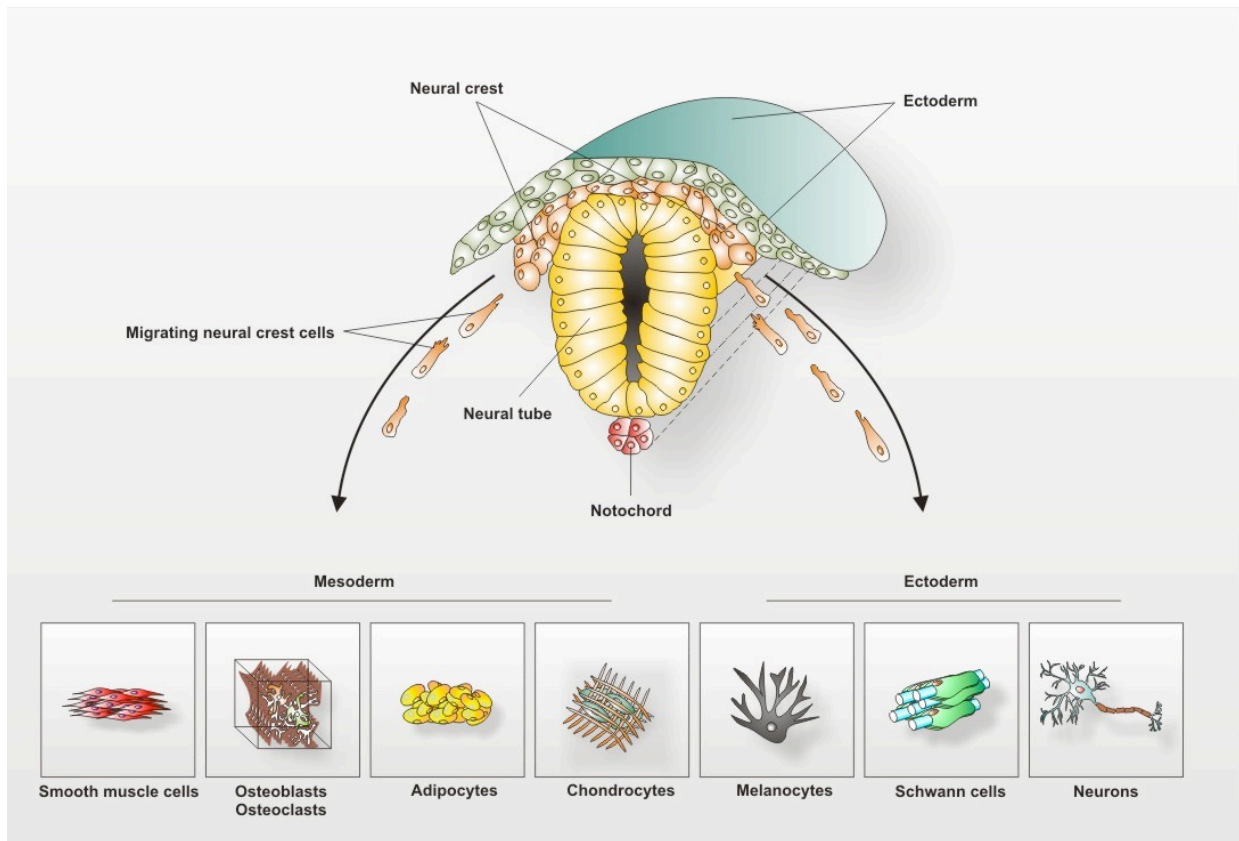
The primordial consequence of neural induction is the reshaping of those cells destined to become the neural precursors of the whole nervous system. Ectodermal cells that reside medially within the embryo undergo an elongation process acquiring a column-shaped body. These cells define the region of the embryo known as neural plate and they are normally referred to as neuroepithelium or neuroectoderm. Furrowing, folding and bending of the neural plate allow the formation of the neural tube. The bending represents an extremely critical step during which the right and the left tips of the neural plate fuse together; the non-neural ectoderm fuse as well, forming a continuous sheet overlying the newly formed roof plate of the neural tube. A group of cells, initially neighbouring the neural plate cells, remain scattered between the non-neural ectodermal cells and the roof plate; these cells are known as neural crest cells and represent the origin of the peripheral nervous system and other non-nervous body structures.



**Neurulation:** Formation of the neural tube and origin of the neural crest cells

### 2.1.1 Neural crest cells and the origin of the peripheral nervous system

Neural crest cells give origin to a surprising number of different specialised tissues in the adult, including cartilage and bone in the head, teeth, endocrine cells, peripheral sensory neurons, all peripheral autonomic neurons (enteric, postganglionic sympathetic, and parasympathetic neurons), all peripheral glia and all epidermal pigment cells. All the aforementioned structures eventually reside in different districts in the developed organism, this fact implies that the neural crest cells must leave their original position in the embryo and reach as well as colonise other zones. One of the first events accompanying the migratory wave is the down-regulation of specific adhesion molecules typically expressed by neuroepithelial cells, such as N-CAM and N-cadherin, and the subsequent epithelial-mesenchymal transition. When these cells accomplish their journey and differentiate, adhesion molecules are normally expressed again according to the specificity of the tissue, which they ultimately populate. As neural crest cells delaminate from the neuroepithelium, they are faced with very different mesodermal environments depending on their axial level. The lineage specification within the neural crest might be explained by two different kind of segregation mechanism: (1) instruction, in which multipotent precursors are instructed by environmental cues to adopt particular fates; (2) selection, in which determined cells, which are only able to adopt one fate, are selected in permissive environments. Data suggest that the migrating population is heterogeneous and characterised by both multipotent and fate-restricted cells. It is important to mention that the neural crest cells form all the PNS, hence neurons and glial cells originate from the same progenitors and it is widely accepted that the sensory–autonomic lineage decision occurs before the neuronal–glial decision.



**Neural crest derivatives:** adult tissues derived from migrating neural cells <http://web.biologie.uni-bielefeld.de>

## 2.2 Proliferation, maturation and migration in the nervous system

The mechanism of generating neurons from a field of neuroectodermal cells is known as neurogenesis. From a cellular point of view, the process of neurogenesis constitutes a gradual progression from multipotent cells to fate-restricted neuronal precursors. Indeed, the very first step of neurogenesis consists in the acquisition of a neural fate by the side of neuroectodermal cells. After neuroepithelial cells initially divide symmetrically to expand the pool of early neural stem cells, neural progenitors then undergo a series of asymmetric divisions to both maintain the stem cell population and become more and more restricted in potential. As the neural tube closes populating cells, organised in a single layer, start to duplicate extensively and they rapidly reach high rate of multiplication with an estimated number of 250,000 new born neurons each minute. This duplication processes paves the way for the formation of three distinct parts of the developing brain: forebrain, midbrain and hindbrain which represent the beginnings of the three major divisions of the brain. The forebrain eventually gives rise to the two cerebral hemispheres, including the thalamus and hypothalamus. The hindbrain corresponds to structures including the cerebellum and, together with midbrain, forms the brain stem. The lumen of the neural tube is known as the



ventricular system, the inner ventricular surface is the site where cells proliferate and this region is generally referred to as Ventricular Zone (VZ). At the same time, also the region next to the VZ, the Subventricular Zone (SVZ), presents dividing cells. Early multiplications have been demonstrated to occur perpendicularly to the VZ, securing both daughter cells to be in contact with the ventricular surface after mitosis. This simple trick provides a way for the increase of stem cells before entering commitment and differentiation stages. Later on development, cells start dividing horizontally to the VZ, giving origin to daughter cells that lose contact with the ventricular surface, exit the cell cycle, differentiate and migrate away from the VZ. Despite by histological examination the VZ morphology appears constant in all the regions, it is easily inferable that there must be a difference in its output capacity, since mature structures originating from different parts of the brain are committed to different specialised jobs. Diversity originates from both intrinsic and extrinsic factors. Intrinsic factors are present in the cell itself, they consist of mRNAs and proteins that get inherited asymmetrically by daughter cells; whereas extrinsic factors are essentially environmental influences, determined by the anterior-posterior segmentation as well as by the dorsal-ventral patterning, set in place before neurogenesis actually starts. This ultimately results in neural progenitors expressing a distinct combination of transcription factors that will regulate their differentiation into specific neuronal subtypes. Moreover, the birthdate of a neuron is an important predictor of cell fate; this means that neurons born at a certain time generally follow similar differentiation pathways. Interestingly, neurons of similar phenotype and birthdate cluster together to form layers, nuclei, or ganglia. One more source of variability and diversity is certainly represented by the SVZ that, for example, gives rise to most of glial cells. Moreover, not all the areas of the CNS contain a SVZ and defined subdivisions have been identified which differ not only in location but also in the type of cells they produce. Following the massive cell expansion, newly born neurons must be relocated in those portions of the brain where they are supposed to play their ultimate function. Two main types of migration mechanisms are known in the CNS: radial and tangential. In radial migration, a particular subset of glial cells (radial glia) provide the tool for neurons to span the thickness of the neural tube and reach the surface of the cerebral cortex. On the other hand, tangential migration does not require neurons to interact with glial cells, suggesting the presence of other signals and mechanisms that promote this process and yet not completely understood. An extraordinary example comes from the neurons populating the olfactory bulb which, closely associated with each other and forming long chains and aggregates, settle in absence of radial glia but thanks to the influence of adhesion molecules and specific signalling

pathways. Similarly, peripheral neurons originating from migrating neural crest cells reach their definitive position under the control of extracellular cues. Semaphorins, ephrin–Eph interactions, glial cell line-derived neurotrophic factor (GDNF) and sonic hedgehog (Shh) are example of factors that cooperate to rule positioning and targeting of peripheral neurons. The terminal location represents for a neuron also the place in which terminal differentiation is achieved. The cell cycle exit and the specification of the fate mark the beginning of the maturation processes for the newly-formed neuron. The final stages will be characterised by the production of the specific neurotransmitters and receptors as well axon guidance and the establishments of innervations. The factors that contribute to the acquisition of the conclusive neuronal function are different and specific for each neuron type, as they depend on the spatial and temporal history of each maturing cell. As an example, POU-homeodomain family genes are known to be expressed during sensory neurons maturation, from worms to mammals. Whereas, LIM transcription factors determine the subtype specificity in CNS motoneurons. The mechanisms that lead to the neuronal differentiation fulfillment is founded on delicate but, at the same time, very well-orchestrated equilibrium. Programmed cell death, termination of migration and inhibition of neuronal differentiation are fine-tuned counteracting proliferation, migration and terminal differentiation, leading to the nervous system structure maturation fulfillment.

### **3. Neuroblastoma cell lines as a valid model to study neuronal differentiation**

Several model organisms have been exploited to study the nervous system development. Going from invertebrates, *Caenorhabditis elegans* and *Drosophila melanogaster*, passing through lower vertebrates, *Danio rerio* and *Xenopus laevis*, to higher vertebrates such as *Gallus gallus* and *Mus musculus*, important anatomical aspects were clarified, revealing how the morphogenesis of the nervous system follows conserved rules in the Animalia kingdom. Moreover, the genome sequencing of organisms like the fruit fly *Drosophila* and the nematode worm *C. elegans* have been now completed. Therefore, they provide a powerful tool for the identification of genes involved in the regulation of the nervous system development since they can be genetically manipulated with little efforts (Kandel, 2000). On the other hand, also cell lines represent an excellent *in vitro* model to study molecular and cellular features characterizing neurons differentiation; in particular neuroblastoma cell lines, which maintain their ability to differentiate in culture (Edjö, 2007).

Neuroblastoma is one of the most common cancer in childhood. Neuroblastomas derive from precursors of the sympathetic branch of the PNS, thus primary tumors can be found at any

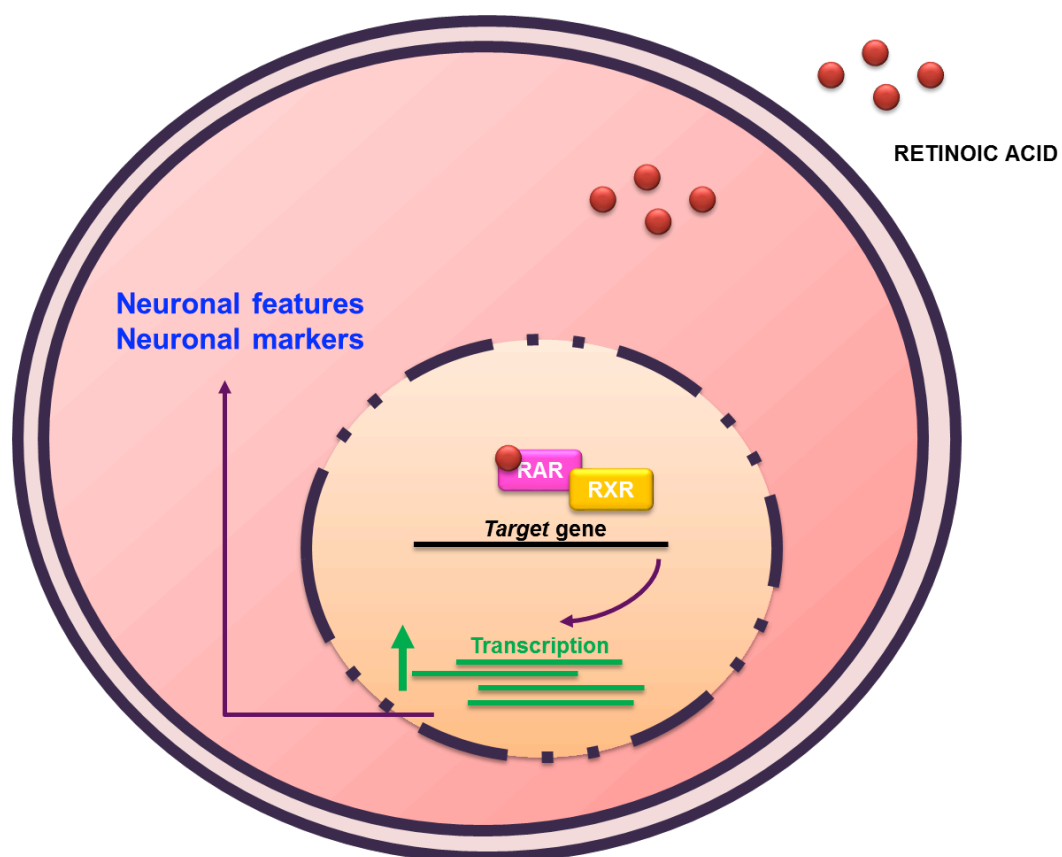
location of the sympathetic nervous system (SNS), such as adrenal medulla and sympathetic ganglia (Edjö, 2007). Evidences suggest that neuroblastoma originates in utero during sympathoadrenal development and that it goes through an embryonic pre-cancer phase (Marshall, 2014). Sympathoadrenal cells take origin from the neural crest in the trunk region of the embryo and undergo a ventral migratory pathway (Huber, 2006). The expression of the proto-oncogene MYCN is high in the early migratory and post-migratory neural crest cells and it regulates both proliferation and differentiation of neural crest cells (Zimmerman, 1986; Wakamatsu, 1997). When it comes to lineage specification, sympathoadrenal precursors' development can diverge into neuronal or chromaffin cells (Huber, 2006). Neuroblastoma cell is thought to arise before this commitment, thus specifically from sympathoadrenal precursors (Marshall, 2014). Although the overall incidence of childhood cancer has been slowly increasing since 1975, cancer in children and adolescents is rare, thus the possibility to perform differentiation studies on primary tumor turns out to be barely feasible (Smith, 2014). Therefore, the best way to investigate molecular and morphological characteristics of sympathetic, or generally neuronal, differentiation is to take advantage of neuroblastoma *in vitro* models. Neuroblastoma cell lines were established starting from the 1970s thanks to the pioneering work of June Biedler, Robert Seeger and they have been used so far as model of tumor cell maturation processes and differentiation (Edjö, 2007). In 1981 Pählman and collaborators succeeded in differentiating SK-N-SH and SH-SY5Y human neuroblastoma cells treating them with 12-O-tetradecanoyl-phorbol-13-acetate (TPA). They demonstrated how TPA induced the development of projections, the production of neurosecretory granules and the increase of neuron-specific markers, as well as the decrease of proliferation rate (Pählman, 1981). From that moment on, phorbol esters, growth factors, neurotrophins and retinoids have been employed as inducers of neuroblastoma differentiation programme (Edjö, 2007).

### **3.1 Retinoids: induction mechanism of neuroblastoma differentiation**

Retinoids gained particular attention and consideration among the other differentiation-inducing factors, both for promoting differentiation of cell lines *in vitro* (Sidell, 1982) and as anticancer therapeutic molecules (Matthay, 1999). The term "retinoids" refers to a multitude of substances including vitamin A, its biologically active derivatives and all their synthetic analogues. All-*trans*-retinoic (ATRA) acid and 9-*cis*-retinoic acid are examples of naturally occurring retinoids, while 13-*cis*-retinoic acid is a synthetic form of retinoid. The mechanism of action of retinoids is exerted by binding to specific nuclear receptors and modulating gene

expression (Evans and Kaye, 1999). Six retinoid receptors have been described so far and they belong to two distinct subfamilies: retinoic acid receptors (RARs),  $\alpha$ ,  $\beta$  and  $\gamma$ , and the retinoid X receptors (RXRs),  $\alpha$ ,  $\beta$  and  $\gamma$  (Chambon, 1995; Rastinejad, 2001). The RARs and RXRs bind the consensus sequence PuGGTCA, also known as RA responsive element (RARE), and consequently trigger gene expression or suppression (Liu, 2005). Given the ability of RARs and RXRs to form both homodimers and heterodimers complexes, the signalling pathways that can spring from retinoids receptors activation are extremely variable and complicated (Nagpal, 1992; Mader, 1993; Evans and Kaye, 1999). In addition, retinoid binding proteins, such as CRBP-I (cellular retinol binding protein-I) and CRABP-II (cellular retinoic binding protein-II), add a further level of complexity since they may also be involved in the retinoids signalling cascade (Smith, 1991; Durand, 1992). The effects of the activation of the retinoid receptors can be observed both at morphological and molecular levels. Neuron projections development, increasing expression of neuronal markers (GAP-43 - growth associated protein-43; NPY - neuropeptide tyrosine; TH - tyrosine hydroxylase etc.) and the accumulation of neurotrophins receptors, like those belonging to the TRK (tropomyosin receptor kinase) family, represent good indicators that neuronal differentiation is triggered *in vitro* (Edjö, 2007). However, outcomes of differentiation protocols might appear slightly different depending on the neuroblastoma cell line studied. For example, LAN-5 cells are known to display characteristics of cholinergic neurons after treatment with retinoic acid (Hill and Robertson, 1997; Hill and Robertson, 1998) and to express typical cholinergic markers such as ChAT (choline acetyl-transferase) and VAcHT (vesicular acetylcholine transporter) (Guglielmi, 2014).

It is not surprising that retinoids can have such an effect on gene expression modulation and in particular on neuronal differentiation stimulation. In fact, they act as very potent morphogens during the early development stages activating Hox genes transcription and determining the caudal patterning of the hindbrain in the embryo (Dupe and Lumsden, 2001). In addition, more recently, it has been proposed a role of RA (retinoic acid) in the coordination of the specification, patterning and alignment of neural and mesodermal tissues that are essential for the organization and function of the neural and skeletal systems (Lee and Skromne, 2014).



Schematic representation of retinoic acid (RA) differentiation triggering

# Chapter 2

MYCN gene expression is required for the onset of the differentiation programme in neuroblastoma cells

“When cells are no longer needed, they die with what can only be called great dignity”  
**Bill Bryson**

## 2.1 Summary

Neuroblastoma is an embryonic tumor of the sympathetic nervous system and is one of the most common cancers in childhood. A high differentiation stage has been associated with a favorable outcome; however, the mechanisms governing neuroblastoma cell differentiation are not completely understood. The MYCN gene is considered the hallmark of neuroblastoma. Even though it has been reported that MYCN plays a role during embryonic development, it is needed its decrease so that differentiation can be completed. We aimed to better define the role of MYCN in the differentiation processes, particularly during the early stages. Considering the ability of MYCN to regulate non-coding RNAs, our hypothesis was that, N-Myc protein might be necessary to activate differentiation (mimicking embryonic development events) by regulating miRNAs critical for this process. We show that MYCN expression increased in embryonic cortical neural precursor cells at an early stage after differentiation induction. To investigate our hypothesis we used human neuroblastoma cell lines. In LAN-5 neuroblastoma cells, MYCN was up-regulated after two days of differentiation induction before its expected down-regulation. Positive modulation of various differentiation markers was associated with the increased MYCN expression. Similarly, MYCN silencing inhibited such differentiation, leading to negative modulation of various differentiation markers. Furthermore, MYCN gene overexpression in the poorly differentiating neuroblastoma cell line SK-N-AS restored the ability of such cells to differentiate. We identified three key miRNAs which could regulate the onset of differentiation programme in the neuroblastoma cells in which we modulated MYCN. Interestingly, these effects were accompanied by changes in the apoptotic compartment evaluated both as expression of apoptosis-related genes and as fraction of apoptotic cells. Therefore, our idea is that MYCN is necessary during the activation of neuroblastoma differentiation to induce apoptosis in cells that are not committed to differentiate.

## 2.2 Background

Neuroblastoma is an embryonic tumour of the sympathetic nervous system and is one of the most common childhood cancers. The clinical signs and symptoms of neuroblastoma are extremely variable (Brodeur, 2003). A high differentiation stage has been associated with a favourable outcome (Brodeur, 2003); however, the mechanisms governing neuroblastoma cell differentiation are not completely understood. Nevertheless, the ability of many neuroblastoma cell lines to maintain their differentiation capability *in vitro* has made them suitable models for studying human neuronal differentiation (Hill, 1997).

It is well known that the MYC family member N-Myc, encoded by MYCN, plays a key role during neuroblastoma differentiation. N-Myc has been found to be overexpressed in approximately 25% of primary neuroblastoma tumours (Munoz, 2006). The MYC gene family is composed of three members, MYC, MYCN and MYCL. The Myc proteins act as transcription factors: they recognise a consensus sequence (CACGTG) known as the E-box sequence and form a heterodimeric complex with their functional partner, Max. The Myc-Max heterodimer recruits other transcriptional co-factors and activates or represses gene expression (Eilers, 2008; Westermarck, 2011). Similarly to the other Myc proteins, N-Myc is a transcription factor that controls the expression of many target genes involved in fundamental cellular processes (Malynn, 2000; Murphy, 2011). c-Myc was found to be overexpressed in Burkitt lymphomas; however, during mouse embryogenesis and in highly proliferative adult tissues it is usually expressed, functioning as an inhibitor of differentiation processes and a promoter of cell proliferation (Pelengaris, 2002). Interestingly, MYCN shows a more targeted expression pattern, with temporal and tissue specificity. It is first detected during the seventh day of pregnancy, is observed at high levels during the ninth and eleventh days and rapidly decreases after the twelfth day (Nau, 1986; Hui, 2001). The importance of MYCN expression during the first steps of developmental processes is demonstrated by mutations in the human MYCN gene being associated with birth defects. Mouse embryos defective for MYCN are unable to survive past embryonic stage E11.5 and exhibit hypoplasia in diverse organs and tissues: strongly reduced thickness of the encephalic walls, reduction of mature neurons in the ganglia of the trunk region, hearts underdeveloped often retaining the S-shape typical of 9-day-old embryos, marked underdevelopment in the lung airway epithelium, failure in the organization of the mesonephros of the genitourinary system, absence of a bulging stomach structures (Sawai, 1991; Charron, 1992; Moens, 1992; Stanton, 1992; Moens, 1993; Sawai, 1993). Moreover, in adult tissues, MYCN is expressed at early stages in developing B cells and at low levels in the brain, testis and heart (Squire, 1986; Zimmerman, 1986).



Nevertheless, it is widely accepted that MYCN expression undergoes a necessary decrease during differentiation processes; otherwise, high MYCN levels lead to a neoplastic phenotype (Thiele, 1988).

The aim of this work was to study the role of the N-Myc protein in neuroblastoma differentiation processes, particularly during the early stages. Our hypothesis was that, N-Myc might be necessary to activate neuroblastoma differentiation (mimicking embryonic development events) by regulating certain non-coding RNAs critical for differentiation.

Indeed, our data demonstrate that MYCN gene expression is required for neuroblastoma cells to activate the differentiation programme in the early stages. We found that N-Myc expression increased during the early differentiation phases, and its downregulation prevented differentiation in human neuroblastoma LAN-5 cells. Moreover, MYCN gene overexpression in the poorly differentiating neuroblastoma cell line SK-N-AS predisposed the cells to complete the differentiation process. These effects were accompanied by modulation of the apoptotic programme and were mediated by non-coding RNAs, which in turn regulated the expression of various apoptosis-related genes.

## 2.3 Results

### 2.3.1 Retinoic acid (RA) triggers differentiation in the human neuroblastoma LAN-5 cell line

First, we performed a comparative western blot analysis of the main proteins studied in the three cell models discussed in the paper (Supplementary Figure 1, Appendix A).

Figure 1a shows neurite outgrowth in LAN-5 cells cultured in a medium supplemented with 10  $\mu$ M RA. Untreated cells continued expansion without changing morphology or shape; however, in RA-treated cells, neurite appeared after the first day of treatment and increased in number and length after five days. Moreover, neurite interconnections were stimulated by RA: the exposure caused the cells to form new networks. The expression of the differentiation marker neurofilament 200 (NF200), was induced by RA (Figure 1b).

Analysis of a group of typical molecular neuronal markers confirmed that RA treatment activated the differentiation programme in LAN-5 cells. Quantitative PCR (qRT-PCR) revealed increasing levels of GAP43, ChAT, MAPT, SLC18A3, ENO2 and CDK5 (Figure 1c); western blotting analysis of GAP43 and ChAT proteins confirmed the qRT-PCR data (Figure 1d).

Differentiation induction was offset by a reduction in the growth of RA-treated cells; the mean doubling time was approximately 27h in control cells and 54 h in RA-treated ones (Supplementary Figure 2a, Appendix A). Retinoic acid prevented cell growth by arresting cells in the G0/G1 phase of the cell cycle (the percentage of cells in G0/G1 was 50.40% in control cells and 71.48% in RA-treated cells after 3 days of growth; Supplementary Figure 2b, Appendix A). Moreover, a BrdU incorporation assay revealed reduced DNA synthesis after RA exposure. The percentage of cells incorporating BrdU was 53% for untreated control cells and 21% for RA-treated cells (Supplementary Figure 2c, Appendix A). Consistent with the increase in the percentage of cells in the G0/G1 cell cycle phase, Cyclin A was down-regulated, and the kinase inhibitor p27<sup>kip1</sup> was up-regulated (Supplementary Figure 2d, Appendix A).

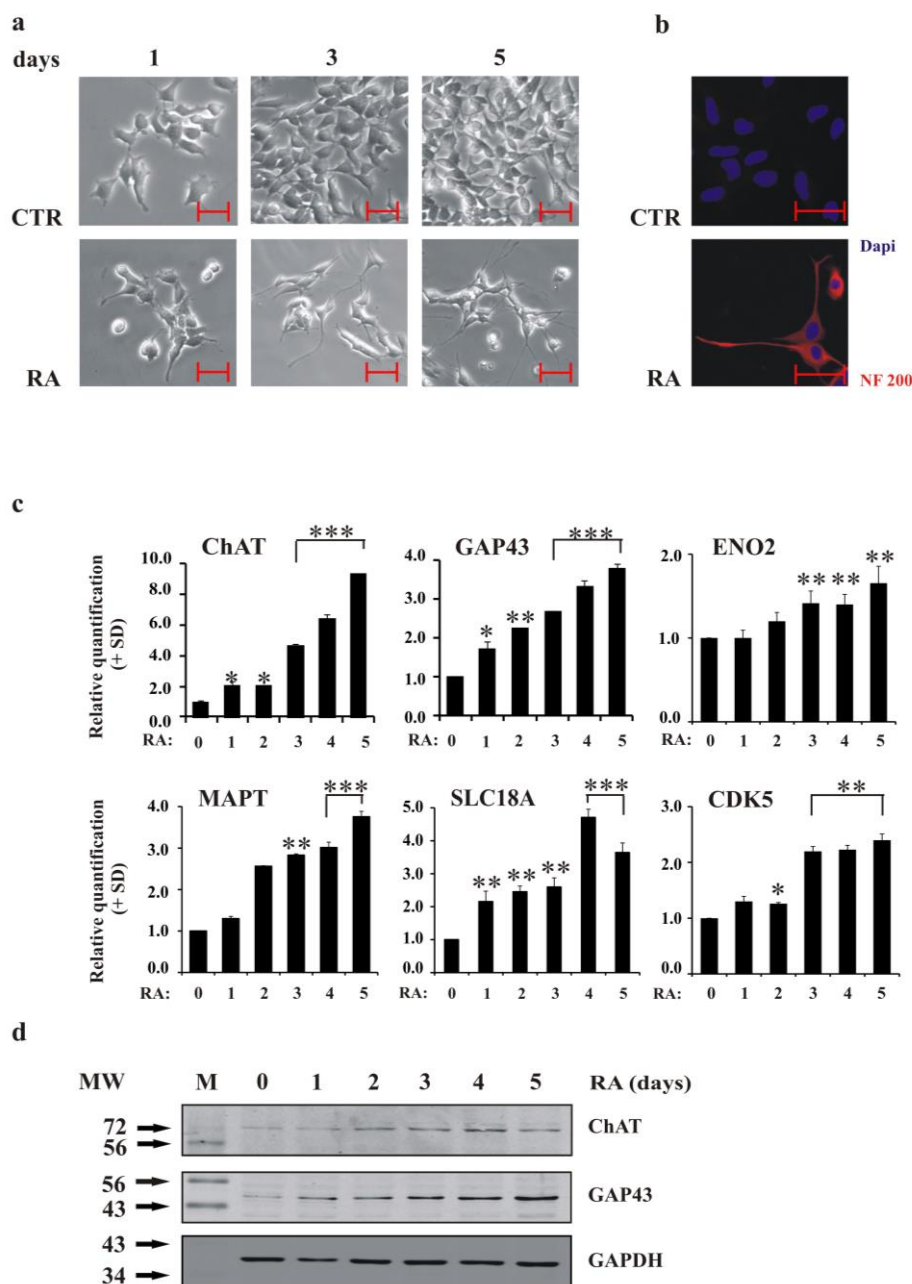


**Figure 1. LAN-5 cells differentiate upon RA stimulus** **a)** Inverted light microscopic images of LAN-5 cells untreated (CTR) or RA-treated for 1, 3 and 5 days. Scale bar, 50  $\mu$ m. **b)** Representative fluorescent images of LAN-5 cells untreated (CTR) or RA-treated for 5 days. Red, NF200 immunostaining; blue, DAPI. Scale bar, 50  $\mu$ m. **c)** The levels of the indicated mRNA in LAN-5 cells untreated (0) or RA-treated for 1, 2, 3, 4 and 5 days. The data are reported as the level of mRNA relative to the respective untreated cells and are the mean + SD ( $n = 3$ ). Statistical significance, \* $p \leq 0.05$ ; \*\* $p \leq 0.01$ ; \*\*\* $p \leq 0.001$ . **d)** Representative blots of the indicated proteins in LAN-5 cells untreated (0) or RA-treated for 1, 2, 3, 4 and 5 days. GAPDH expression was used to normalise protein loading. The experiment was repeated three times with similar results. M, molecular weight markers; MW, molecular weight.

### **2.3.2 N-Myc expression increases during the early phases of RA-induced differentiation in cells of neural origin**

LAN-5 cells showed an increase in N-Myc protein when exposed to RA. The maximal N-Myc expression was evident between the first and the third day of treatment (Figure 2a). Afterwards, N-Myc expression levels started to decrease. Analysis of MYCN levels using qRT-PCR confirmed the results observed by western blot analysis, revealing a maximum of an approximately 3-fold-enrichment of its mRNA during the early induction of differentiation (Figure 2b). We also examined the mRNA levels of a well-known down-regulated downstream target of N-Myc, N-Myc downstream-regulated gene 1 (NDRG1) (Melotte, 2010), to verify the functional implications of MYCN up-regulation. As expected, qRT-PCR analysis revealed that the modulation of the N-Myc target NDRG1 inversely paralleled MYCN modulation during differentiation (Figure 2b). The analysis of the sub-G1 fraction, indicative of apoptosis, during the RA-induced differentiation in LAN-5 cells revealed a peak in the sub-G1 region between the third and the fourth day of differentiation, when N-Myc expression was maximal (Figure 2c).

The MYCN expression analysis conducted in mouse cortical embryonic neural progenitor cells induced to differentiate revealed that the MYCN levels in these cells tracked those observed in LAN-5 cells during differentiation (Figure 2d). Evidently, MYCN expression increased during the early phases of differentiation and then decreased as expected. The observed increase in CDK5 expression was consistent with the activation of differentiation. Interestingly, a significant decrease in MYC expression was observed from the early phases of differentiation, further supporting the idea that the MYC and MYCN genes might play different roles in the differentiation programme.

### **2.3.3 N-Myc is necessary to activate the differentiation programme in LAN-5 neuroblastoma cells**

To determine whether and to what extent MYCN plays a determining role in early differentiation, we silenced its expression in MYCN-amplified LAN-5 cells. We introduced an artificial miRNA to interfere with N-Myc expression. We evaluated N-Myc levels after down-regulation, comparing Mock cells and MYCN-KD ones during RA treatment for 4 days (Figure 3a). We obtained a decrease in protein levels of approximately 70%, maintained at similar level during RA-induced differentiation. The down-regulation of the MYCN transcripts was approximately 40%, and the levels of the N-Myc downstream target NDRG1 were significantly up-regulated (Figure 3b).

Phase contrast microscopy revealed a strong reduction of neurite formation in MYCN-KD cells even after RA treatment. In contrast, Mock cells continued to present neurite extensions (Figure 3c). In the same differentiation conditions in MYCN-KD cells we did not observe any significant expression of the neurite marker NF200 (Figure 3d).

We studied plasma membrane polarisation using flow cytometry and fluorescent dyes responsive to acute changes in the plasma membrane potential to determine functional effects of MYCN down-regulation in LAN-5 cells. As expected, MYCN-KD cells were characterised by a reduced ability to polarise the plasma membrane compared to Mock cells. (Figure 4a). In addition, the membrane hyperpolarisation usually observed in RA-differentiated cells was prevented when the MYCN gene was down-regulated (Figure 4b). We evaluated cell death in Mock and MYCN-KD cells by assessing the mitochondrial membrane potential. We found that the MYCN-silenced cells did not show any cell death after RA treatment, whereas the control Mock cells exposed to RA exhibited apoptosis (Figure 4c), suggesting that MYCN might be necessary in the early phases of differentiation to induce apoptosis in cells not committed to differentiation.

The expression of the molecular neuronal markers previously analysed in the differentiating LAN-5 cells was also studied after MYCN silencing. We observed inhibited expression levels of all four markers analysed at day three after RA treatment (Figure 4d).

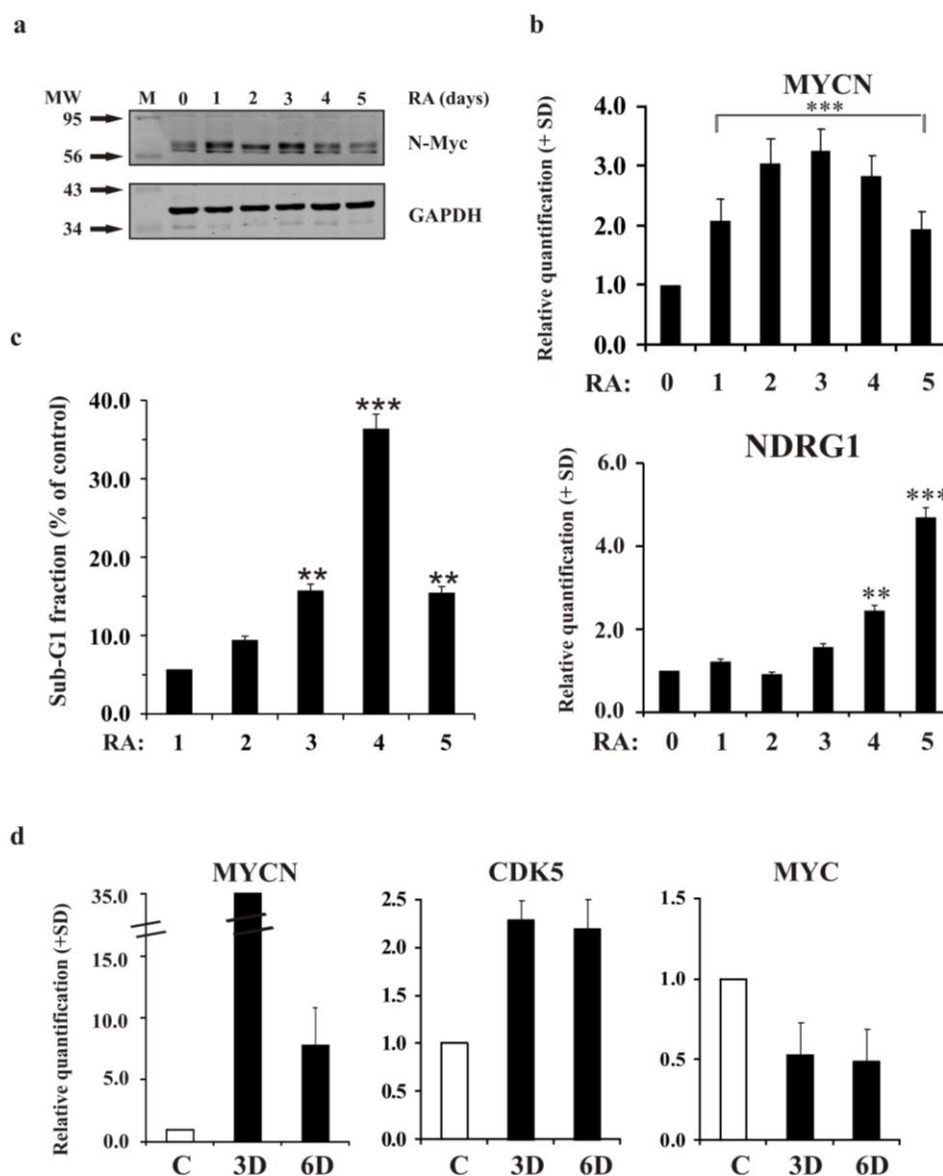


**Figure 2. MYCN increases during the first days of differentiation in LAN-5 cells and in mouse cortical embryonic neural progenitors** **a**) Representative blots of the N-Myc protein in LAN-5 cells untreated (0) or RA-treated for 1, 2, 3, 4 and 5 days. GAPDH expression was used to normalise protein loading. The experiment was repeated three times showing similar results. M, molecular weight markers; MW, molecular weight. **b**) Levels of the indicated mRNA in LAN-5 cells untreated (0) or RA-treated for 1, 2, 3, 4 and 5 days. The data are reported as the level of mRNA relative to the respective untreated cells and are the mean + SD (n = 3). Statistical significance, \*\*p<0.01; \*\*\*p<0.001. **c**) Sub-G1 fractions estimated on the DNA content histograms in LAN-5 cells treated with RA for 1, 2, 3, 4 and 5 days. Data are reported as percent of control. Statistical significance, \*\*p<0.01; \*\*\*p<0.001. **d**) The levels of the indicated mRNA in mouse cortical embryonic neural progenitor cells undifferentiated (white) or induced to differentiate for 3 and 6 days (black). The data are reported as the level of mRNA relative to the respective untreated cells and are the mean + SD (n = 3). Statistical significance, \*\*p<0.01; \*\*\*p<0.001.

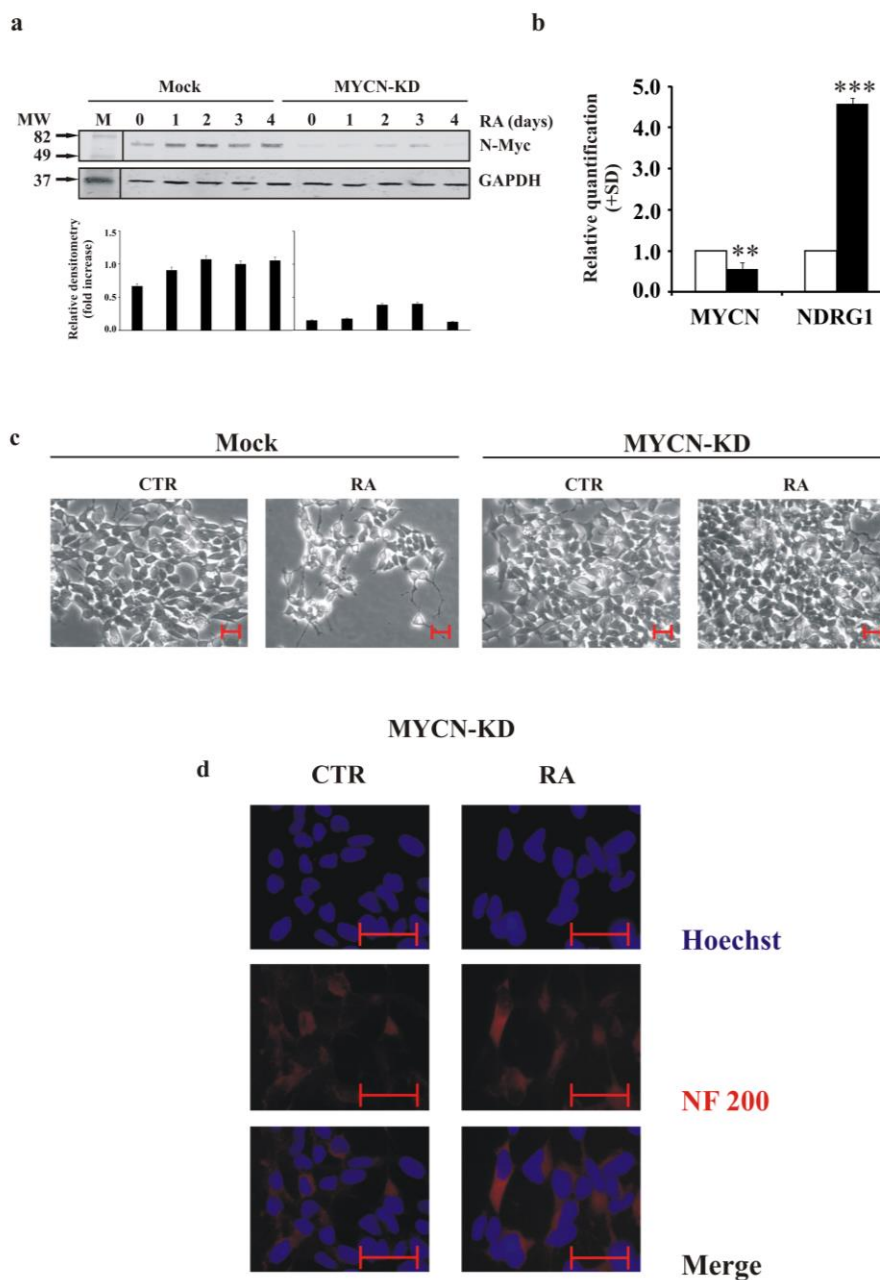


**Figure 3. MYCN gene silencing in LAN-5 cells inhibits neurite outgrowth and NF200 expression after RA induction** **a)** Upper panel, representative blots of the N-Myc protein in LAN-5 cells silenced for MYCN gene (MYCN-KD) or in control cells (Mock) untreated (0) or RA-treated for 1, 2, 3, 4 and 5 days. M, molecular weight markers; MW, molecular weight. Lower panel, blots densitometry as analysed by ImageJ software. Values are averages + SD of three independent experiments with similar results. GAPDH expression was used to normalise protein loading. **b)** The levels of the indicated mRNA in MYCN-KD LAN-5 cells (black) or in control cells (white). The data are reported as the level of mRNA relative to the respective control cells and are the mean + SD ( $n = 3$ ). Statistical significance, \*\* $p \leq 0.01$ ; \*\*\* $p \leq 0.001$ . **c)** Inverted light microscope images of MYCN-KD LAN-5 cells or in control cells, untreated (CTR) or RA-treated for 3 days. Scale bar, 50  $\mu\text{m}$ . **d)** Representative fluorescent images of MYCN-KD LAN-5 cells untreated (CTR) or RA-treated for 3 days. Red, NF200 immunostaining; blue, Hoechst. Scale bar, 50  $\mu\text{m}$ .

### **2.3.4 N-Myc overexpression induces differentiation in poorly differentiating neuroblastoma cells**

The SK-N-AS neuroblastoma cell line shows a very poor capacity to differentiate after stimulation with RA, and these cells have a single copy of the MYCN gene, thus showing no overexpression of this gene (Suenaga, 2009). We overexpressed the MYCN gene in these cells (Figure 5a) and studied differentiation activation after RA induction. The overexpression of the MYCN gene was also confirmed by the protein level (Figure 5b). Figure 5c shows the micrographs of SK-N-AS Mock and SK-N-AS MYCN<sup>+</sup> cells, untreated or treated with RA for three days. In the presence of the MYCN gene, RA activated differentiation in SK-N-AS cells, as indicated by the neurite outgrowth, with most of them showing a bipolar shape. The number of cells with neurites increased by approximately 90% in MYCN<sup>+</sup> cells after RA treatment. The neurite length was significantly increased in MYCN<sup>+</sup> cells (Figure 5d; Mock cells, mean=121  $\mu$ M, median=120  $\mu$ M, range=60-254  $\mu$ M; MYCN<sup>+</sup> cells, mean=213  $\mu$ M, median=208  $\mu$ M, range=115-375  $\mu$ M). NF200 immunostaining confirmed the ability of SK-N-AS MYCN<sup>+</sup> cells to differentiate; NF200 was clearly expressed in these cells after RA exposure (Figure 5e). The analysis of GAP43, CDK5 and ENO2 differentiation marker genes corroborated that MYCN overexpression in SK-N-AS cells rendered these cells prone to differentiation after RA exposure (Figure 5f).



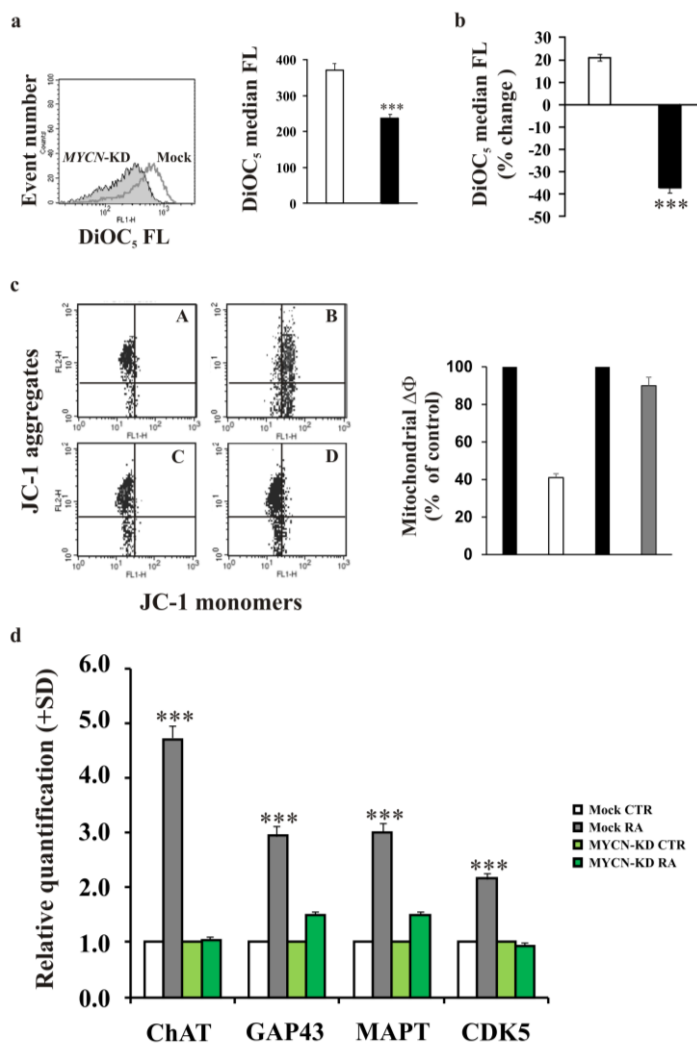


**Figure 4. MYCN gene silencing produces a depolarisation of the plasma membrane and inhibits the RA-induced up-regulation of differentiation markers** **a**) FACS analysis of the DiOC<sub>5</sub> fluorescence distribution in MYCN-KD LAN-5 cells (full histogram) or in Mock control cells (empty histogram). Right, FACS histograms; left, median values of the DiOC<sub>5</sub> fluorescence distributions in MYCN-KD LAN-5 cells (black) or in Mock control cells (white). The experiment was repeated three times showing similar results. **b**) The percent variation of the median values of the DiOC<sub>5</sub> fluorescence distributions in MYCN-KD LAN-5 cells (black) or in Mock control cells (white) after RA treatment. The experiment was repeated three times showing similar results. **c**) Mitochondrial membrane potential analysed by JC-1 staining in Mock control LAN-5 untreated (A) and RA-treated (B) cells compared to MYCN-KD LAN-5 untreated (C) and RA-treated (D) cells (left panel). In the right panel are shown the  $\Delta\Phi$  values calculated on the FACS cytograms following the formula described in Materials and Methods section. Data are reported as percent of control and are average of at least three separate experiments. Bars represent standard deviation. **d**) The levels of the indicated mRNA in MYCN-KD LAN-5 cells untreated (light green) or RA-treated for 3 days (green) and in Mock control cells untreated (white) or RA-treated for 3 days (dark grey). The data are reported as the level of mRNA relative to the respective untreated cells and are the mean + SD (n = 3). Statistical significance, \*\*\*p $\leq$ 0.001.

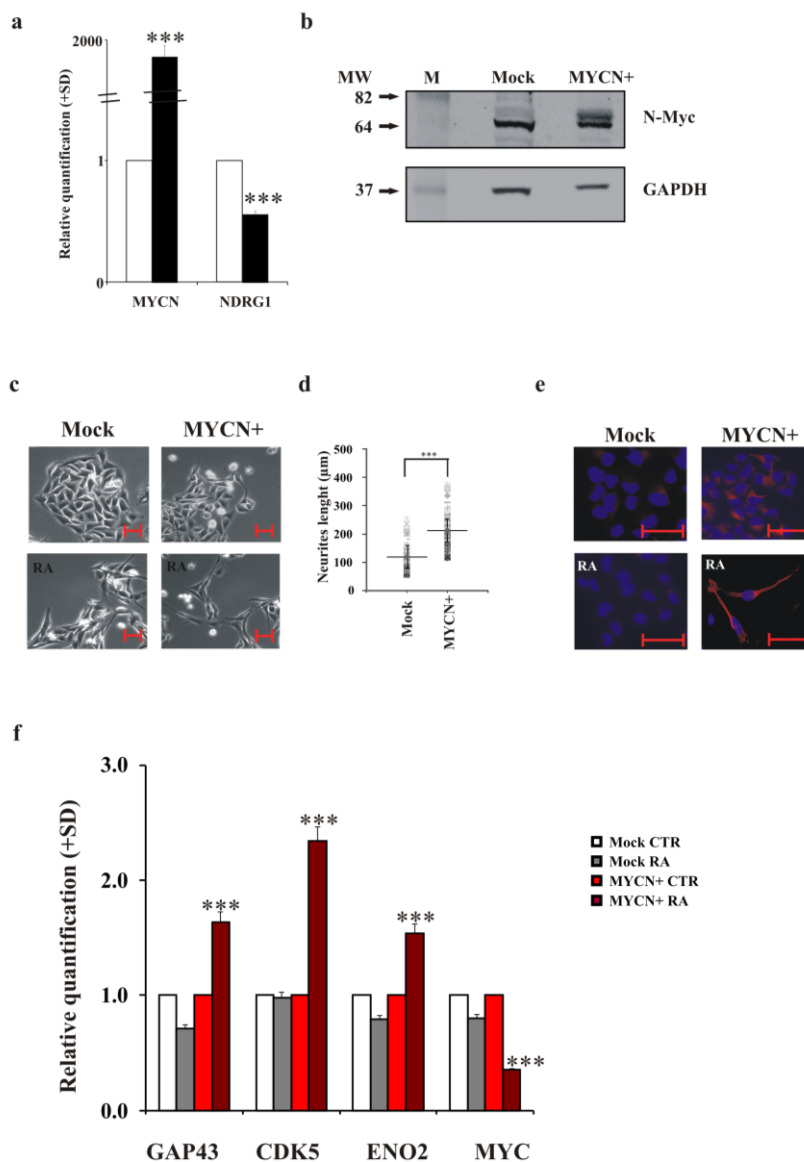


**Figure 5. MYCN overexpression in the SK-N-AS cells restores their ability to differentiate after RA** **a)** The levels of the indicated mRNA in SK-N-AS Mock (white) and SK-NAS MYCN+ (black) cells. The data are reported as the level of mRNA relative to the respective Mock cells and are the mean + SD (n = 3). Statistical significance, \*\*\* $p \leq 0.001$ . **b)** Representative blots of the N-Myc protein in SK-N-AS Mock and SK-N-AS MYCN+ cells. GAPDH expression was used to normalise protein loading. The experiment was repeated three times showing similar results. M, molecular weight markers; MW, molecular weight. **c)** Inverted light microscope images of SK-N-AS Mock and SK-N-AS MYCN+ untreated or RA-treated for 3 days. Scale bar, 50  $\mu\text{m}$ . **d)** Distribution of the neurite outgrowth length as measured in SK-N-AS Mock and SK-N-AS MYCN+ treated with RA for 3 days. Statistical significance, \*\*\* $p \leq 0.001$ . **e)** Representative fluorescent images of SK-NAS Mock and SK-N-AS MYCN+ untreated or RA-treated for 3 days. Red, NF200 immunostaining; blue, DAPI. Scale bar, 50  $\mu\text{m}$ . **f)** The levels of the indicated mRNA in SK-N-AS Mock and SK-N-AS MYCN+ untreated (white or light red, respectively) or RA-treated for 3 days (grey or red, respectively). The data are reported as the level of mRNA relative to the respective control cells and are the mean + SD (n = 3). Statistical significance, \*\*\* $p \leq 0.001$ .

### 2.3.5 MYCN modulation modifies the expression of miRNAs involved in apoptosis preceding neuronal differentiation

The analysis of specific miRNAs selected by *in silico* analysis (miRWalk - Dweep, 2011) and reported to be regulated by MYCN and at the same time involved in apoptosis and neuron development, revealed changes in the expression of miR-20a, miR-9 and miR-92a. We found that these miRNAs were up-regulated in MYCN-silenced LAN-5 cells (Figure 6a). In contrast, when MYCN was overexpressed in the SK-N-AS cells, the same miRNAs were down-regulated (Figure 6b). In particular, the p53-family members have been reported to be regulated by these miRNAs. For this reason, we performed PCR Array analysis of the p53 signalling pathway (Figure 6c). As expected, and consistent with the expression of miR-20a, miR-9 and miR-92a, the expression pattern observed in LAN-5 MYCN-KD cells was opposite to that in SK-N-AS MYCN+ cells with regard to genes known to be involved in cell death regulation. We found that pro-apoptotic CASP9 and BAI1 genes were up-regulated in the MYCN overexpressing cells; whereas, the anti-apoptotic BCL2 gene was down-regulated in the same MYCN condition. By contrast, CASP9 and BAI1 were down-regulated and BCL2 up-regulated when MYCN was silenced. As well as, genes known to be involved in the activation of apoptotic programme such as E2F1, E2F3, GADD45A, and FOXO3 were up-regulated in MYCN-amplified and down-regulated in MYCN-silenced cells, respectively. In addition, despite an analysis of validated miRNA targets using miRWalk database reported miR-20a, miR-9 and miR-92a target TP53, TP73 and TP63 mRNAs, the PCR Array analysis did not reveal any modulation of TP53 mRNA levels (data not shown); while an up-regulation of both TP73 (about 7-fold) and TP63 (more than 2-fold) was observed in MYCN overexpressing cells (Figure 6c).

### 2.3.6 Inhibition of miR-20a, miR-9 and miR-92a in the wild type SK-N-AS cells restores apoptosis and their differentiation ability

We inhibited miR-20a, miR-9 and miR-92a in MYCN-non-amplified SK-N-AS cells avoiding any possible interference by MYCN (Figure 7a).

The pro-apoptotic genes (CASP9, FOXO3, E2F1, E2F3 and TP73) were up-regulated by miRNAs inhibition after both 24h and 48h. By contrast, TP63 was not up-regulated suggesting no correlation between miR-20a, miR-9 and miR-92a and TP63 expression (Figure 7b). Interestingly, RA was able to activate apoptosis after miRNAs inhibition in SK-N-AS cells (Figure 7c, *panel D*). While, control cells did not present any significant induction of apoptosis by RA treatment (Figure 7c, *panel B*).

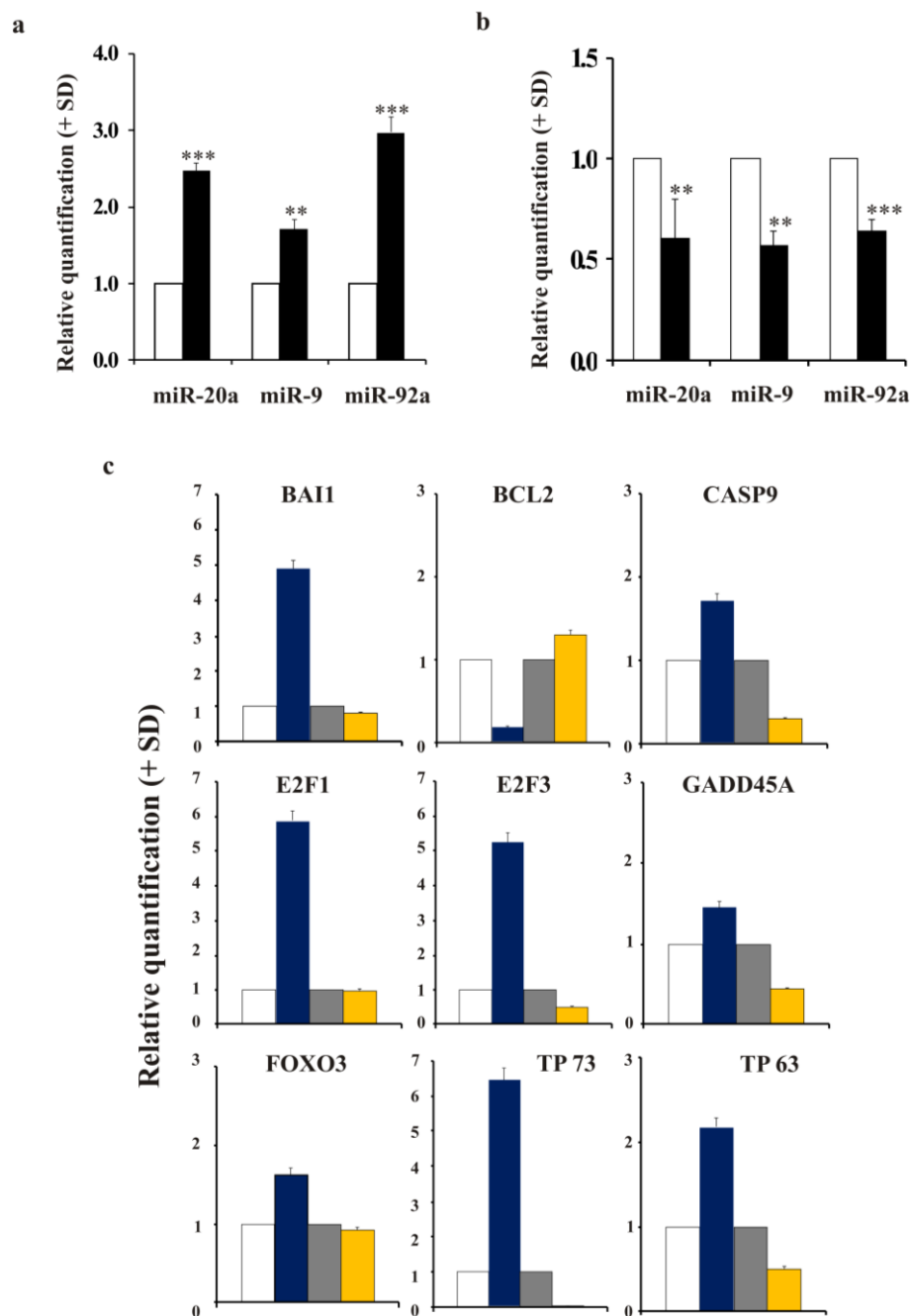


**Figure 6. miRNAs are inversely regulated in MYCN-silenced and MYCN-up-regulated neuroblastoma cells, and its expression is associated to a different modulation of apoptosis-related genes** **a)** The levels of the indicated hsa-miR in MYCN-KD LAN-5 cells (black) or in Mock control cells (white). The data are reported as the level of miRNA relative to the respective untreated cells and are the mean + SD (n = 3). Statistical significance, \*\* $p \leq 0.01$ ; \*\*\* $p \leq 0.001$ . **b)** The levels of the indicated hsa-miR in SK-N-AS MYCN+ cells (black) or in Mock control cells (white). The data are reported as the level of miRNA relative to the respective untreated cells and are the mean + SD (n = 3). Statistical significance, \*\* $p \leq 0.01$ ; \*\*\* $p \leq 0.001$ . **(c)** The levels of the indicated mRNA in SK-N-AS Mock (white), SK-N-AS MYCN+ (blue), LAN-5 Mock (grey) and LAN-5 MYCN-KD (yellow). The data are reported as the level of mRNA relative to the respective control cells and are the mean + SD (n = 3).

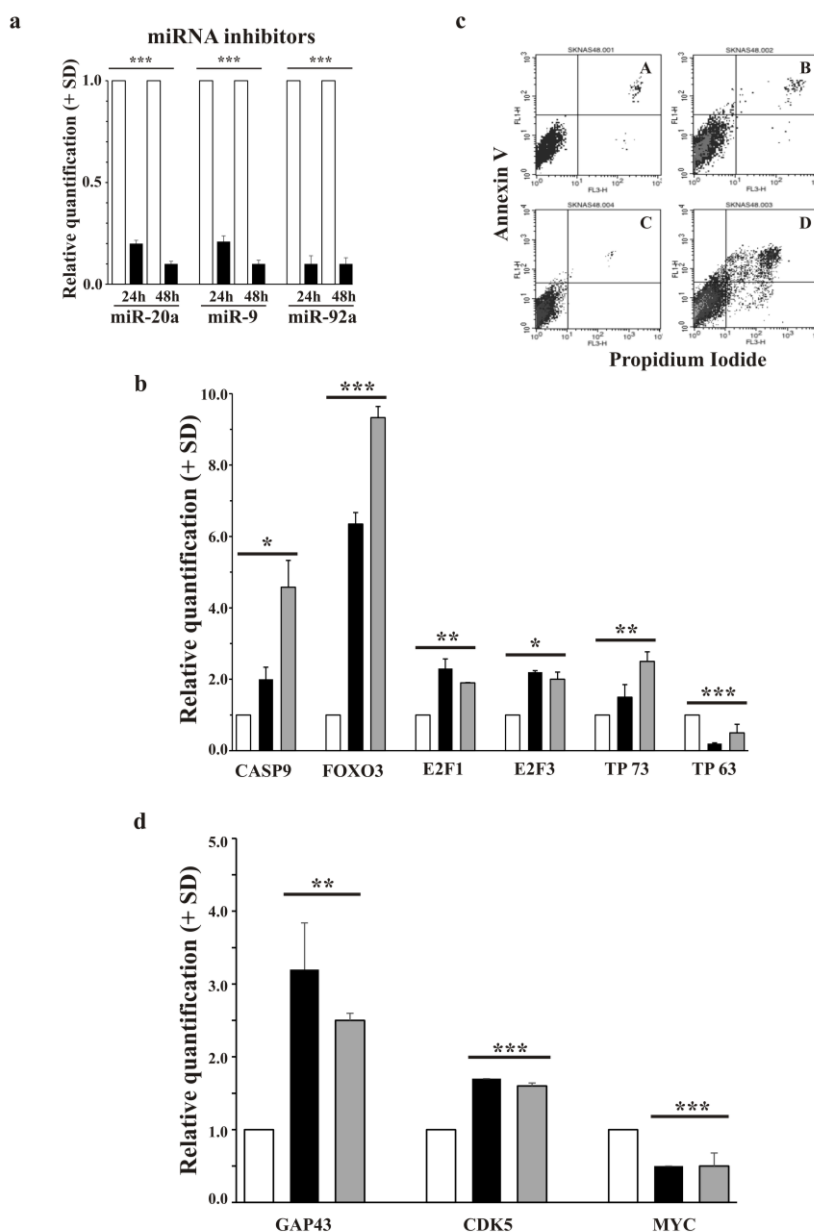


**Figure 7. miR-20a, miR-9 and miR-92a inhibition in wild type SK-N-AS cells leads to apoptotic death induction and expression of differentiation-related genes** **a)** The levels of the indicated miRNAs in inhibitor negative control (white) and miRNA inhibitor (black) cells at 24h and 48h after transfection. The data are reported as the level of mRNA relative to the respective miRNAs negative control cells and are the mean + SD (n = 3). Statistical significance, \*\*\*p<0.001. **b)** The levels of the indicated mRNA in inhibitor negative control (white), miRNA inhibitor at 24h (black) and miRNA inhibitor at 48h (grey). The data are reported as the level of mRNA relative to the respective miRNAs negative control cells and are the mean + SD (n = 3). Statistical significance, \*p<0.05; \*\*p<0.01; \*\*\*p<0.001. **c)** FACS analysis of the Annexin V fluorescence distribution in inhibitor negative control untreated (panel A) and RA-treated (panel B) cells and miRNA inhibitor untreated (panel C) and RA-treated (panel D) at 48h after transfection. The experiment was repeated three times showing similar results. **d)** The levels of the indicated mRNA in inhibitor negative control (white), miRNA inhibitor at 24h (black) and at 48h (grey) after transfection. The data are reported in RA-treated condition. The data are the mean + SD (n = 3). Statistical significance, \*\*p<0.01; \*\*\*p<0.001.

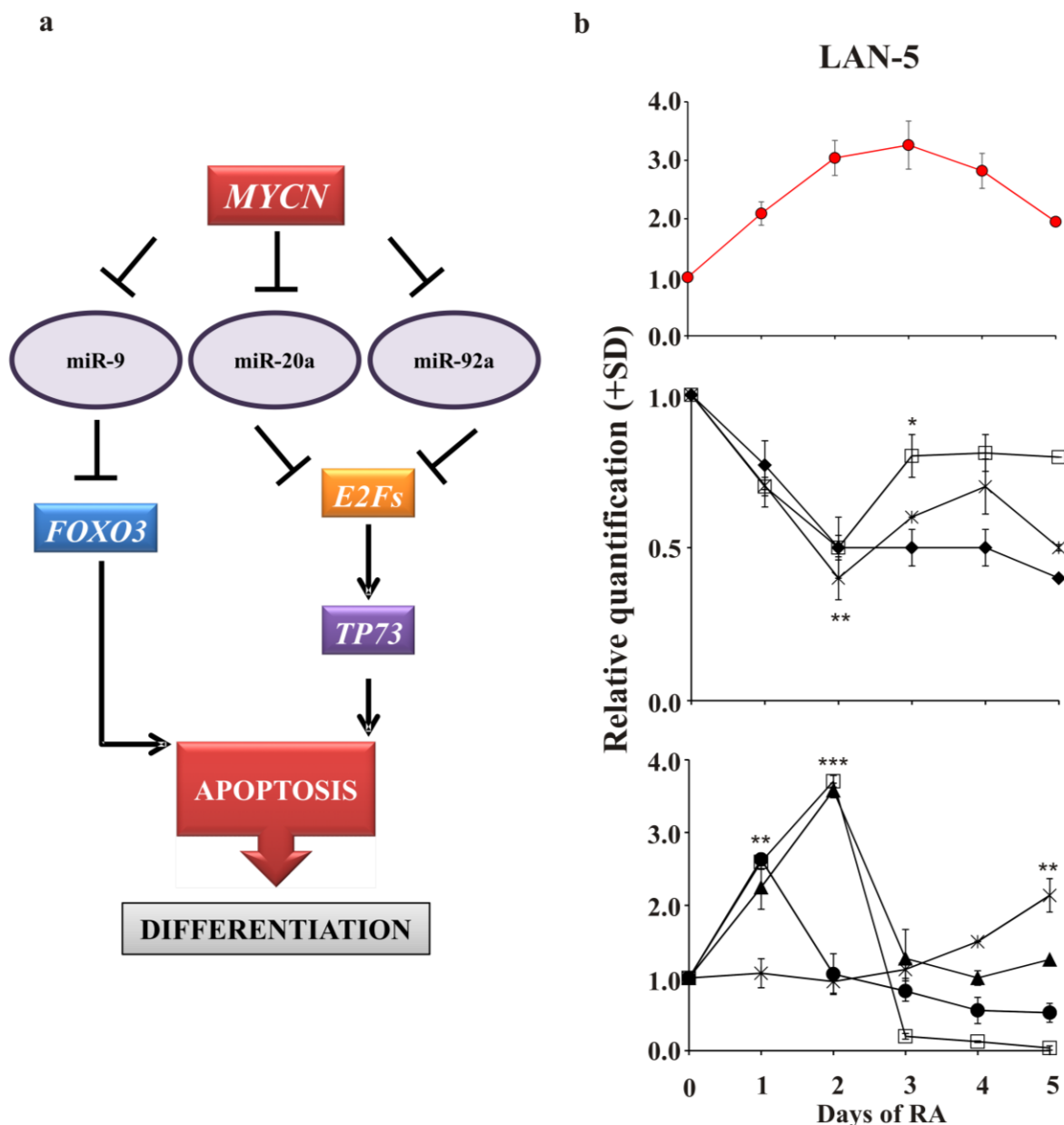


**Figure 8. Model of the hypothetical role of MYCN during the early phases of neuroblastoma differentiation** **a)** MYCN overexpression inhibits miR-9, miR-20a and miR-92a. We hypothesise that this inhibition allows targets of these miRNAs (E2F genes, TP73 and FOXO3) to be up-regulated and in turn to activate apoptosis in those cells not committed to differentiate but still proliferating. In contrast, MYCN down-regulation allows the overexpression of miR-9, miR-20a and miR-92a, preventing the up-regulation of apoptosis-related genes, thus inhibiting apoptosis and subsequent differentiation. **b)** Upper panel, the levels of MYCN gene in LAN-5 cells untreated (0) or RA-treated for 1, 2, 3, 4 and 5 days. Middle panel, the levels of miR-20a (diamond), miR-9 (open square) and miR-92a (star). Lower panel, the levels of E2F1 (closed circle), E2F3 (open square), FOXO3 (triangle), TP73 (star). The data are reported as the level of mRNA relative to the respective untreated cells and are the mean + SD (n = 3). Statistical significance, \* $p \leq 0.05$ ; \*\* $p \leq 0.01$ ; \*\*\* $p \leq 0.001$ .

Differentiation markers were up-regulated after the inhibition of the three miRNAs at both 24h and 48h in the presence of RA induction (Figure 7d). As expected, MYC was down-regulated in differentiating cells.

In Figure 8a we summarised our data presenting a hypothetical mechanism by which MYCN could trigger the onset of differentiation programme in neuroblastoma cells. To further validate this hypothesis we analysed the expression kinetics of miRNAs and apoptotic genes presented in the model (Figure 8b, *middle* and *lower panels*). To make data reading easier we reported the kinetics of MYCN gene (Figure 8a, *upper panel*; see also Figure 2b). As MYCN gene is up-regulated during RA treatment the three miRNAs are down-regulated and consequently their targets are up-regulated.

## 2.4 Conclusions

Several studies of MYC- and MYCN-knockout mice have revealed that embryos of these mice could not survive until gestation (Sawai, 1991; Charron, 1992; Stanton, 1992; Davis, 1993; Knoepfler, 2002), suggesting that the MYC family genes are required for normal development at the beginning of organogenesis. In particular, Knoepfler et al. showed that N-Myc plays an important role in complete nervous system development. In fact, loss of N-Myc function during embryogenesis interrupts the ability of neural progenitors to expand, differentiate and populate the brain, causing neurological dysfunction after birth. Unlike c-Myc, which is expressed in all proliferating cells, N-Myc expression is more restricted. Appropriate spatial and temporal expression of N-Myc is important for normal embryonic development (Strieder, 2003). Accordingly, we show that up-regulation of the MYCN gene is restricted to the early stages of differentiation induction in mouse cortical embryonic neural progenitor cells. In addition, as expected, MYC gene expression decreased during differentiation progress. These data suggest that the MYCN gene might play a critical role in the activation of neuronal differentiation. Nevertheless, as also reported by others (Sidell, 1982; Amatruda, 1985; Thiele, 1988), differentiation completion was later associated with a decrease in MYCN expression. It is likely that the N-Myc protein, as a transcription factor, is necessary at the onset of neuronal differentiation to establish the expression of a set of genes essential for subsequent phases.

To examine the role of N-Myc in the neuronal differentiation programme, we used the human neuroblastoma cell line LAN-5, which show MYCN gene amplification (Ribatti, 2002). The LAN-5 cell line, similarly to many others neuroblastoma cell lines, maintains the ability to differentiate in vitro in the presence of specific stimuli, such as RA (Ribatti, 2002; Edjö, 2004). In fact, our results confirm that LAN-5 cells treated with RA form neurites; express the neuronal marker NF200, an intermediate filament that provides structural stability to the axon; and show the induction of a series of neuronal molecular markers. In agreement with previous papers (Sidell, 1982; Pählman, 1984), GAP43 and MAPT were up-regulated in differentiated LAN-5 cells; in addition, ChAT and SLC18A appeared to have increased expression after differentiation induction in the LAN-5 cell line, which is normally committed to cholinergic differentiation (Hill, 1997). As expected, successful development is associated with cell proliferation inhibition, demonstrated by cell cycle analysis performed using various approaches.

In addition to what has been observed previously (Sidell, 1982; Amatruda, 1985; Thiele, 1988), we found peak MYCN expression during the first days of RA-induced differentiation



in LAN-5 cells. We demonstrated the functionality of the increased N-Myc protein through expression analysis of the N-Myc target NDRG1, which decreased as expected (Melotte, 2010).

Furthermore, differentiation was inhibited by MYCN silencing in the same model; this was indicated by the failure of neurite outgrowth, the decrease in known neuronal molecular markers and the loss of NF200 expression during differentiation. In addition, the plasma membrane of the MYCN-KD LAN-5 cells depolarised and was no longer able to hyperpolarise in response to differentiation stimuli. Plasma membrane polarisation is a parameter known to be essential for differentiated neuronal cells (Sundelacruz, 2009).

In addition, when MYCN is overexpressed in cells with a poor differentiation capacity, developmental processes are restored. This pattern was observed in SK-N-AS MYCN<sup>+</sup> cells, in which neurite outgrowth occurred, and the expression of NF200 and known molecular neuronal markers increased after RA treatment.

These data, taken together, demonstrate that N-Myc protein expression is required to activate the differentiation processes in neuroblastoma cells.

To explore the mechanisms by which N-Myc could trigger differentiation in neuroblastoma cells, we studied the expression levels of miR20a, miR-9 and miR-92a which have been reported to be involved in differentiation processes and to be modulated by MYCN (Schulte, 2008; Stallings, 2009). Through the up- or down-regulation of the MYCN gene, we observed that all the three miRNAs were decreased or increased, respectively. Consistently, the inverse relationship between these miRNAs and the cell differentiation status suggests that their down-regulation is needed for differentiation triggering. In fact, according to the miRWalk database, two of the validated targets of these miRNAs are the retinoic acid receptor genes RARA and RARG (Li, 2009; Liu, 2012). The up-regulation of miR-92 following MYCN silencing and its down-regulation by RA treatment are in agreement with Chen and Stallings (2007), who showed that the expression of different miRNAs correlates with neuroblastoma prognosis, differentiation and apoptosis, also in response to RA. Moreover, consistently with Haug et al. (2011) who found that miR-92 inhibits the secretion of the tumour suppressor gene DKK3 in neuroblastoma, our data demonstrated the down-regulation of miR-92a in cells with a restored ability to differentiate, characteristic of a less malignant phenotype. Our findings are also supported by the data of Jee et al. (2012), which showed that inhibition of miR-20a expression induces definitive motor neuron survival and neurogenesis. Consistent with results of Yoo et al. (2009), showing that miR-9 is repressed in neural proliferating

progenitors and is sequentially re-expressed in post-mitotic neurons, is the modulation of miR-9 we observed in LAN-5 cells during the RA kinetics (see Figure 8b, *middle panel*).

In agreement with O' Donnell et al. (2005) and Coller et al. (2007) we demonstrated that miR-20a negatively regulates the E2F factor genes. The transactivating p73 isoforms are transcriptionally induced by E2F and contribute to E2F-mediated apoptosis (Irwin, 2000, Stiewe, 2000; Zaika, 2001). Consistent with these data, up-regulation of TP73 and E2F was observed in MYCN+ cells and after miRNAs inhibition in SK-N-AS cells. Moreover, as expected, when MYCN was down-regulated, and miR-20a and miR-92a were consequently up-regulated, E2F and TP73 were inhibited. The role of p73 in the induction of neuronal differentiation has been previously highlighted by De Laurenzi et al. (2000), who showed an increase in p73 protein levels after RA stimuli in murine neuroblastoma cells. In apparently disagreement with our data, they also showed reduced N-Myc protein levels after RA treatment as a marker of neuronal differentiation (De Laurenzi, 2000). Indeed, they analysed N-Myc expression after 6 days of RA treatment, whereas, although our data demonstrated a peak in N-Myc protein expression between the second and the third day of differentiation induction, we also observed a subsequent decrease at day 5 of differentiation. It is likely that N-Myc, by down-regulating miR-20a and miR-92a, produces the increase in E2Fs gene expression, which in turn induces TP73 transcription. Interestingly, RA treatment in LAN-5 cells confirmed the presence of a hierarchy between E2Fs and TP73 which are overexpressed at day 1 and day 4 of RA treatment, respectively.

In addition, we found FOXO3 up-regulated in differentiating MYCN+ cells and in RA-treated LAN-5 cells. The human FOXOs transcription factor family regulates the expression of genes associated with multiple biological process such as cell cycle arrest and apoptosis (Eijkelenboom, 2013). As demonstrated by Senyuk et al. (2013), miR-9 is able to bind directly to the 3' UTR of FOXO3. In fact, when we silenced the MYCN gene in LAN-5 cells, an increase in miR-9 and a consequent decrease in FOXO3 mRNA levels were obtained. These data are further demonstrated by the increase in FOXO3 expression achieved after inhibiting miRNAs in SK-N-AS cells.

We reasoned that the miR-20a, miR-9 and miR-92a inhibition in MYCN+, as well as, in RA-treated LAN-5 cells and the subsequent pro-apoptotic genes increase could be a necessary step prior to differentiation programme. In fact, the inhibition of miR-20a, miR-9 and miR-92a in the MYCN-non-amplified SK-N-AS cells restored the ability of these cells to respond to RA treatment, as demonstrated by Annexin V assay and differentiation-related genes expression analysis.

Even though the overexpression of MYCN in SK-N-AS cells resulted in a down-regulation of miR-92a and an up-regulation of TP63 we did not observe an increase of TP63 after inhibiting miR-92a. It is likely, that other pathways downstream MYCN are involved in TP63 regulation. More studies are needed to establish if TP63 is directly or indirectly activated by N-Myc.

Therefore, we hypothesise that MYCN is necessary during the activation of neuroblastoma differentiation to induce apoptosis in cells that are not committed to differentiation but are still proliferating. Programmed cell death is a necessary physiological process and involves a large number of developing neurons during nervous system development (Oppenheim, 1991) and in adult neurons (Kim, 2011).

## 2.5 Materials and Methods

### Cell line maintenance, differentiation and treatments

LAN-5 and SK-N-AS human neuroblastoma cell lines (both gifts of Dr. Doriana Fruci) were grown in RPMI-1640 medium (Gibco) supplemented with 10% FBS (Hyclone), 2 mM L-glutamine, 100 U/L penicillin and 100 µg/L streptomycin in a humidified incubator containing 5% CO<sub>2</sub> at 37°C. LAN-5 cells contain amplified MYCN,<sup>28</sup> whereas SK-NAS cells are MYCN single copy (Suenaga, 2009).

Embryonic neural precursor cells (eNPC; gift of Prof. Stefano Biagioni and Dr. Emanuele Cacci) were cultured and differentiated as previously described (Cacci, 2008).

For differentiation experiments, LAN-5 cells were seeded at a density of  $5 \times 10^3$  cells/cm<sup>2</sup>. The following day, the cells were induced to differentiate with 10 µM retinoic acid (ATRA, designated RA throughout the paper; Sigma) in “differentiation medium” composed of 50% fresh and 50% conditioned culture medium. The cells were fed after 3 days with differentiation medium containing fresh RA. RA was dissolved in dimethyl sulphoxide (DMSO; Sigma) and stored as a stock solution at -80°C. SK-NAS cells were seeded at a density of  $3.5 \times 10^3$  cells/cm<sup>2</sup>. The following day, the cells were induced to differentiate by adding 1 µM RA in a “differentiation medium” composed of RPMI + 1% FBS. Because of the light sensitivity of RA, all incubations were performed under subdued lighting. The DMSO concentration in each experiment was always  $\leq 0.01\%$ , which was not toxic and did not induce differentiation.

A comparative western blot analysis has been conducted in the three cell lines employed in this work to evidence basal expression level of the main mentioned proteins (Supplementary Figure S1).

### Western Blot

Cultured cells were washed twice with 1X PBS and then incubated for 1 min in 1X PBS added with 0.5 mM PMSF (Sigma-Aldrich) and 1X Complete Protease Inhibitors (Sigma-Aldrich) scraped, harvested and briefly sonicated. Proteins were suspended in urea buffer (8 M urea, 100 mM NaH<sub>2</sub>PO<sub>4</sub>, and 10 mM Tris pH 8) and the protein concentration was determined by the Bradford assay. The proteins were subjected to SDS–polyacrylamide gel electrophoresis with NuPAGE kit (Life Technologies) according to manufacturer's instructions. The resolved proteins were blotted overnight onto nitrocellulose membranes, which then were blocked in 1X PBS containing 5% non-fat milk for at least 1 hour. The blots

were incubated with the following primary anti-human antibodies: rabbit polyclonal anti-N-Myc (C-19; Santa Cruz Biotechnology); mouse monoclonal anti-GAP43 (GAP-7B10; Sigma-Aldrich); rabbit polyclonal anti-CDK5 (Cell Signaling Technology); mouse monoclonal anti-cyclin A (C-19; Santa Cruz Biotechnology); rabbit polyclonal anti-p27<sup>kip1</sup> (C-19; Santa Cruz Biotechnology); goat polyclonal anti-ChAT (Millipore); mouse monoclonal anti-GAPDH (6C5; Millipore); and mouse monoclonal anti-HSP 72/73 (Ab1-W27; Oncogene Science Inc.). The membranes were then incubated for 45 min with the appropriate secondary antibody: donkey anti-rabbit IRdye800 (LI-COR); donkey anti-mouse IRdye800 (LI-COR) or donkey anti-goat IRdye800 (LI-COR). The membranes were then analysed with a Licor Odyssey Infrared Image System in the 800 nm channel. Blot scan resolution was 150 dpi.

### **Immunofluorescence**

The cells were seeded on coverglass supports in complete medium and treated with RA for the indicated times. The cells were fixed with 4% (w/v) paraformaldehyde and permeabilised in PBS containing 0.1% Triton-X100. NF200 was detected using an anti-NF200 monoclonal antibody (N52; Sigma). Alexa Fluor 594 goat anti-mouse antibody (Molecular Probes) was used as a secondary antibody. The antibodies were diluted in PBS. Cell nuclei were stained with 1 mg/ml DAPI in PBS for 5 min. Finally, the cells were washed in PBS and briefly rinsed in ddH<sub>2</sub>O, and the coverglass slips were mounted in ProLong Gold anti-Fade Reagent (Molecular Probes). Images were acquired with an Olympus BX51 fluorescence microscope and analysed with I.A.S. software (Delta Sistemi, Legnano (VR), Italy). The brightness and contrast of the acquired images were adjusted, and the figures were generated using Adobe Photoshop 7.0.

### **Total RNA preparation and quality control**

The cells were seeded in complete medium and harvested after the different treatments; total RNA was isolated using a Total RNA purification kit (Norgen Biotek). RNA quantity was determined by absorbance at 260 nm using a NanoDrop UV-VIS spectrophotometer. The quality and integrity of each sample was confirmed using a BioAnalyzer 2100 (Agilent RNA 6000 Nanokit); samples with an RNA Integrity Number (RIN) index lower than 8.0 were discarded.

### Real-time RT-PCR analysis

RNA was reverse-transcribed with a High-Capacity cDNA Reverse Transcription Kit (Applied Biosystem) according to the manufacturer's instructions. Equal amounts of cDNA were then subjected to real time PCR analysis with an Applied Biosystems 7900HT thermal cycler, using the SensiMix SYBR Kit (Bioline) and specific primers, each at a concentration of 200 nM.: GAPDH (unigene Hs.544577) F: AGCCACATCGCTCAGACA e R: GCCCAATACGACCAAATCC; TBP (unigene Hs.590872) F: GAACATCATGGATCAGAACAACA e R: ATAGGGATTCCGGGAGTCAT; MAPT (unigene Hs.101174) F: ACCACAGCCACCTTCTCCT e R: CAGCCATCCTGGTTCAAAGT; MYCN (unigene Hs.25960) F: CCACAAGGCCCTCAGTACC and R: TCCTCTTCATCATCTTCATCATCT; GAP43 (unigene Hs.134974) F: GAGGATGCTGCTGCCAAG and R: GGCACCTTCCTTAGGTTTGGT; ChAT (unigene Hs.302002) F: CAGCCCTGATGCCTTCAT and R: CAGTCTTCGATGGAGCCTGT; SLC18A3 (unigene Hs.654374) F: CCAGCCACTCCTCAACCTT and R: GATATGGAACGGGTCACAGG and R: CCTTGAACACAGTCCGTAGG; ENO2 (Hs.511915) F: ACTTTGTCAGGGACTATCCTGTG and R: TCCCTACATTGGCTGTGAACT; CDK5 (Hs.647078) F: GCGATGCAGAAATACGAGAA and R: CCTTGAACACAGTCCGTAGG; Mycn (Mm.16469) F: CCTCCGGAGAGGATACCTTG and R: TCTCTACGGTGACCACATCG; Myc F: CCTAGTGCTGCATGAGGAGA and R: TCTTCCTCATCTTCTTGCTCTTC; Cdk5 (Mm.298798) F: TGGACCCTGAGATTGTGAAGT and R: GACAGAATCCCAGGCCTTTC. Each experiment was performed in triplicate. The expression data were normalised using the Ct values of GAPDH and TBP.

To validate mRNA levels of genes identified by PCR array, we reverse-transcribed RNA with a High-Capacity cDNA Reverse Transcription Kit (Applied Biosystem) according to the manufacturer's instructions. Equal amounts of cDNA were then subjected to real time PCR analysis with an Applied Biosystems 7900HT thermal cycler, using the 2X RT<sup>2</sup> SYBR Green/ ROX qPCR Master Mix (Qiagen) and specific primers, each at a concentration of 400 nM: E2F1 (PPH00136G; unigene Hs. 654393); E2F3 (PPH00917F; unigene Hs. 269408); CASP9 (PPH00353B; unigene Hs. 329502); FOXO3 (PPH00807A; unigene Hs. 220950); TP63 (PPH01032F; unigene Hs. 137569); TP73 (PPH00725A; unigene Hs. 697294).

### **Cell cycle analysis**

Cell cycle analysis was performed by pulse-chase bromodeoxyuridine (BrdU, Sigma) incorporation and propidium iodide (PI) DNA staining. For BrdU incorporation a pulse of 10  $\mu$ M BrdU was added to the cell culture during the last 30 min before harvesting. Cells were fixed in ethanol 70% at + 4 °C for at least 1 hour, and then processed as previously described (REF Natoli). Primary anti-BrdU (BD Biosciences) and secondary FITC-conjugated F(ab')<sub>2</sub> rabbit anti-mouse IgG (DAKO) antibodies were used to detect the BrdU. Finally, after washing in PBS/BSA 0.5%, cells were stained with a solution containing 5  $\mu$ g/mL PI and 75 KU/mL RNase overnight in dark. For PI staining cells fixed in ethanol 70% for at least 1 hour were stained in a solution containing 50  $\mu$ g/mL PI and 75 KU/mL RNase for at least 30 min in the dark. In each case, 20,000 events per sample were acquired by using a FACScan cytofluorimeter and the CellQuest BD software. BrdU positive cells represent the fraction of the cell population synthesizing DNA. The percentages of the cells in the different cell cycle compartments were estimated on linear PI histograms by using the MODFIT software.

### **Neurite quantification**

After RA treatment, the cells were viewed with a Leica DM IRB inverted phase contrast microscope at 200X. The cells were scored as differentiated if the length of the neurite extensions was at least twice the diameter of the cell body. The neurites were evaluated based on the percentage of cells bearing neurites as determined from the cell culture images, which facilitated tracing the individual neurites and eventual branch points. A total of >300 cells was examined in 5 randomly chosen fields in each treated and untreated sample. The projection images were semiautomatically traced with NIH ImageJ using the NeuronJ plugin. The total dendritic length of each individual neuron was analysed.

### **miRNA Assays**

Equal amounts of RNA were reverse transcribed with the TaqMan® MicroRNA Reverse Transcription Kit (Applied Biosystem), according to the manufacturer's instructions, with a custom 1X RT primer pool (hsa-miR-20a ID 000580; hsa-miR-9 ID 000583; hsa-miR-92a ID 000431). Real time PCR analysis was performed with an Applied Biosystem 7900HT thermal cycler using 20X Individual TaqMan® MicroRNA Assays.

### **miRNA inhibition**

SK-N-AS cells were seeded at a density of  $5 \times 10^4$  cells/cm<sup>2</sup>. After 24h cells were transfected overnight in the presence of 10% FBS, both with mirVana miRNA inhibitors and mirVana miRNA inhibitor Negative Control. Lipofectamine RNAiMAX Reagent (Life Technologies) was used as transfection reagent according to manufacturer's instructions. We transfected hsa-miR-92a (MH10916, ambion), hsa-miR20a (MH10057, ambion) and hsa-miR9 (MH10022, ambion) all together setting a concentration of approximately 10 nM each, in order to obtain the final concentration of 30 nM. The mirVana miRNA inhibitor Negative Control was used to the final concentration of 30 nM. After transfection cells were treated with RA (see Cell line maintenance, differentiation and treatments). Samples were harvested at 24h and 48h to perform mRNA expression analysis and at 48h to detect apoptosis.

### **PCR Array**

RNA was reverse transcribed with a High-Capacity cDNA Reverse Transcription Kit (Applied Biosystem) according to the manufacturer's instructions. Equal amounts of cDNA were then subjected to real time PCR analysis with a Bio-Rad iQ5 thermal cycler. Each sample was mixed with 2X RT<sup>2</sup> SYBR Green/ ROX qPCR Master Mix (Qiagen) and added to each 96-well plate Human p53 Signaling Pathway PCR Array (PAHS-027A; Qiagen), according to the manufacturer's instructions.

### **Apoptosis detection**

Apoptosis was detected in the specific conditions by using Annexin V assay, mitochondrial membrane potential measurement, estimation of sub-G1 fraction. Description of these methods have been detailed in previous papers (Gatti, 2009; Maresca, 2012).

### **MYCN silencing**

Proliferating LAN-5 cells were transfected with a plasmid (pcDNA6.2-GW/EmGFP-miR-MYCN) targeting MYCN mRNA and a non-silencing plasmid (pcDNA6.2-GW/EmGFP-miR-Neg) with no homology to mammalian genes, using Lipofectamine2000 (Life Technologies) according to the manufacturer's instructions. We used 2  $\mu$ g of plasmid. After transfection, the cells were selected with blasticidin for 2 weeks before performing experiments.



**MYCN overexpression.** Proliferating SK-NAS cells were transiently transfected with a plasmid carrying the MYCN construct driven by the CMV promoter or a BlueScript control vector using Lipofectamine2000 (Life Technologies) according to the manufacturer's instructions. We used 2 µg of DNA per sample. At 24h after the transfection, the cells were induced to differentiate by exposure to RA for 3 days using a specific differentiation protocol (see above).

### **Plasma membrane potential analysis**

LAN-5 plasma membrane potential was measured by flow cytometry using the voltage-sensitive fluorescent dye DiOC<sub>5</sub> (Molecular probes). The cells were harvested and washed once in PBS + 0.1 M glucose, and  $1 \times 10^6$  cells were incubated in a solution containing 50 nM DiOC<sub>5</sub> at 37 °C for 15 min. The samples were then washed once in PBS + 0.1 M glucose and immediately assessed by flow cytometry. As a depolarised control, we used a sample post-incubated with the oxidative phosphorylation inhibitor 4-trifluoromethoxyphenylhydrazine (FCCP); as a hyperpolarised control, we used a sample incubated with the potassium-specific transporter valinomycin. Propidium iodide at a final concentration of 10 µg/ml was added to each sample immediately before the measurements to exclude non-viable cells from the analysis. A total of 10,000 events was acquired for each sample using a FACScan cytofluorimeter.

### **Statistical analysis**

Statistical significance of differences between groups was tested by paired Student's t-test or, if there were more than two groups, by one-way ANOVA.

## 2.6 Acknowledgements

I would like to thank all the people that contributed to the realisation of this work published on Cell Death and Disease (doi: 10.1038/cddis.2014.42.), Chiara Cinnella, Marta Nardella, Giovanna Maresca, Alessandra Valentini, Delio Mercanti, Armando Felsani and Igea D'Agnano. I would also like to thank Carla Musa for her support during the preparation of the manuscript.

This work was partially supported by a joint Grant CNR-EBRI “Molecular and cellular mechanisms of brain plasticity” and by PNR-CNR Aging Program 2012-2014.

# Chapter 3

Massive change of transcription profile following activation of the differentiation programme by choline acetyltransferase forced expression in N18TG2 neuroblastoma cells

“In the beginning there is the stem cell”  
**Stewart Sell**

### 3.1 Summary

As previously reported the mouse neuroblastoma N18TG2 clone is defective for biosynthetic neurotransmitter enzymes showing an incapacity to differentiate into neurons. The forced expression of choline acetyltransferase (ChAT) in these cells results in the synthesis and release of ACh and hence in the expression of neurospecific features and markers. To further characterise how the forced expression of ChAT triggered differentiation, we investigated the genome wide expression profiling differences between the N18TG2 cells and its ChAT-transfected derived 2/4 clone. Progression of the neuronal developmental programme in the 2/4 cells was confirmed by the up-regulation of several differentiation-related genes and by the decrease of typical cell cycle-related gene expression. At the same time, we observed a massive reorganisation in cytoskeletal proteins in terms of gene expression, with the particular accumulation of the nucleoskeletal lamina component Lamin A/C in differentiating cells. Our hypothesis is that, as the cytoskeleton needs to be rearranged during neuronal differentiation to guarantee the acquisition of specialised structures such as dendrites and axons, so also the nucleoskeleton must cooperate providing nuclear components that can contact, directly or not, cytoskeletal proteins. These interactions might be crucial in what is known as nucleokinesis during neurons migration and establishment of neurons synapses. Consistently, Lamin A/C knock-down in 2/4 cells led to the down-regulation of specific genes involved in differentiation and axon guidance processes and to the up-regulation of genes known to regulate self-renewal and stemness. This data suggest that Lamin A/C might play a crucial role in the ChAT-dependent molecular differentiation cascade.

### 3.2 Background

Differentiation can be defined as a very “tricky machinery” by which immature cells achieve a more advanced stage of development and, as consequence, a specific function. Particularly, neuronal differentiation is the process through which newly formed neurons acquire specific features, changing their shape, size and molecular composition depending on the function they will acquire. The core of neuron function is their ability to establish specialized contacts (synapsis) with nearby cells and send specific messages through neurotransmitters which differ among different neuronal subtypes. Thus in mature brain, neurotransmitters act as mediators of communication between neurons and target cells; however, neurotransmitter synthesising enzymes and receptors appear at early stages of neurogenesis, before axons reach and establish contacts with their targets (Nguyen, 2001), suggesting that they play a role during the nervous system development. Several evidences show that neurotransmitters act as developmental signals that influence proliferation, differentiation, synapse maturation and neuronal survival during the earliest stages of brain development (Lauder, 1993; Mattson, 1998; Bovetti, 2011). Acetylcholine (ACh) is an ancient signaling molecule, present in bacteria, algae, protozoa, sponge and primitive plants and fungi (Horiuchi, 2003; Wessler and Kirkpatrick, 2008). Since its discovery as neurotransmitter its pleiotropic role as a general signaling system has been suggested as indicated by its synthesis and release in cells other than neurons, e.g. epithelial, endothelial, mesenchymal and immune cells (Ruediger and Bolz, 2007), as well as by the complexity of ACh signaling patterns, downstream nicotinic and muscarinic receptors (Wessler, 2008). The murine neuroblastoma clone N18TG2 defective for biosynthetic neurotransmitter enzymes has been used to elucidate the role of ACh synthesis and release in the advancement of the differentiation program. In 1976, Nelson et al. described the ability of NG108-15 hybrid cells, derived by fusion of mouse neuroblastoma N18TG2 and rat glioma C6BU1 cells, to form synapsis with striated muscle cells, while both N18TG2 and C6BU1 cells lack this capacity. The formation of functional synapsis between the hybrid and muscle cells was accompanied by a remarkable difference in the expression of the choline acetyltransferase (ChAT), active in the hybrid (Hamprecht, 1977) and not in the parental neuroblastoma line. This study suggested the role of acetylcholine in promoting neuron differentiation (Nelson, 1976). Further evidences about the involvement of ACh in neuronal differentiation came from studies showing that the transfection of ChAT cDNA in N18TG2 cells led to the isolation of stable clones with ChAT activity, a consistent ACh synthesis and release and a consequent acquisition of neuron

specific features (Bignami et al., 1997; Biagioni et al., 2000; De Jaco et al., 2002; Salani et al., 2009).

In this study, we investigated the effects induced by ChAT transfection in the N18TG2 neurotransmitter-defective neuroblastoma cells on whole genome-wide profile expression. The rescue of the ability to synthesise and release the neurotransmitter in ChAT-expressing 2/4 clone induced a massive modulation of gene expression, including genes involved in proliferation, cell differentiation and cytoarchitecture rearrangements. Interestingly, among the genes specifically up-regulated in the ChAT-expressing clone, we also identified genes related to nuclear envelope functionality. In particular, the nuclear lamina component Lamin A/C was induced in ChAT-expressing 2/4 clone and appeared to have a role in cytoskeletal changes and differentiation processes. Nuclear lamins are intermediate filament (IF) proteins that were originally identified as components of nuclear lamina, providing structural support and organisation to the nuclear envelope (Aebi et al., 1986; Sullivan et al. 1999). However, in 2006 Constantinescu and colleagues clearly demonstrated how Lamin A/C could be considered as a marker of mouse and human embryonic stem cell differentiation suggesting that this protein is not simply a structural and scaffolding protein. In addition, more recently, Maresca and colleagues (2012) have pointed out that LMNA knock-down affect neuronal differentiation in neuroblastoma cells.

### 3.3 Results

#### 3.3.1 The transcription profile of the 2/4 clone shows extensive modifications by comparison with the N18TG2 parental cell line

We performed a microarray analysis of untreated cells (CTR) and RA treated cells during a four-day culture period to evaluate the effects on gene expression due to the synthesis and release of ACh in 2/4 cells with respect to N18TG2 parental cells (Figure 1).

From the whole microarray, containing ~ 60,000 probes, a total number of 13744 transcripts were fished out for the analysis, setting a fluorescent expression threshold  $> 100$ . The experiment was performed in duplicate allowing us to filter out  $\text{Log}_2$  intensity values with a coefficient of variation (CV)  $> 2.0$  avoiding the introduction of biases in further analysis.

Figure 1a reports the number of transcripts analysed in total and in each conditions: N18TG2 untreated (CTR) and RA-treated (RA), as well 2/4 untreated (CTR) and RA-treated (RA). The intersections of the Venn diagram represents common analysed transcripts within categories.

The hierarchical cluster analysis was carried out on normalised data (aligned to 75<sup>th</sup> percentile). As expected, 2/4 cells tended to cluster at the opposite extremes of the clustering pattern displaying their ability to respond to RA treatment and activate differentiation programme. On the other hand, also N18TG2 cells displayed differences but they turned to cluster together at the centre of the clustering pattern. This indicates that the 2/4 cell line was more affected by the differentiation stimulus triggered with RA than the parental cell line N18TG2, thus confirming the ability of ChAT-transfected derived clone to be committed to a more mature phenotype (Figure 1b).

These data suggested that the 2/4 cell line underwent an outstanding regulation of a massive numbers of transcripts following RA acid treatment. Interestingly, this modulation is mainly due to the restored production of ACh and, consequently, stimulation of ACh receptors in these cells since they originally shared the same genetic background with the parental cell line N18TG2.

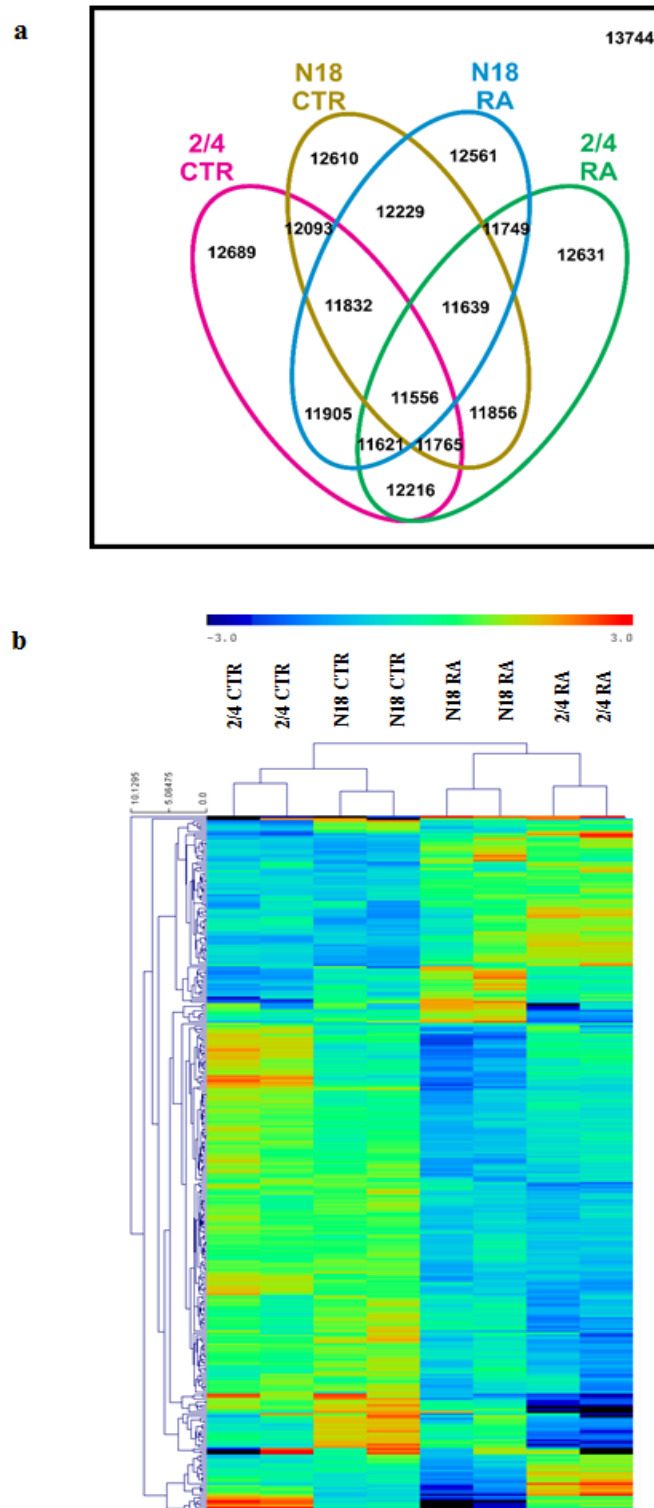


**Figure 1. Microarray total transcripts analysis and clustering** **a)** Venn diagram of the total number of transcripts analysed and their intersections in the four experimental conditions: N18TG2 (named N18) untreated (CTR) and RA-treated (RA), 2/4 untreated (CTR) and RA-treated (RA). Transcripts were fished out from a total of ~60K probes setting a threshold of minimum fluorescence signal  $> 100$ . **b)** Hierarchical clustering of samples, using Euclidean distance metric and average linkage clustering. We show the RNAs differential both for 2/4 cells and N18TG2 cells (named N18). Log<sub>2</sub> data normalised to the 75th percentile were used and each gene was centered to its mean value.



### 3.3.2 ChAT forced exogenous expression modifies cell cycle and neuronal differentiation regulation

As a first approach we decided to compare transcription profile of N18TG2 and 2/4 cells after RA treatment to investigate the different ability of these two cell lines to be responsive to differentiation stimuli. Figure 2a shows the Venn diagrams of the down- and up-regulated RNAs after RA treatment. Both cell lines exhibited changes of their gene expression profile. Despite in both cell lines RA induced modifications, the number of down- and up-regulated RNAs resulted significantly different, with only 171 common down-regulated transcripts and 76 common up-regulated transcripts between N18TG2 and 2/4 cells. 1345 and 520 were the differentially down-regulated transcripts for 2/4 and N18TG2, respectively. At the same time 651 RNAs were up-regulated in 2/4 cells against 334 up-regulated RNAs in N18TG2. Taken together these numbers suggested 2/4 cells to be more sensitive to the presence of RA. To investigate which pathways and cellular mechanisms were triggered, DAVID Bioinformatics Database was used to perform a functional analysis of both common and differential genes lists. Figure 3 and Figure 4 show selected categories of DAVID analysis of genes regulated in N18TG2 and 2/4 cells after RA treatment and the corresponding Enrichment score and P-value. Genes belonging to common categories were related to the known ability of RA to promote transcription of Hox genes (Dupe and Lumsden, 2001), group of genes that control the body plan of the embryo along the anterior-posterior axis, or to regulate metabolic processes (Brun, 2013). Most interestingly, differential categories revealed how specifically 2/4 were affected by the presence of RA in the modulation of cell cycle and neuronal differentiation (Figure 4, *second and fourth tables*). Mitotic cell cycle and related processes, such as chromosome condensation, spindle formation and DNA replication were down-regulated, whereas neuron projection and synapse formations as well as transmission of nerve impulse were promoted in 2/4 cells. Surprisingly, neurogenesis and changes in the cytoskeletal architecture of cells were inhibited in N18TG2 RA-treated parental clone (Figure 4, *first table*). We then analysed transcripts modulation in 2/4 CTR and RA-treated cells compared to N18TG2 cells in the same conditions, respectively. We identified 659 down-regulated and 884 up-regulated shared mRNAs between 2/4 CTR and RA-treated. 350 and 3292 genes were differentially down-regulated in 2/4 CTR and RA-treated cells, respectively. Moreover, 2/4 CTR cells showed 538 differentially up-regulated transcripts against the 1115 specifically expressed only in 2/4 RA-treated cells. Once again, 2/4 RA-treated cells appeared to be more prone to gene expression changes in the presence of a differentiation stimulus.

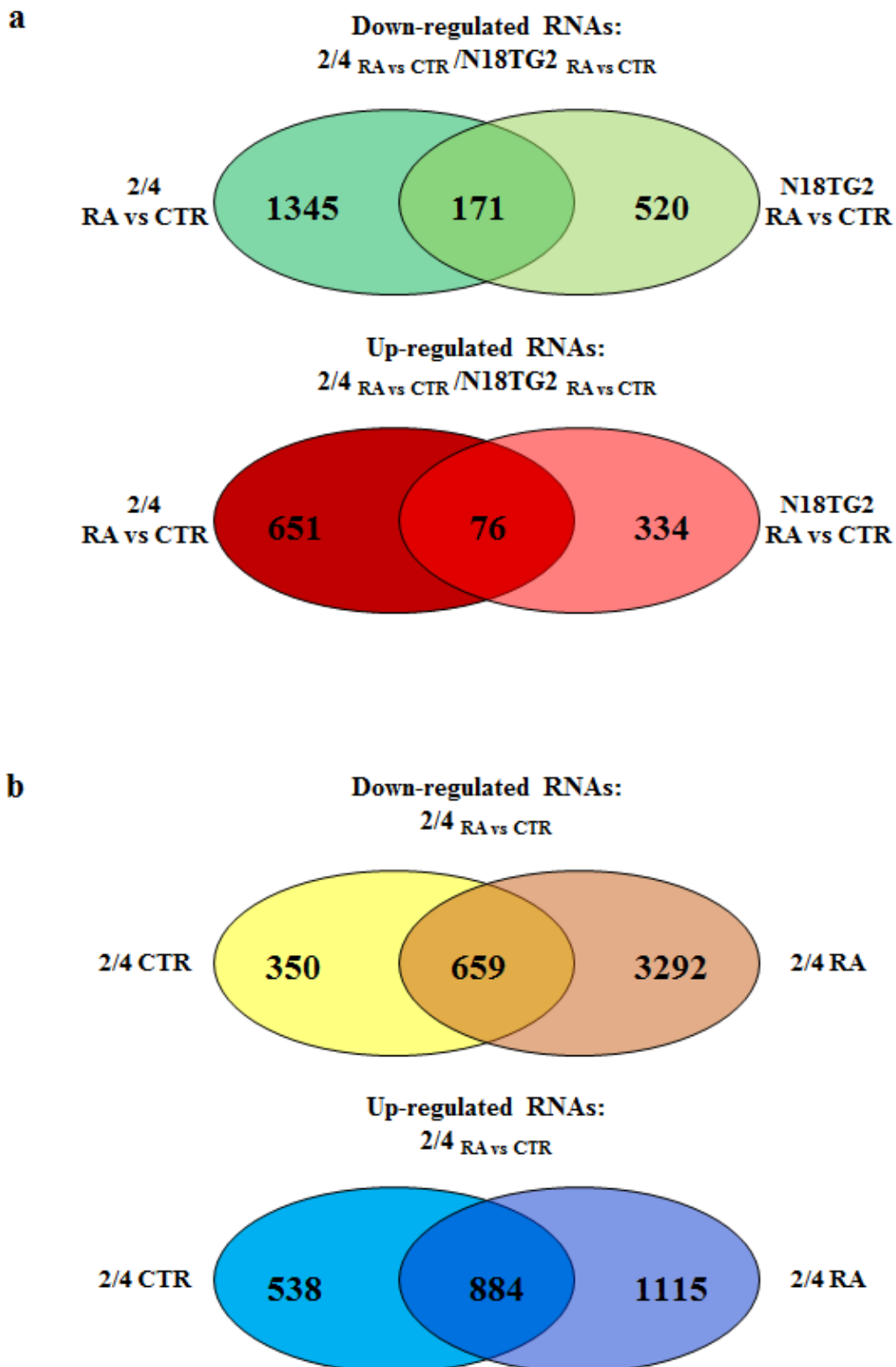


**Figure 2.** Common and differentially expressed RNAs in  $2/4_{RA\ vs\ CTR} / N18TG2_{RA\ vs\ CTR}$  and  $2/4_{RA\ vs\ CTR}$  a) Common and differentially expressed RNAs in  $2/4$  and N18TG2 cells obtained comparing RA samples to untreated (CTR) samples across cell lines and then comparing selected RNAs, with a minimum 2.0 fold change ratio in linear scale, between cell lines. b) Common and differentially expressed RNAs in  $2/4$  untreated (CTR) and RA-treated cells. Only RNAs with a minimum 2.0 fold change ratio in linear scale were selected.

**Common categories 2/4<sub>RA vs CTR</sub> /N18TG2<sub>RA vs CTR</sub> Down**

Enrichment Score	Term	P-value
2.594	GO:0055114~oxidation reduction	0.001266
2.039	GO:0000786~nucleosome	8.09E-05
1.392	IPR013091:EGF calcium-binding	0.012449
1.341	GO:0006631~fatty acid metabolic process	0.011534

**Common categories 2/4<sub>RA vs CTR</sub> /N18TG2<sub>RA vs CTR</sub> Up**

Enrichment Score	Term	P-value
1.347	GO:0048598~embryonic morphogenesis	0.021891

**Figure 3. Selected common DAVID categories in 2/4<sub>RA vs CTR</sub> /N18TG2<sub>RA vs CTR</sub> and 2/4<sub>RA vs CTR</sub>** *First table:* common categories generated with the list of down-regulated RNAs in 2/4 RA-treated cells comparing to N18TG2 RA-treated cells. *Second table:* common categories generated with the list of up-regulated RNAs in 2/4 RA-treated cells comparing to N18TG2 RA-treated cells. For each category Enrichment score and P-value are reported. Categories with an Enrichment Score < 1.3 and P-value > 0.05 were filtered out from further analysis.

**Differential categories 2/4<sub>RA vs CTR</sub> /N18TG2<sub>RA vs CTR</sub> Down in N18**

Enrichment Score	Term	P-value
2.230	GO:0008092~cytoskeletal protein binding	9.96E-04
2.011	GO:0051493~regulation of cytoskeleton organization	4.49E-05
1.459	SP_PIR_KEYWORDS~neurogenesis	0.006276
1.326	GO:0008360~regulation of cell shape	0.01706

**Differential categories 2/4<sub>RA vs CTR</sub> /N18TG2<sub>RA vs CTR</sub> Down in 2/4**

Enrichment Score	Term	P-value
19.359	GO:0000278~mitotic cell cycle	6.51E-22
11.533	GO:0000779~condensed chromosome, centromeric region	2.32E-12
3.205	GO:0005819~spindle	9.86E-07
1.868	SP_PIR_KEYWORDS~dna replication	0.003056
1.452	IPR000789:Cyclin-dependent kinase, regulatory subunit	0.006829

**Differential categories 2/4<sub>RA vs CTR</sub> /N18TG2<sub>RA vs CTR</sub> Up in N18**

Enrichment Score	Term	P-value
1.794	GO:0031669~cellular response to nutrient levels	0.004082
1.549	GO:0006350~transcription	0.002007
1.413	mmu03040:Spliceosome	0.007983
1.379	GO:0051028~mRNA transport	0.035424

**Differential categories 2/4<sub>RA vs CTR</sub> /N18TG2<sub>RA vs CTR</sub> Up in 2/4**

Enrichment Score	Term	P-value
3.027	GO:0043005~neuron projection	1.40E-05
2.616	GO:0045202~synapse	9.97E-05
2.123	GO:0019226~transmission of nerve impulse	1.31E-04
1.762	GO:0006928~cell motion	8.16E-04

**Figure 4.** Selected differential DAVID categories in 2/4<sub>RA vs CTR</sub> /N18TG2<sub>RA vs CTR</sub> and 2/4<sub>RA vs CTR</sub> *First table and second table:* differential categories generated with the list of down-regulated RNAs in 2/4 RA-treated cells comparing to N18TG2 RA-treated cells. *Third and fourth table:* differential categories generated with the list of up-regulated RNAs in 2/4 RA-treated cells comparing to N18TG2 RA-treated cells. For each category Enrichment score and P-value are reported. Categories with an Enrichment Score < 1.3 and P-value > 0.05 were filtered out from further analysis.

The study of the differential categories emerged from the comparison of untreated and treated cells unveiled how, even in the absence of RA, 2/4 cells are characterised by a less proliferative inclination (Figure 6, *first table*) and at the same time by the ability to promote cytoskeletal rearrangements, normally required for neurons differentiation. However, the changes in terms of axonogenesis, synapse formation and cell cycle deregulation were induced also by the presence of RA (figure 6, *third and fourth tables*), confirming the ability of these cells to respond to differentiation stimuli.

qPCR was used to validate microarray results. We selected 12 genes, which could be considered as representative of the main clusters identified by DAVID Database. Figure 7 reports the fold change values (Log scale) of the selected genes, in 2/4 clone compared to N18TG2 cells in the absence (CTR; Figure 7a) or in the presence of retinoic acid treatment (RA; Figure 7b). qPCR and microarray data were compared and results are shown in Figure 7c: the box plot displays the correlation of the fold change values originated by the microarray and the qPCR experiments. Consistently with microarray analysis, we observed a down-regulation of those genes involved in proliferation (Ccn3, Rb1, Lef1) and stemness (Nestin and Prominin1) and an up-regulation of differentiation-related genes (Cdk5, Cend1, Nav1, Rab6b, Syn1, Syn2 and Tubb3) both in untreated and RA-treated cells. As far as 2/4 cells, RA treatment only enhanced the expression changes of genes related with cell cycle exit and neuronal differentiation, compared with 2/4 untreated cells (Figure 7a and 7b).

The analysis of cell cycle and neurite outgrowth in 2/4 cells strongly supported gene expression profiling results. In fact, in the 2/4 clone, cell cycle analysis revealed a significant increase of the G0/G1 phase percentages with a concomitant reduction of the S and G2-M phase percentages compared with the N18TG2 cells (Figure 8a). RA did not produce a significant effect on cell cycle phases distribution in N18 cells while, 2/4 clone showed a decrease of S-phase population after RA treatment (data not shown). Western blot analysis of CycA and p27 proteins confirmed FACS data, showing an up-regulation of CycA and a down-regulation of p27 in N18TG2 cells (Figure 8b). As previously reported (Salani et al, 2009), 2/4 cells appeared to extend longer neurites and form more complex neurite networks than N18TG2 cells following both in untreated (CTR) and RA conditions (Figure 8c). RA treatment induced the expression of the characteristic marker of neuronal differentiation NF200 in the 2/4 clone (Figure 8d).

**Common categories 2/4<sub>RA vs CTR</sub> Down**

Enrichment Score	Term	P-Value
1.607	GO:0007049~cell cycle	4.64E-04
1.575	GO:0000279~M phase	0.00633
1.460	mmu04120:Ubiquitin mediated proteolysis	0.001342

**Common categories 2/4<sub>RA vs CTR</sub> Up**

Enrichment Score	Term	P-Value
3.080	GO:0045202~synapse	7.92E-05
2.706	GO:0031175~neuron projection development	5.71E-05
2.278	GO:0007010~cytoskeleton organization	0.001846
2.232	GO:0008092~cytoskeletal protein binding	8.09E-05
1.907	GO:0006887~exocytosis	0.004293
1.762	SP_PIR_KEYWORDS~microtubule	4.22E-04
1.442	GO:0008021~synaptic vesicle	7.23E-05

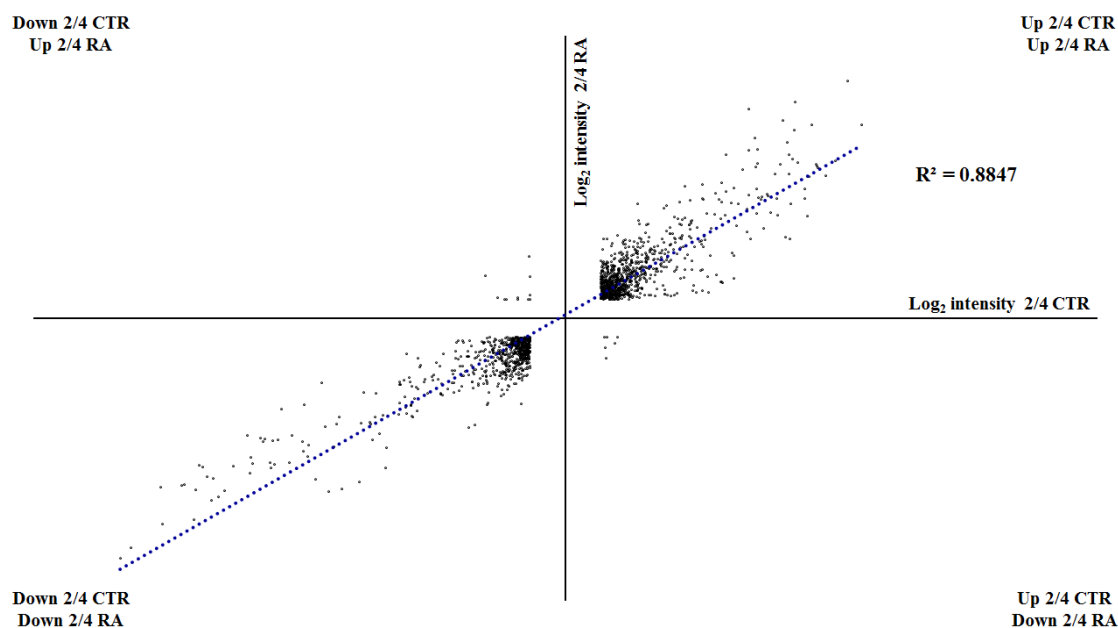


**Figure 5. Selected common DAVID categories in 2/4<sub>RA vs CTR</sub>** *First table:* common categories generated with the list of down-regulated RNAs in 2/4 RA-treated cells comparing to 2/4 untreated cells (CTR). *Second table:* common categories generated with the list of up-regulated RNAs in 2/4 RA-treated cells comparing to 2/4 untreated cells (CTR). For each category Enrichment score and P-value are reported. Categories with an Enrichment Score < 1.3 and P-value > 0.05 were filtered out from further analysis. *Lower panel:* correlation plot between Log<sub>2</sub> intensity fluorescence values of 2/4 cells transcripts in untreated (CTR) and RA-treated conditions. Uniquely genes belonging to common categories were considered. R<sup>2</sup> was generated by Excel and is displayed in the graph.

**Differential categories 2/4<sub>RA vs CTR</sub> Down in CTR**

Enrichment Score	Term	P-Value
1.665	GO:0002009~morphogenesis of an epithelium	0.00297
1.644	mghPathway:Growth Hormone Signaling Pathway	0.010134
1.522	mmu04010:MAPK signaling pathway	3.53E-06
1.489	GO:0030335~positive regulation of cell migration	0.014752

**Differential categories 2/4<sub>RA vs CTR</sub> Up in CTR**

Enrichment Score	Term	P-Value
2.428	GO:0031967~organelle envelope	1.61E-04
2.323	GO:0044430~cytoskeletal part	7.72E-04

**Differential categories 2/4<sub>RA vs CTR</sub> Down in RA**

Enrichment Score	Term	P-Value
29.338	SP_PIR_KEYWORDS~cell cycle	2.87E-35
18.753	GO:0005694~chromosome	6.97E-31
3.916	SP_PIR_KEYWORDS~translocation	4.29E-07

**Differential categories 2/4<sub>RA vs CTR</sub> Up in RA**

Enrichment Score:	Term	P-Value
2.537	GO:0031175~neuron projection development	2.38E-04
2.446	GO:0045202~synapse	1.22E-06
2.024	GO:0005938~cell cortex	3.57E-05
1.877	GO:0030427~site of polarized growth	0.003694
1.383	GO:0050770~regulation of axonogenesis	0.004676

**Figure 6.** Selected differential DAVID categories in 2/4<sub>RA vs CTR</sub> Differential categories generated with the list of modulated RNAs in 2/4 RA-treated cells comparing to 2/4 untreated cells (CTR). Categories are shown according to their down- or up-regulation in CTR cells (*first* and *second table*, respectively) and in RA-treated cells (*third* and *fourth table*, respectively). For each category Enrichment score and P-value are reported. Categories with an Enrichment Score < 1.3 and P-value > 0.05 were filtered out from further analysis.

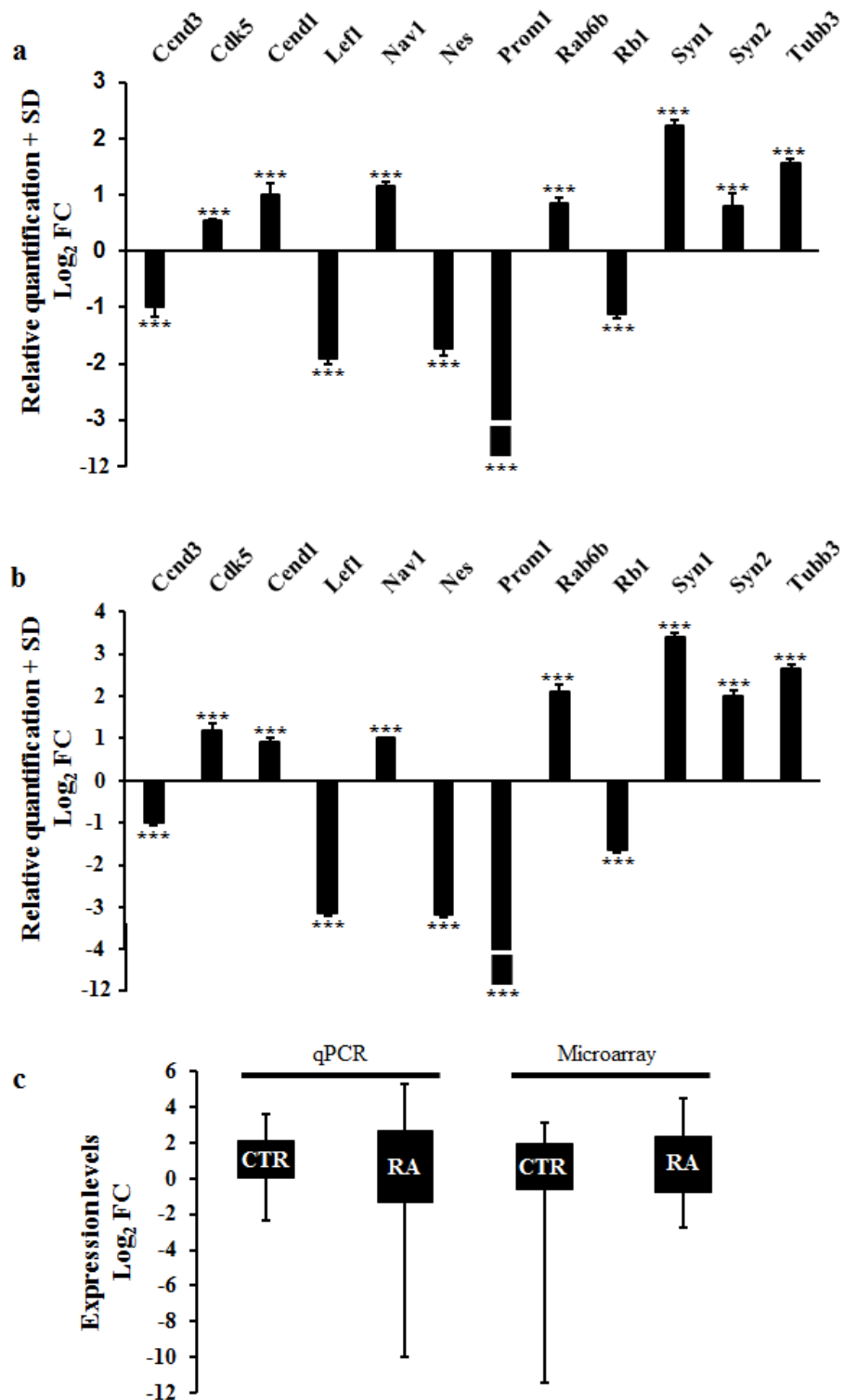


**Figure 7. qPCR microarray data validation** **a)** Levels of the indicated mRNA in 2/4 cells untreated (CTR) cells. The data are reported as the level of mRNA relative to the respective N18TG2 untreated (CTR) cells (0,  $x$  axis) and are the mean + SD ( $n = 3$ ). Statistical significance,  $***p \leq 0.001$ . **b)** Levels of the indicated mRNA in 2/4 cells RA-treated (RA) cells. The data are reported as the level of mRNA relative to the respective N18TG2RA-treated (RA) cells (0,  $x$  axis) and are the mean + SD ( $n = 3$ ). Statistical significance,  $***p \leq 0.001$ . **c)** Box plot of Log<sub>2</sub> FC data comparison between qPCR and microarray transcripts values presented in **a** and **b** bar plots, showing the correlation obtained using the two different techniques.



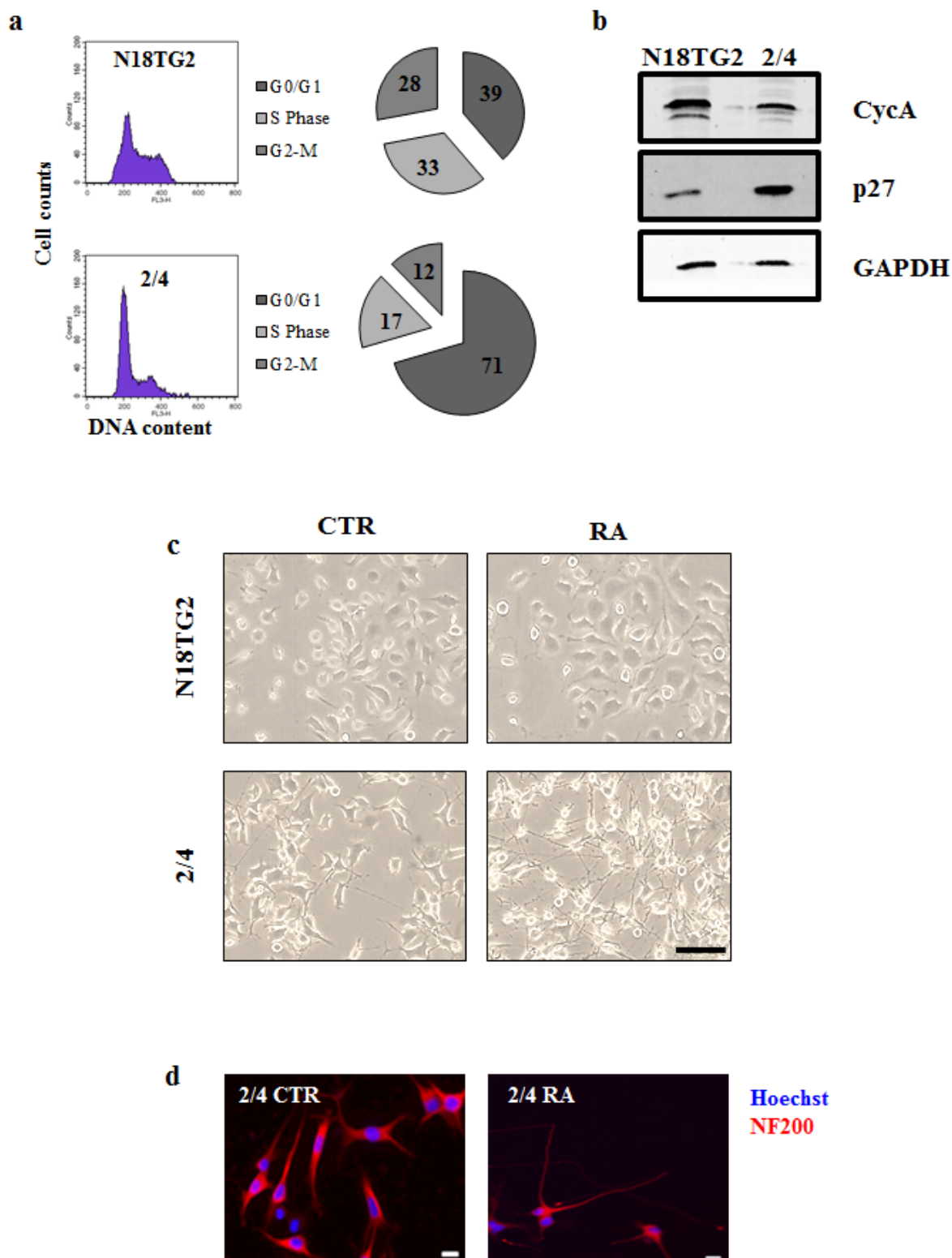


**Figure 8. RA treatment induces proliferation and differentiation changes in 2/4 cells** **a)** Cell cycle FCM analysis of N18TG2 and 2/4 cells in untreated conditions. Cell cycle-phases percentages are reported for each graph. **b)** Representative blots of the CycA and p27 proteins in N18TG2 and 2/4 cells in untreated conditions. **c)** Inverted light microscopic images of N18TG2 and 2/4 cells untreated (CTR) or RA-treated (RA) for 3 days of RA. Scale bar, 50 $\mu$ m. **d)** Representative fluorescence images of 2/4 cells untreated (CTR) or RA-treated (RA) for 3 days. Red, NF200 immunostaining; blue, Hoechst staining. Merge images are shown. Scale bar, 50 $\mu$ m.

### 3.3.3 Lamin A/C is specifically up-regulated after ChAT transfection in 2/4 cells

Among the gene categories which appeared to be specifically up-regulated in 2/4 clone compared to N18TG2 cells we identified in particular one category named GO:0031967~organelle envelope. This category emerged as a result of a group of genes related to nucleus functionality. In particular, Lamin A transcripts exhibited an up-regulation in 2/4 cells compared to N18TG2 cells in untreated conditions. The large number of genes implicated in the processes activated by ChAT transfection, which also makes cell more responsive to RA, indicates a consistent rearrangement of gene expression and poses the question of the mechanisms and factors involved in this processes. Several studies demonstrated that nuclear lamins are directly involved in the regulation of multiple cellular processes (Wilson and Foisner, 2010). We then decided to investigate the expression pattern of the two main nuclear lamina components Lamin A/C and Lamin B in both N18TG2 and 2/4 cells. Interestingly, we observed a specific up-regulation of Lamin A/C in 2/4 clone in untreated and RA-treated conditions. Immunofluorescent images reported in Figure 9 clearly show Lamin A/C nuclear localization only in 2/4 clone, with no significant signal increase after the treatment with RA; whereas nuclear localization for Lamin B can be observed in both cell types and in both conditions. Western blot analysis revealed a significant up-regulation of Lamin A/C in 2/4 cells compared to N18TG2 cells; RA treatment further increased the expression levels of Lamin A/C in 2/4 cells (Figure 10). On the other hand, Lamin B showed no significant expression changes in both cell lines, even after RA treatment (Figure 10).

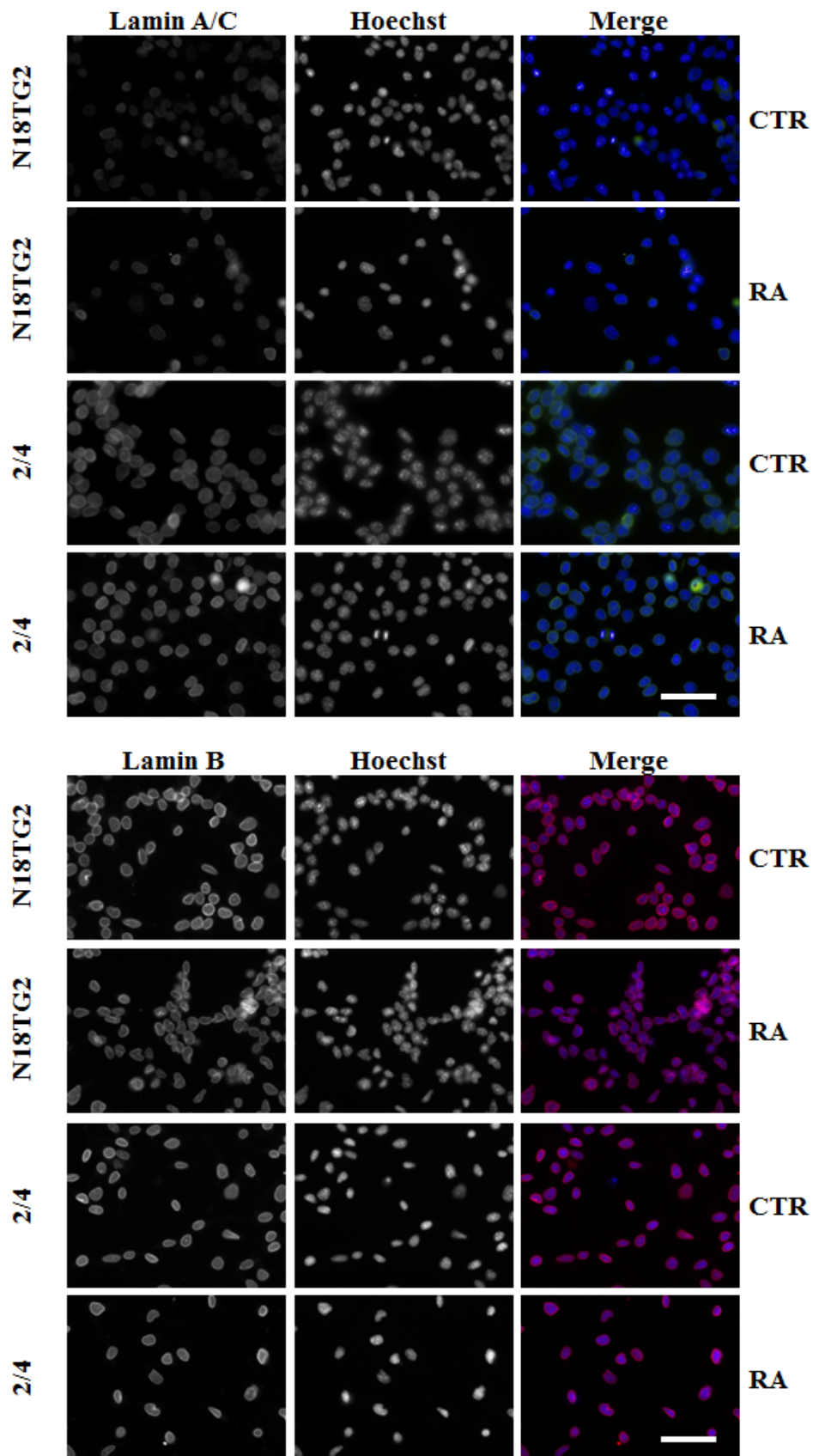


**Figure 9. Lamin A/C increases in 2/4 cells** Representative fluorescence images of N18TG2 and 2/4 cells both in untreated (CTR) or RA-treated (RA) conditions for 3 days. *Right-upper panels*, Lamin A/C immunostaining; *right-lower panels*, Lamin B immunostaining; *middle panels*, Hoechst; *left panels*, merge. Scale bar, 50 $\mu$ m.

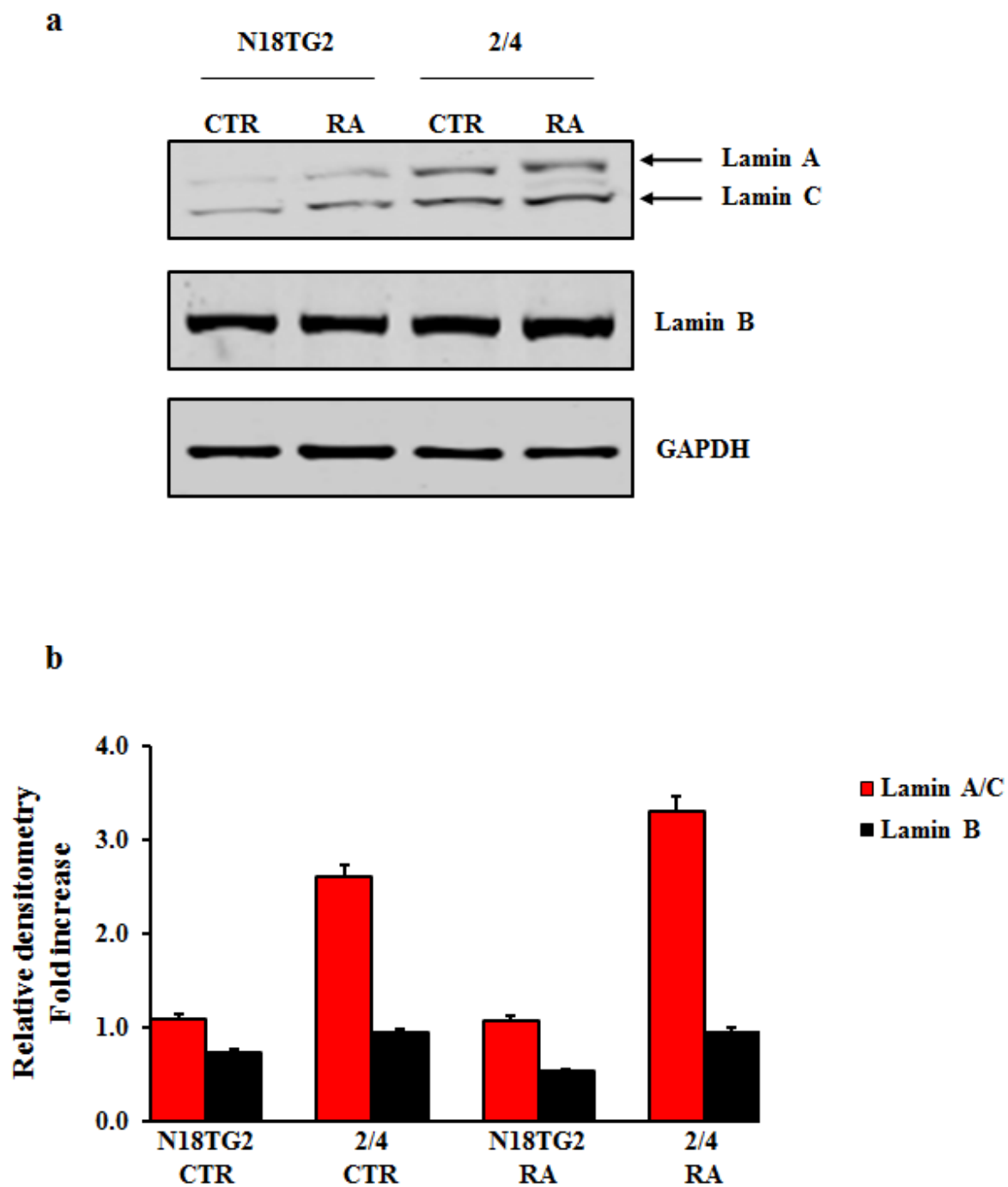


**Figure 10. Lamin A protein is up-regulated the most in 2/4 cells** *Upper panel*, representative blots of the Lamin A/C and Lamin B proteins in N18TG2 and 2/4 cells untreated (CTR) or RA-treated (RA) for 3 days. *Lower panel*, blots relative densitometry as analysed by ImageJ software. Values are the mean  $\pm$ SD of three independent experiments. GAPDH expression was used to normalize protein loading.

### 3.3.4 Acetylcholine receptor agonist and antagonist modulate Lmna expression in N18TG2 and 2/4 cells

N18TG2 cells are defective for the production of choline acetyltransferase and hence for the synthesis of ACh; however, similarly to 2/4 cells, express acetylcholine receptors. Lamin A/C appeared to be significantly expressed in ChAT-transfected cells, also in absence of RA, suggesting a possible role of ACh receptors pathways in the expression of this protein. To determine if ACh receptors stimulation could induce Lamin A/C expression, we stimulated N18TG2 cells with the well-known ACh analogue and cholinergic agonist carbachol. We performed a carbachol treatment kinetics and observed an up-regulation of Lmna gene since the first hour of stimulation. Levels of Lmna mRNA continued to increase up to 6h and 12h of treatment (Figure 11, *left-upper panel*). The gene transcription activation following the agonist kinetics in N18TG2 is specifically restricted to Lamin A/C nuclear envelope protein since Lmnb1 and Lmnb2 genes were not induced in N18TG2 cells after carbachol treatment (Figure 11, *left-middle and left-lower panel*). Consistently with the agonist treatment, the muscarinic receptor antagonist atropine down-regulates Lmna transcript in 2/4 cells (Figure 11 *middle-upper panel*). However, the nicotinic receptor antagonist mecamylamine did not influence the expression of either Lmna or Lmnb genes in 2/4 clone (Figure 11, *right panels*). This observation suggests a specific role of acetylcholine muscarinic receptors and not of nicotinic receptors in the increase of Lamin A/C expression in 2/4 clone.

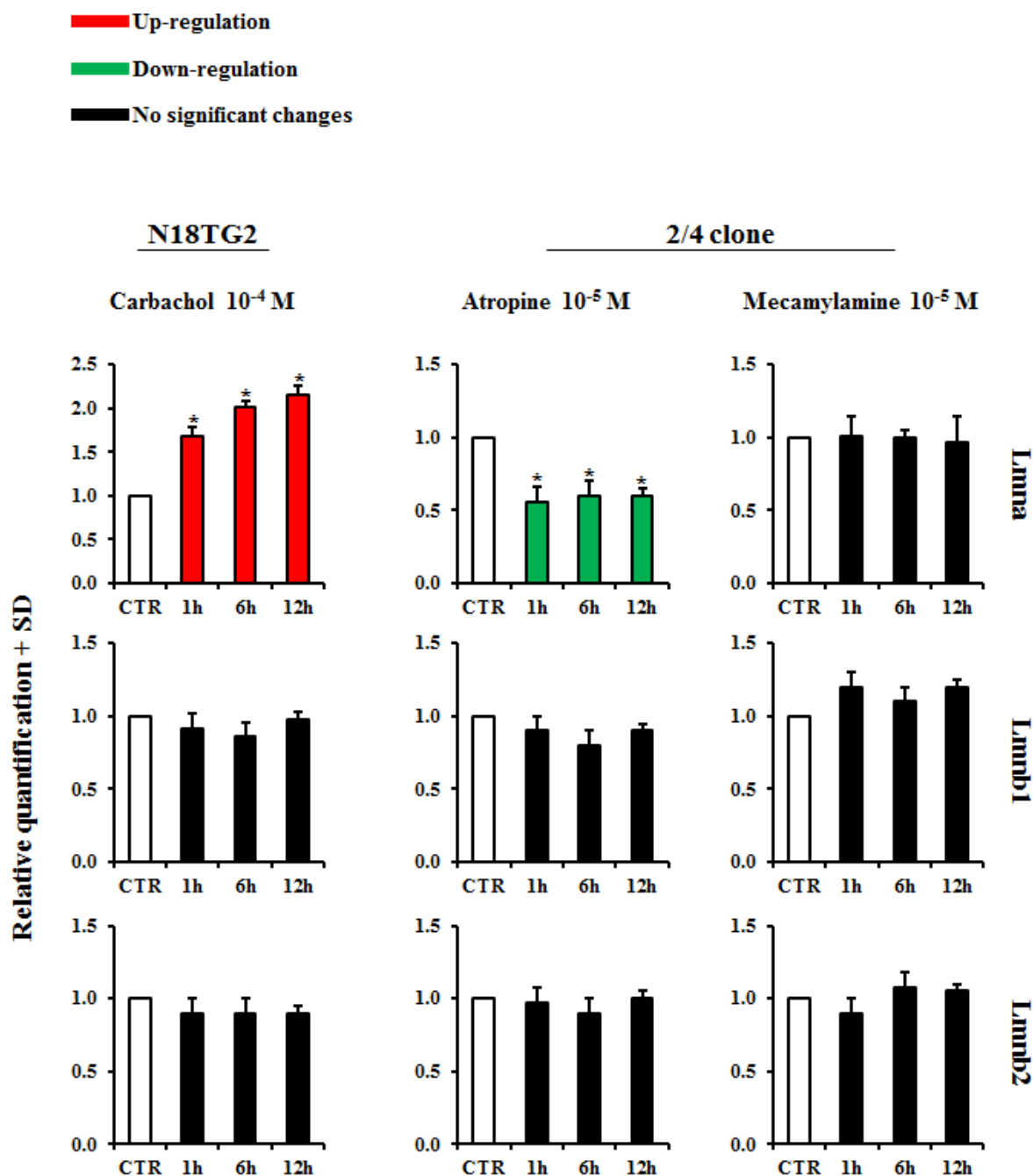


**Figure 11. Muscarinic receptors control *Lmna* expression in 2/4 cells** *Right panels*, levels of the indicated mRNA in N18TG2 cells treated with carbachol  $10^{-4}$  M for 1, 6 and 12 hours. The data are reported as the level of mRNA relative to the respective N18TG2 untreated (CTR) cells and are the mean + SD ( $n = 3$ ). Statistical significance,  $*p \leq 0.05$ . *Middle and left panels*, levels of the indicated mRNA in 2/4 cells treated with atropine and mecamylamine  $10^{-5}$  M, respectively, for 1, 6 and 12 hours. The data are reported as the level of mRNA relative to the respective 2/4 untreated (CTR) cells and are the mean + SD ( $n = 3$ ). Statistical significance,  $*p \leq 0.05$ .

### 3.3.5 Lamin A/C interactomics network and forced knock-down suggest an involvement of this nuclear envelope protein in ChAT-dependent differentiation cascade

We performed an interactomics study using the Cognoscente web tool to visualise all the known Lamin A/C-interacting proteins (Figure 12a). To investigate the interactomics network of Lamin A/C protein and maximise the search space, we carried out the analysis using a threshold Radius = 2 (see Materials and Methods). Moreover, the analysis was specifically restricted to the *Mus musculus* taxonomic category. We found that 24 of the interactors displayed in the generated network were at the same time up-regulated specifically in 2/4 cells in the microarray data and play an important role in cytoarchitecture regulation (Figure 12b), thus suggesting Lamin A/C might be involved in the network/pathway rearrangements of the cyto- and nucleo-skeleton during differentiation.

We then silenced *Lmna* gene in 2/4 cells. We obtained a 90% down-regulation of *Lmna* mRNA and a 40% Lamin A/C protein decrease after 24h and 48h of siRNA silencing (Figure 13, a and b). The siRNA knock-down of *Lmna* gene in differentiating cells further highlight the importance of the interaction of Lamin A/C with cytoskeletal-regulating proteins such as, CDK5 and Nav1. Additionally, it confirmed an intimate correlation between Lamin A/C expression, expression of differentiation-related genes (*Cdk5*, *Cend1*, *Nav1*, *Syn1* and *Syn2*) and negative modulation of proliferation/stemness genes (*Lef1* and *Prom1*) (Figure 13c). We also analyzed the mRNA levels of *Ccnd3*, *Nes*, *Rab6b*, *Rb1* and *Tubb3* after *Lmna* gene knock-down, but we did not observe any significant alteration of their expression (data not shown).

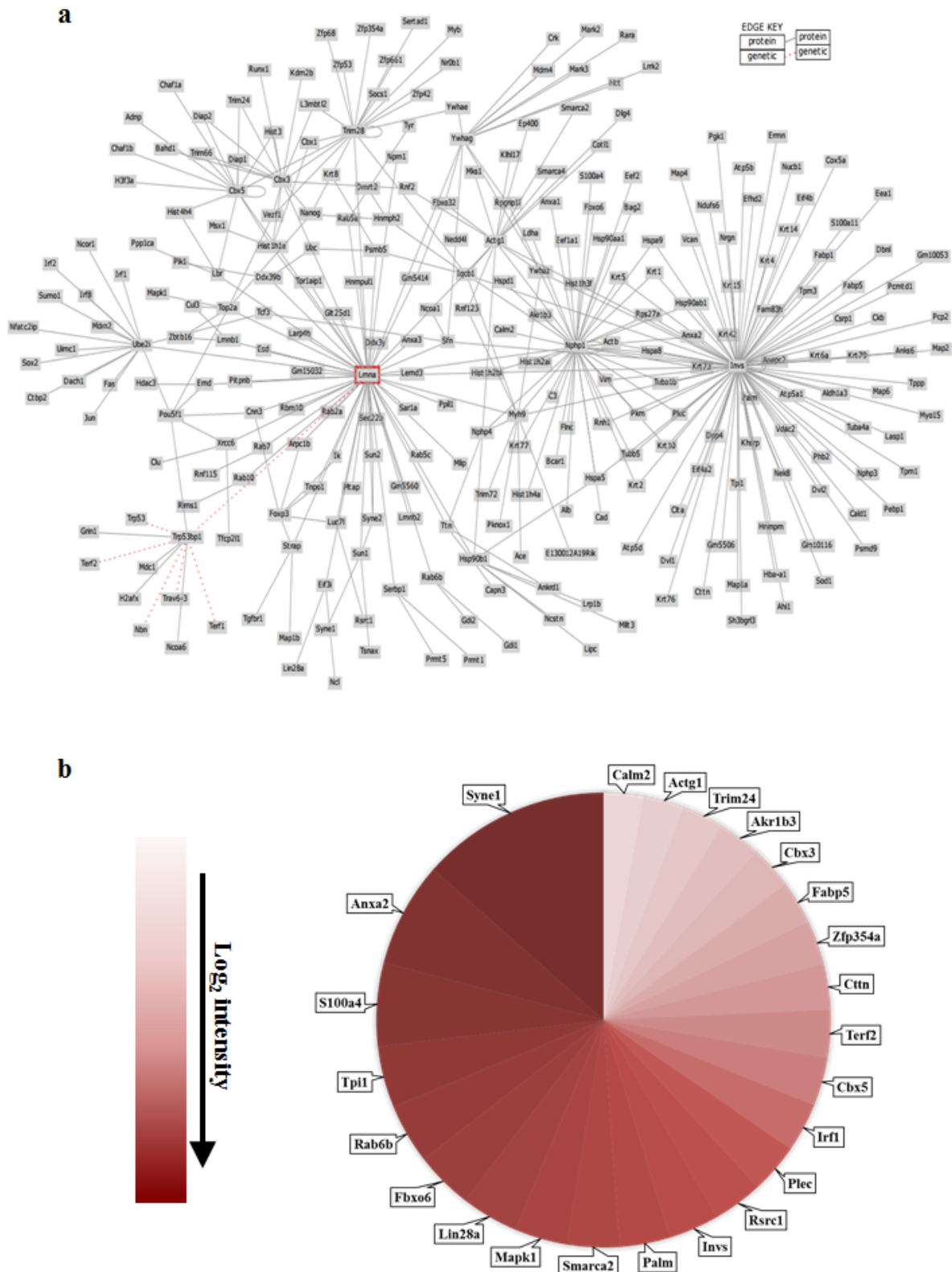


**Figure 12. Lmna gene interactomics network** **a)** Interactomics network of Lmna gene generated with Cognoscente database. The query gene (Lmna) is indicated with red line. Grey connections represent known protein-protein interactions; red-dotted connections represent known protein-gene interactions. **b)** Pie chart of the Lamin A/C interactors up-regulated in 2/4 cells. Genes are shown according to their  $\text{Log}_2$  intensity ascending order going from light to dark colour.



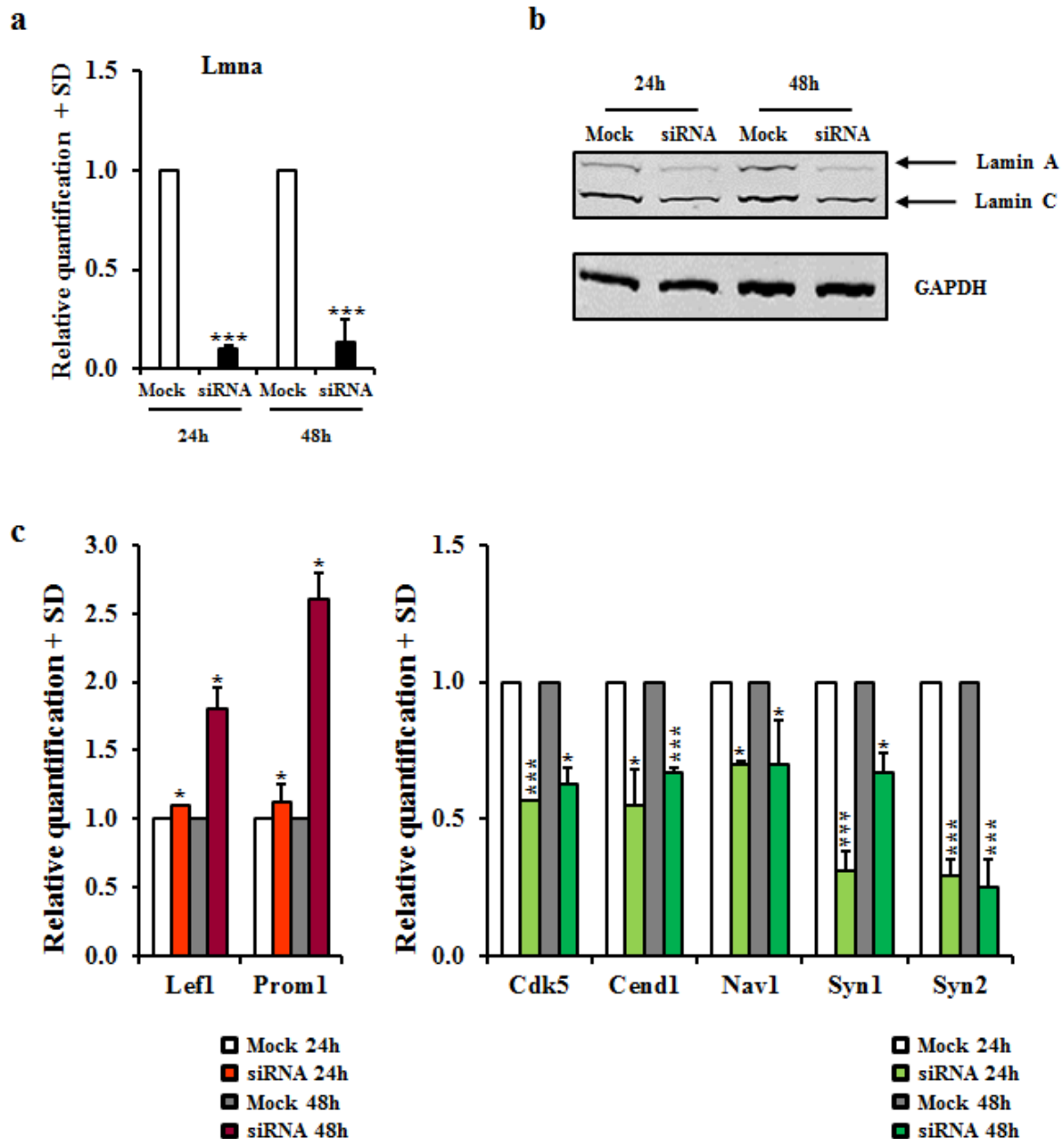


**Figure 13. Lmna gene silencing in 2/4 cells affects stemness and differentiation** **a)** Levels of the Lmna mRNA in 2/4 cells transfected with the siRNA Silencer Select for 24 and 48 hours. The data are reported as the level of mRNA relative to the respective 2/4 cells transfected with the siRNA Silencer Select Negative Control (Mock) and are the mean + SD ( $n = 3$ ). Statistical significance,  $***p \leq 0.001$ . **b)** Representative blots of the Lamin A/C protein in 2/4 cells transfected with the siRNA Silencer Select Negative Control for 24 hours (Mock 24h), 48 hours (Mock 48h) and with the siRNA Silencer Select for 24 hours (siRNA 24h), 48 hours (siRNA 48h). GAPDH expression was used to normalise protein loading. **c)** Levels of the indicated mRNA in 2/4 cells transfected with siRNA Silencer Select for 24 hours (*left panel*, light red bars; *right panel*, light green bars) and 48 hours (*left panel*, dark red bars; *right panel*, dark green bars). The data are reported as the level of mRNA relative to the respective 2/4 cells transfected with the siRNA Silencer Select Negative Control for 24 hours (white bars) and for 48 hours (grey bars) and are the mean + SD ( $n = 3$ ). Statistical significance,  $*p \leq 0.05$ ;  $***p \leq 0.001$ .

### 3.4 Conclusions

Increasing evidences from different experimental models suggest that neurotransmitters play an important role during nervous system development. In fact, they are detected at early stages of neurogenesis before synapse formation meaning that they take part in alternative functions before acting as signal molecules in neurotransmission (Biagioni, 2000). In this scenario, ACh has been extensively studied both for its neurotransmitter and non-neurotransmitter role and the N18TG2 murine neuroblastoma cell line, defective for neurotransmitter synthesis, represents an interesting model to study ACh role during neuronal differentiation.

Here we provide evidence that the exogenous expression of ChAT in 2/4 cells produced massive changes in gene expression with respect to N18TG2. An important transcripts modulation occurred even in "basal" untreated 2/4 cells indicating that the solely production of ACh represents the necessary and sufficient condition to stop proliferation and trigger differentiation. Therefore, stimulation with RA, a known regulator of many processes during neuronal development, enhanced the effects already produced by the rescue of ACh synthesis in 2/4 cells. RA treatment in N18TG2 also led to a quite extensive gene expression modulation, but the categories emerged as up-regulated were mainly due to cellular responses to nutrients changes. These data can be explained as a result of serum deprivation used concurrently to RA addition to the cell medium to promote differentiation. Differently to 2/4 cells, N18TG2 did not respond to cell medium modifications promoting cell cycle exit and cell differentiation, indicating that these cells are affected by an inability to differentiate essentially due to the neurotransmitter-defective phenotype. Analysis of the expression of single genes belonging to the generated categories corroborates the ability of 2/4 clone to stop proliferation and enter differentiation programme. This switching is clearly indicated by the higher expression in 2/4 cells of Cend1 gene, involved in neuronal precursor cell cycle exit and differentiation promotion (Politis, 2007). We also examined the expression of an important regulator of stemness, Lef1, which has been recently demonstrated to activate Oct4 and Nanog expression, two important components of the embryonic stem cells (ESC) pluripotency machinery and to physically interact with Nanog (Huang and Qin, 2010). In agreement with these data we also showed the down-regulation of two other stemness markers, Nes, encoding for Nestin a type VI intermediate filament protein, generally expressed in neuronal precursors cells and Prom1, encoding for CD133 a transmembrane glycoprotein, that since its isolation in 1997 has become one of the most valuable cell surface markers with clinical value for cancer stem cells identification (Weigmann, 1997; Corbeil,

2013). These findings, taken together with microarray results, demonstrate that the production of acetylcholine in 2/4 cells determines molecular changes which are crucial for the accomplishment of a mature neuronal phenotype.

What about morphological changes? Neurons are probably one of the most specialised type of cells of an organism (Stewart and Shen, 2015). Their shape determines their function and functionality. For example, the extent of dendritic arbors, at least in peripheral nervous system sensory neurons, physically defines their receptive fields (Hall and Treinin, 2011), and axonal topology is known to affect synaptic output (Sasaki, 2012). The cytoskeleton reorganization plays a central role in establishing and maintaining the shaping of developing neurons forming dendrites and axons, essential to the various roles of neurons (Susuki and Rasband, 2008; Kapitein and Hoongenraad, 2011; Bennett and Lorenzo, 2013; Machnicka, 2014). Consistently with these evidences we observed a modulation of cytoskeletal-related genes in 2/4 cells in both untreated and RA-treated conditions. In agreement, CDK5 transcript is increased in differentiating cells supporting previously reported data about CDK5 role in neural development and function, such as neuron migration, axon guidance, dendrites formation and synapse organization (Causeret, 2007; Tanabe, 2014; Kawauchi, 2014; Shah and Lahiri, 2014). Functional clustering of up-regulated transcripts in 2/4 RA-treated cells unveiled the overrepresentation of gene ontology categories such as, GO:0044430~cytoskeletal part, GO:0006928~cell motion, GO:0043005~neuron projection and GO:0045202~synapse. In fact, concurrently to CDK5, many other cytoskeleton-associated genes are overexpressed in differentiating cells both in absence and presence of RA treatment, suggesting that ACh production is, once again, fundamental to pave the way also for morphological rearrangements (for a complete list of genes see Appendix B). They include genes coding for proteins related to fiber formation (Tubb3) and proteins with a more dynamic function, as axon migration (Nav1 – van Haren, 2009). Also relevant is the up-regulation of Rab6 which through its interaction with dynein has been suggested to play a role in retrograde transport (Wanschers, 2008).

Intriguingly, we demonstrate that 2/4 cells are characterised by a specific increasing expression of the nucleoskeleton protein Lamin A/C compared to the other major component of nuclear lamina, Lamin B. Nuclear lamina was originally considered to be no more than a structural component of the nuclear envelope, proving a scaffold for the nucleus. Nowadays, Lamins have gained a place of honor in far more complex roles in the maintenance of normal cellular physiology (Burke and Stewart, 2013). As to be expected, Lamin A/C is listed into two main GO categories, GO:0031967~organelle envelope and GO:0044430~cytoskeletal

part, which are overrepresented in 2/4 cells in untreated conditions. A challenging process during neurogenesis and neuronal migration is represented by nuclear movements (Zhang, 2009). The overwhelming size of the nucleus compared to other cellular compartments, as well as the asynchronous movements of the nucleus and extending processes, suggest there must be a dedicated pathway to promote nuclei translocation during brain development (Li-Huei Tsai, 2005). Dynein, Lis1 and other cytoplasmic proteins have been described to connect microtubules to the nucleus during nucleokinesis (Zhang, 2009). Tsai and Gleeson (2005) illustrated how the centrosome plays an important role in promoting nucleokinesis pulling force from microtubules and dynein motors. However, the factors connecting the nuclear envelope (NE) to these complexes remain to be determined (Zhang, 2009). González-Granado and colleagues (2014) recently described how lamin-A increased upon T-cells activation and interacted with the linker of nucleoskeleton and cytoskeleton complex (LINC) to promote F-actin polymerization, which is a critical step for immunological synapse formation and antigen presentation. Consistently, western blot analysis of lamins in N18TG2 and 2/4 cells proved an enhancement of A-type lamins expression in differentiating cells, with a particular increase for Lamin A transcript, also reported in the GO categories. Despite a slight change is observed also in N18TG2 cells, this can be explained by the existence of RA-responsive element located within Lamin A/C promoter (Okumura, 2000). However, nuclear localization signal of Lamin A/C by immunofluorescence clearly show how the number of Lamin A/C expressing cells per field and the expression levels of Lamin A/C are prominent in 2/4 cells, even in CTR samples, with respect to non differentiating cells. Moreover, in accordance with previously reported data showing that stimulation with muscarinic receptor agonists induces cytoskeletal remodelling (Street, 2006) and expression of cytoskeleton-associated genes (Teber, 2004), we provided evidence that also the nucleoskeleton of differentiating neurons can be specifically affected by muscarinic receptor agonist stimulation, leading to *Lmna* transcription activation. These data are further corroborated by interactomics analysis of Lamin A/C protein. Several interactors known to be involved in cytoarchitecture aspects, such as cytoskeletal maintenance (*Actg1* - Belyantseva, 2009), actin remodelling (*Cttn* - Navratil, 2014) and left-right axis orientation (*Invs* - Yokoyama, 1993) are co-expressed with Lamin A/C in 2/4 cells. In addition, genes related to synapse maturation and functionality such as *Palm* and *Calm2* (Arstikaitis, 2008; Kang, 2012) and vesicular traffic pathways *Rab6b* (Grigoriev, 2007; Wanschers, 2008), show a linked expression pattern with A-type lamins. Extremely notable is the up-regulation of *Plec* (Plectin) and *Syne1* (*Nesprin1* or spectrin repeat containing, nuclear envelope 1). Plectin

proteins normally anchor IF (intermediate filaments) networks, both of nuclear and cytoplasmic origin, and they mediate their cross talk with the actin and tubulin cytoskeleton (Wiche and Winter, 2011); furthermore Nesprin 1, able to interact with both actin (Zhang, 2002) and plectin (Wilhelmsen, 2005), is also known to bind Sun1 and Sun2, which directly contact Lamin A and other lamin-associated proteins, through its KASH domain linking with the SUN domain (Zhong, 2010; Haque, 2010; Dahl, 2012). Interestingly, Smith and colleagues have recently depicted how the expression of Syne1/Nesprin1 is differentiation-related and how its siRNA down-regulation correlates with a more undifferentiated, stem cell-like and RA non-responsive phenotype. Similarly, Lmna siRNA knock-down produce an up-regulation of stemness-related genes (Lef1 and Prom1) and down-regulation of differentiation-related genes (Cend1, Syn1 and Syn2) in 2/4 cells. Additionally, Lmna decreased expression is associated to the expression levels reduction of two cytostructural-related genes, CDK5 and Nav1.

All these data taken together strongly support the idea that cytoarchitecture rearrangements are critical during neuronal development. Despite cytoplasmic proteins have received a major attention during the years for their implications in the establishment of neuronal morphology (Schlager, 2010), here we point out a possible role of a nuclear lamina protein, Lamin A/C, in determining a coordinated and consistent nucleoskeleton re-organisation during cytoskeletal changes occurring in neuronal differentiation.

### 3.5 Materials and Methods

#### Cell line maintenance, differentiation and treatments

N18TG2 and 2/4 murine neuroblastoma cell lines were grown in DMEM medium (Sigma) supplemented with 10% FBS (Hyclone), 2 mM L-glutamine, 100 U/L penicillin and 100 µg/L streptomycin at 37°C and maintained in a humidified incubator containing 10% CO<sub>2</sub>. 2/4 clone was maintained in the presence of 200 µg G418. For differentiation experiments N18TG2 cells and 2/4 cells were seeded at a density of  $5 \times 10^3$  cells/cm<sup>2</sup>. The following day, the cells were induced to differentiate with 1 µM retinoic acid (ATRA, designated RA throughout the paper; Sigma) in a “differentiation medium” composed of DMEM + 1% FBS. RA was dissolved in dimethyl sulphoxide (DMSO; Sigma) and stored as a stock solution at -80°C. Because of the light sensitivity of RA, all incubations were performed under subdued lighting. The DMSO concentration in each experiment was always  $\leq 0.01\%$ , which was not toxic and did not induce differentiation. For agonist and antagonist treatments N18TG2 cells and 2/4 cells were seeded at a density of  $5 \times 10^3$  cells/cm<sup>2</sup>. After 24h cells were exposed to carbachol  $10^{-4}$ M, atropine (Sigma-Aldrich)  $10^{-5}$ M and mecamylamine (Sigma-Aldrich)  $10^{-5}$ M. Samples were collected at 1, 6 and 12h after the exposure.

#### Western Blot

Cultured cells were washed twice with 1X PBS and then incubated for 1 min in 1X PBS added with 0.5 mM PMSF (Sigma-Aldrich) and 1X Complete Protease Inhibitors (Sigma-Aldrich) scraped, harvested and briefly sonicated. Proteins were suspended in urea buffer (8 M urea, 100 mM NaH<sub>2</sub>PO<sub>4</sub>, and 10 mM Tris pH 8) and the protein concentration was determined by the Bradford assay. The proteins were subjected to SDS–polyacrylamide gel electrophoresis with NuPAGE kit (Life Technologies) according to manufacturer's instructions. The resolved proteins were blotted overnight onto nitrocellulose membranes, which then were blocked in 1X PBS containing 5% non-fat milk for at least 1 hour. The blots were incubated with the following primary anti-mouse antibodies: goat polyclonal anti-Lamin A/C diluted 1:400 in 5% non-fat milk (N-18; Santa Cruz Biotechnology); goat polyclonal anti-Lamin B diluted 1:500 in 5% non-fat milk (M-20; Santa Cruz Biotechnology); mouse monoclonal anti-GAPDH (6C5; Millipore). After four washes (10 min/each) in 1X PBS and 0.1% Tween20, the membranes were incubated for 45 min with the appropriate secondary antibody: donkey anti-goat IRdye800 (LI-COR) or donkey anti-mouse IRdye800 (LI-COR).

The membranes were then analyzed with a Licor Odyssey Infrared Image System in the 800 nm channel. Densitometry analysis were performed using ImageJ software.

### **Immunofluorescence**

The cells were seeded on coverglass supports in complete medium and treated with RA for 3 days. The cells were fixed with 100% ice-cold methanol for 10 min and rehydrated with PBS ++ (1X PBS added with MgCl<sub>2</sub> and CaCl<sub>2</sub>) for 10 min. Cells were then incubated in a blocking solution in PBS++, 5% non-fat milk, 0.5% Tween20 for 30 min. Coverglasses were incubated for 1h and 30' using the following antibodies: goat polyclonal anti-Lamin A/C diluted 1:50 (N-18; Santa Cruz Biotechnology), goat polyclonal anti-Lamin B diluted 1:30 (M-20; Santa Cruz Biotechnology) and mouse monoclonal anti-NF200 diluted 1:200 (N52; Sigma-Aldrich). Alexa Fluor 488 donkey anti-goat, Alexa Fluor 594 donkey anti-goat antibody and Alexa Fluor 594 goat anti-mouse (Molecular Probes) were used as secondary antibodies. Primary antibodies were diluted in PBS++, 5% non-fat milk, 0.5% Tween20, whereas secondary antibodies were diluted in 1X PBS. Cell nuclei were stained with 1 mg/ml Hoechst in 1X PBS for 10 min. Finally, the cells were washed in 1X PBS and briefly rinsed in ddH<sub>2</sub>O and the glass coverslips were mounted in ProLong Gold anti-Fade Reagent (Molecular Probes). Images were acquired with an Olympus AX70 fluorescence microscope and analyzed with cellSens Standard software 1.8.1 (Olympus Corporation). The brightness and contrast of the acquired images were adjusted, and the figures were generated using Adobe Photoshop 7.0.

### **Total RNA isolation and quality control**

The cells were seeded in complete medium and harvested after the different treatments; total RNA was isolated using a Total RNA purification kit (NorgenBiotek). RNA quantity was determined by absorbance at 260 nm using a NanoDrop UV-VIS spectrophotometer. The quality and integrity of each sample was confirmed using a BioAnalyzer 2100 (Agilent RNA 6000 Nanokit); samples with an RNA Integrity Number (RIN) index lower than 8.0 were discarded.

### **RNA labelling and Microarray hybridization**

RNA samples were reverse-transcribed to cDNA. cRNA was obtained and then samples were amplified, labelled with Cy3 using the Low Input Quick Amp Labeling Kit One-Color (Agilent Technologies). cRNA labelled samples were purified with RNeasy KIT (Qiagen)

according to manufacturer's instructions. Quality control was performed to evaluate cRNA quantity and dye integration by NanoDrop measurement. The gene expression profiling was performed using the One-Color Microarray Agilent Platform according to the standard Agilent protocol for gene expression. Samples were hybridized on 8X60K whole mouse genome oligonucleotide microarrays, (Design grid ID 028005). 600ng of labeled cRNA was fragmented for 30 min at 60°C in 1X Fragmentation Buffer (Agilent Technologies) and loaded onto the array in 1XGEx Hybridization Buffer (Agilent Technologies). Array was incubated at 60°C in a rotating hybridization buffer chamber for 17h. Array was washed in GE Wash Buffer 1 and 2 (Agilent Technologies) for 1 min and then transferred in acetonitrile for 1 min. Post-hybridization image acquisition was accomplished using the Agilent Scanner G2564C. Data extraction from the scanner images was done by Feature Extraction.

### **Microarray normalization and statistical analysis**

Data filtering and normalization were performed using Agilent GeneSpring GX 11.0. All the features with the flag `gIsWellAboveBG=0` (too close to background) were filtered out and excluded from the following analysis. Filtered samples were normalized (aligned) to the 75th percentile. Subsequent statistical analysis was done using Microsoft Excel. Expressed genes were selected by a fold change threshold = 2.0 in linear scale and a minimum fluorescence level >100. The experiment was performed in duplicate on the same array and expression values with a coefficient of variation > 2.0 were filtered out and excluded for further analysis. The investigation of over- and under- represented functional annotations was performed using the chart and cluster algorithms of DAVID web tool (Huang et al, 2009). Hierarchical sample clustering was obtained by MultiexperimentViewer (Saeed et al, 2006). Updated microarray probe annotations were downloaded from the official website (<https://earray.chem.agilent.com>).

### **Real-time RT-PCR analysis**

RNA was reverse-transcribed with a High-Capacity cDNA Reverse Transcription Kit (Applied Biosystem) according to the manufacturer's instructions. Equal amounts of cDNA were then subjected to real time PCR analysis with an Applied Biosystems 7900HT thermal cycler, using the SensiMix SYBR Kit (Bioline) and specific primers, each at a concentration of 200 nM.: Ccnd3 F: GGAAGATGCTGGCATACTGG and R: CCAGGTAGTTCATAGCCAGAGG; Cdk5 F: TGGACCCTGAGATTGTGAAGT and R: GACAGAATCCCAGGCCTTTC; Cend1 F: TCATCCCGTGAAGCGAAT and R:



TCTGGGCATTATATGGGTGTC; Lef1 F: TGCCTACATCTGAAACATGGTG and R: CAAGCTTCCATCTCCAGAAGAG; Nav1 F: AAAGGGCCAGCTTACCAACA and R: TGCTGTTGGATCGGGTGATT; Nes F: TCCCTTAGTCTGGAAGTGGCTA and R: GGTGTCTGCAAGCGAGAGTT; Prom1 F: GCCCAAGCTGGAAGAATATG and R: CAGCAGAAAGCAGACAATCAA; Pgk1 F: AACTGGCCAAGCTACTGTG and R: ATCTGCTTAGCTCGACCCAC; Ppia F: CCCACCGTGTCTTCGACAT and R: CCAGTGCTCAGAGCTCGAAA; Rab6b F: TGGTTTTCTAGGGGAGCAG and R: GGTTGCCTGGTAGGTGTTGT; Rb1 F: GAGCTCATGAGAGACCGACA and R: CACCTTGCAGATGCCATACA; Syn1 F: GGAAGGGATCACATTATTGAGG and R: TGCTTGTCTTCATCCTGGTG; Syn2 F: CCTTGGAGATTATGACATCAAGGT and R: GCCACCAGGTTAAGCTCTGA; Tubb3 F: GCGCATCAGCGTATACTACAA and R: TTCCAAGTCCACCAGAATGG. Each experiment was performed in triplicate. The expression data were normalised using the Ct values of Pgk1 and Ppia.

### Cell cycle analysis

Cell cycle distribution was performed by FACS analysis. Cells were fixed in ethanol 70% and stained in a solution containing 50 µg/mL PI and 75 KU/mL RNase for at least 30 min in the dark. In each case, 20,000 events per sample were acquired by using a FACScan cytofluorimeter and the CellQuest BD software. The percentages of the cells in the different cell cycle phases were estimated on linear PI histograms by using the MODFIT software.

### siRNA knock down

2/4 cells were seeded at a density of  $5 \times 10^3$  cells/cm<sup>2</sup> in complete medium. After 24h cells were transfected with both siRNA Silencer Select (siRNA ID s69253) and siRNA Silencer Select Negative Control in Opti-MEM medium (Life Technologies). Lipofectamine RNAiMAX Reagent (Life Technologies) was used as transfection reagent according to manufacturer's instructions. The final concentration of both siRNA and siRNA Negative Control was set at 15nM. Samples were harvested at 24 and 48 h to perform mRNA expression analysis and western blot analysis.

### Interactomics analysis

Cognoscente, a database and visualization tool for biomolecular interactions that have been documented in the literature, was used to design the interactomic profile of Lamin A/C. Analysis was carried out setting a Radius = 2, meaning that all the known interactors and all

the known intermediates were visualised. The genes list generated by Cognoscente was compared to the list of mRNAs specifically up-regulated in 2/4 cells both in untreated and RA-treated conditions.

### **Statistical analysis**

Statistical significance of differences between groups was tested by paired Student's t-test or, if there were more than two groups, by one-way ANOVA.

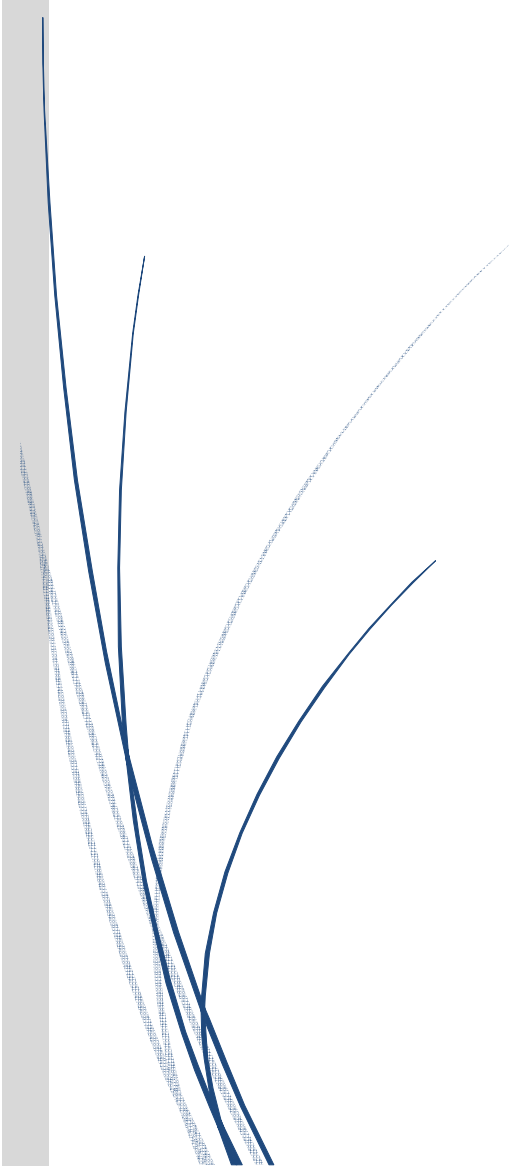
### **3.6 Acknowledgements**

I would like to thank all the people that contributed to the realisation of this work: Marta Nardella, Carla Musa, Ivan Arisi, Andrea Ennio Storti, Mara D'Onofrio, Cacci Emanuele, Biagioni Stefano, Gabriella Augusti-Tocco, Igea D'Agnano and Armando Felsani.

A vertical grey bar on the left side of the page. A dark blue arrow-shaped banner points to the right, containing the text 'Chapter 4' in white serif font.

# Chapter 4

## General Discussion

A series of thin, dark blue lines of varying lengths and curves, some overlapping, extending from the bottom left towards the center of the page.

“Any man could, if he were so inclined, be the  
sculptor of his own brain”  
**Santiago Ramón y Cajal**

#### 4. General discussion

Precise interconnections shared by many millions of neurons represent the foundation for the multitude tasks performed by our nervous system. Classical anatomical studies, conducted by Santiago Ramón y Cajal at the beginning of the 20<sup>th</sup> century, unraveled interesting details about the structure and organization of the nervous system and paved the way for more recent studies intended to elucidate cellular and molecular mechanisms of the developing neurons. Outstanding advances have been made thanks to the identification of several factors determining neural stem cells expansion, renewal and fate specification as well, formation of dendrites, axons and synaptic connection/plasticity. A mix of genetic and epigenetic features (intrinsic factors) and external cues (extrinsic factors) are critical for the differentiation process of each nerve cell (Kandel, 2000).

This thesis work touched upon two important, and yet not completely clarified, aspects of neurons development: regulation of apoptosis and role of the neurotransmitters. In both cases original and novel data have been presented; on one hand the very well-known oncogene MYCN has been related to programmed cell death (PCD) during the early stages of differentiation, on the other hand a genome-wide study was carried out to highlight the non-synaptic properties of the acetylcholine neurotransmitter. As for the regulation of cell death it was believed, for a long time, that the majority of events occurred in post-mitotic neurons competing for limiting amounts of target-derived neurotrophic signals, so it was believed that the unique role of neurotransmitters was exerted after synaptic connections establishment (Rao and Jacobson, 2005). However, it is now evident that cell death and synthesis of the neurotransmitters occur in immature nervous system before the elaboration of neuritic processes and formation of synaptic contacts (Lauder, 1993; Bovetti, 2011; Lossi, 2015). Thus, apoptosis and release of neurotransmitter are time-regulated during development and act differently according to the prior or post synapsis completion.

##### 4.1 Dying to become a neuron

Occurrence of PCD early in the development of the nervous system is a processes well conserved during evolution, in fact it can be observed in several organisms, ranging from *Caenorhabditis elegans* to mouse. It is now clear that, undifferentiated populations of cells, typically proliferative and/or newly postmitotic, undergo apoptosis in the nervous system. However, unlike neurotrophic cell death resulting from trophic withdrawal, the molecular pathways behind early PCD are largely unknown (Yeo and Gautier, 2004).

The comprehension of programmed cell death in neural precursors cells remain one of the most intriguing, but still controversial, issue in developmental neurobiology (Voyvodic, 1996; Sommer and Rao, 2002). Despite the efforts in giving an estimation of death rate, results were extremely variable and dependent on the different techniques applied; with percentages ranging from 50% -70% to 0.3%-1.7% of proliferating cells destined to die (Blaschke, 1996; Blaschke, 1998; Thomaidou, 1997).

From a molecular point of view some aspects have been clarified. It has been demonstrated that *apaf-1*<sup>-/-</sup>, *caspase-9*<sup>-/-</sup>, and *caspase-3*<sup>-/-</sup> mice clearly show an impairment of nervous system development and die before birth, underlying how much apoptosis is important during early embry development (Rao and Jacobson, 2005). However, factors controlling apoptosis in precursors cells appear dissimilar to those in mature neurons, where Bax- and Bak-mediated mitochondrial dysfunction to trigger cell death (Rao and Jacobson, 2005; Wei, 2001). Generally speaking, the same regulators of other physiological aspects of neuronal development, such as cell proliferation and differentiation, coordinate cell death. The result is a sophisticated, as well complicated, balance between cell death and survival stimuli (Yeo and Gautier, 2004).

Molecules involved in early neural development as well as PCD in other developmental processes				
Type of molecule	Location of developmental PCD	Role in developmental PCD	Role in early neural development	Putative link with apoptosis
Bone morphogenetic proteins (BMPs)	r3 and r5	Required for PCD in r3 and r5, and limb bud	Inhibits neural induction Induces of dorsal cell fates in neural tube Coordinates proliferation and differentiation of dorsal cell types	TAK1 bridges interactions between BMP receptors and XIAP (Yamaguchi et al., 1999).
	Necrotic zones in limb bud			
Wnt	r3 and 5	Required for BMP-mediated PCD in r3 and r5	Inhibition of Wnt signaling required for anteriorization Involved in BMP-mediated dorsal induction, neural crest fate induction, proliferation, and survival	<i>hid</i> interacts genetically with Wg signaling in <i>Drosophila</i> (Cox et al., 2000).
	Necrotic zones in limb bud	Inhibition of Wnt signaling induces PCD in limb bud		
c-Jun N-terminal kinases (JNKs)	Neural folds in hindbrain	Required for PCD in hindbrain neural folds		JNK pathway regulates apoptotic machinery (Lin, 2002 and references therein).
	Neuroepithelium in forebrain	Required for survival in forebrain neuroepithelium		
Sonic Hedgehog (Shh)	Ventral VZ in neural tube	Overexpression increases PCD in ventral VZ Suppresses apoptosis in axial tissues following removal of notochord and FP	Induction of ventral cell fates in neural tube Coordinates proliferation and differentiation of ventral cell types	Caspase cleavage of intracellular domains of Patched is required for Patched-mediated apoptosis (Thibert et al., 2003).
Growth Factors: fibroblast growth factors (FGFs), insulin and insulin-like growth factors (IGFs), and neurotrophins	Various cell types within the nervous system: proliferating precursors to differentiated neurons (see text)	Promote survival of various cell types (see text)	Proliferation and differentiation context-dependent effects.	IL-3 and IGF-1 phosphorylates BAD, leading to binding with 14-3-3 (Datta et al., 1997).

VZ, ventricular zone; FP, floorplate; r, rhombomere; CNS, central nervous system.

Table by Yeo and Gautier, 2004

As reviewed by Yeo and Gautier (2004), protagonists of the early stages of embryo development, such as BMPs, Wnt, Shh and growth factors, also regulate PCD (for details see the table above). Chapter 2 of this thesis work clearly demonstrated how a very well-known proliferative gene like MYCN can also trigger apoptosis through the down-regulation of anti-apoptotic miRNAs, confirming that death and proliferation are characterised by a delicate interplay during neuronal differentiation.

What is the physiological meaning of PCD? Why does it occur before terminal differentiation? These are the most important questions to address. Several explanations have been proposed, going from the necessity to eliminate cells that acquire errors during differentiation and regulate the response to morphogenetic factors (spatial and temporal aspects) to monitor cells that get damaged as a consequence of proliferation (Yeo and Gautier, 2004). An attractive hypothesis is that PCD could be a novel form of regulating commitment of precursors to become mature neurons. In *Xenopus* early development, maintaining neuronal cells uncommitted, through the constitutive expression of Notch signalling, abrogates PCD; as well, PCD inhibition through overexpression of Bcl-2, results in increased number of both neural and neuronal cell types (Yeo and Gautier, 2003). The increase not only in neuronal cells number, but also in the neural subset strongly supports the idea that PCD is not exclusively meant to regulate cell mass but it has an active role in neuronal determination (Yeo and Gautier, 2003). Consistently, when neural cells are prevented to further differentiate PCD is reduced (Yeo and Gautier, 2003). Intriguingly, a very extreme theory has been proposed on cell death regulation describing PCD as the default fate of all the cells in the nervous system, such that only those receiving the correct and sufficient stimuli can survive and differentiate (Raff, 1992).

Novel protagonists have been identified through the years. Interestingly, and similarly to what described in Chapter 2 of this thesis, the expression of two members of the p53 family,  $\Delta Np73$  and TAp63 changes in sympathetic neurons following NGF withdrawal, strongly supporting the idea of their role in developmental neuronal apoptosis (Jacobs, 2005; Kristiansen and Ham, 2014).

Although, we are still far from a coherent and integrated view, evidences demonstrate that PCD, like cell division and differentiation, is an integral process of normal development.

## 4.2 Neurotransmitters as morphogens

Questioning on what kind of instructions are needed in embryonic neurons to get wired into a functioning brain has fascinated developmental biologists for decades. Morphogens play a key role in shaping the nervous system. With the term "morphogens" are indicated a plethora of developmental signals that exert specific effects on receptive cells according to concentration (Lauder and Schambra, 1999). Neurotransmitters can be defined as morphogens since they can act as morphogenetic factors in a dose-dependent manner in neural and non-neural tissues. These evidences raise the possibility that synaptic transmission is just an evolved specialised function of neurotransmitters, originating from phylogenetically old jobs (Lauder and Schambra, 1999).

The genome-wide study reported in Chapter 3 illustrated how dramatic the restored ability of neurotransmitter synthesis can be for the accomplishment of differentiation processes, going from cell cycle exit to the acquisition of a mature phenotype. Moreover, data showed (Chapter 3) that cytoskeletal and nucleoskeletal proteins are affected by neurotransmitters synthesis. It is known that intracellular levels of  $\text{Ca}^{2+}$  are essential for controlling neurons migration, which implies reorganization of the cytoskeleton, and that these levels are maintained by neurotransmitters activation of specific receptors (Manent and Represa, 2007). Doherty and colleagues (2000) described how a concerted cooperation between CAMs and MAPK signalling determine shape remodelling in developing neurons. Interestingly, the model presented in Chapter 3 is based on two kind of receptors that can be activated by the acetylcholine neurotransmitter: the muscarinic receptors, upstream a MAPK cascade, and the nicotinic receptors, controlling calcium intracellular flux.

Are the neurotransmitters this powerful as morphogens? The answer to this question is yes. It has been found that, in particular for the AChRs, perinatal manipulations of the cholinergic system result in major changes of cortical structure and cortex differentiation (Lauder and Schambra, 1999).

However, defining the molecular effects of neurotransmitter release remain a steep challenge as neurotransmitters can regulate growth, differentiation, and plasticity of neurons, demonstrating how a multitude of complex signaling pathways can be affected by a single molecule (Lauder and Schambra, 1999). Therefore, focusing on simple and accessible models, such as isogenic cell lines uniquely differing for the neurotransmitter synthesis production and release, could represent a feasible strategy to decipher the multiple effects of a single "morphogen" on differentiation processes.



Multiple efforts have been made so far to depict the nervous system development regulation in the embryo and it is undeniable that much has not been completely disclosed yet. Having said that, the nervous system is not "hard-wired", in fact neuronal circuits continue to remodel in response to environmental stimuli even during adulthood overemphasizing the complexity of this charming and "fickle" structure.

## REFERENCES

### Chapter 1

**All the information from section 1. to section 2.2 were rearranged from:**

Kandel E, Schwartz J, Jessell T, Jessell TM, Schwartz JH. Principles of Neural Science, Fourth Edition. McGraw-Hill Medical Publishing Division. 2000 Jan.

Bangalore L. Brain Development. First Edition. Gray Matter series. Chelsea House Publishing, New York. 2007 May.

Rao SM, Jacobson M. Developmental Neurobiology, Fourth Edition. Kluwer Academic/Plenum Publishers, New York. 2005.

Chambon P. The molecular and genetic dissection of the retinoid signaling pathway. Recent Prog Horm Res. 1995;50:317-32.

Dupé V and Lumsden A. Hindbrain patterning involves graded responses to retinoic acid signalling. Development. 2001 Jun;128(12):2199-208.

Durand B, Saunders M, Leroy P, Leid M, Chambon P. All-trans and 9-cis retinoic acid induction of CRABP II transcription is mediated by RAR-RXR heterodimers bound to DR1 and DR2 repeated motifs. Cell. 1992 Oct 2;71(1):73-85.

Edsjö A, Holmquist L, Pählman S. Neuroblastoma as an experimental model for neuronal differentiation and hypoxia-induced tumor cell dedifferentiation. Semin Cancer Biol. 2007 Jun;17(3):248-56.

Evans TR and Kaye SB. Retinoids: present role and future potential. Br J Cancer. 1999 Apr;80(1-2):1-8.

Finger S. Ch. 1: The brain in antiquity. Origins of neuroscience: a history of explorations into brain function. Oxford Univ. Press. 2001 ISBN 978-0-19-514694-3.

- Guglielmi L, Cinnella C, Nardella M, Maresca G, Valentini A, Mercanti D, Felsani A, D'Agnano I. MYCN gene expression is required for the onset of the differentiation programme in neuroblastoma cells. *Cell Death Dis.* 2014 Feb 20;5:e1081.
- Hill DP and Robertson KA. Characterization of the cholinergic neuronal differentiation of the human neuroblastoma cell line LA-N-5 after treatment with retinoic acid. *Brain Res Dev Brain Res.* 1997 Aug 18;102(1):53-67.
- Hill DP and Robertson KA. Differentiation of LA-N-5 neuroblastoma cells into cholinergic neurons: methods for differentiation, immunohistochemistry and reporter gene introduction. *Brain Res Brain Res Protoc.* 1998 Mar;2(3):183-90.
- Huber K. The sympathoadrenal cell lineage: specification, diversification, and new perspectives. *Dev Biol.* 2006 Oct 15;298(2):335-43.
- Kandel E, Schwartz J, Jessell T, Jessell TM, Schwartz JH. *Principles of Neural Science*, Fourth Edition. McGraw-Hill Medical Publishing Division. 2000 Jan; ISBN: 0838577016.
- Lee K and Skromne I. Retinoic acid regulates size, pattern and alignment of tissues at the head-trunk transition. *Development.* 2014 Nov;141(22):4375-84.
- Liu T, Bohlken A, Kuljaca S, Lee M, Nguyen T, Smith S, Cheung B, Norris MD, Haber M, Holloway AJ, Bowtell DD, Marshall GM. The retinoid anticancer signal: mechanisms of target gene regulation. *Br J Cancer.* 2005 Aug 8;93(3):310-8.
- Mader S, Chen JY, Chen Z, White J, Chambon P, Gronemeyer H. The patterns of binding of RAR, RXR and TR homo- and heterodimers to direct repeats are dictated by the binding specificities of the DNA binding domains. *EMBO J.* 1993 Dec 15;12(13):5029-41.

- Matthay KK, Villablanca JG, Seeger RC, Stram DO, Harris RE, Ramsay NK, Swift P, Shimada H, Black CT, Brodeur GM, Gerbing RB, Reynolds CP. Treatment of high-risk neuroblastoma with intensive chemotherapy, radiotherapy, autologous bone marrow transplantation, and 13-cis-retinoic acid. Children's Cancer Group. *N Engl J Med*. 1999 Oct 14;341(16):1165-73.
- Nagpal S, Saunders M, Kastner P, Durand B, Nakshatri H, Chambon P. Promoter context- and response element-dependent specificity of the transcriptional activation and modulating functions of retinoic acid receptors. *Cell*. 1992 Sep 18;70(6):1007-19.
- Rastinejad F. Retinoid X receptor and its partners in the nuclear receptor family. *Curr Opin Struct Biol*. 2001 Feb;11(1):33-8.
- Påhlman S, Odelstad L, Larsson E, Grotte G, Nilsson K. Phenotypic changes of human neuroblastoma cells in culture induced by 12-O-tetradecanoyl-phorbol-13-acetate. *Int J Cancer*. 1981 Nov 15;28(5):583-9.
- Sidell N. Retinoic acid-induced growth inhibition and morphologic differentiation of human neuroblastoma cells in vitro. *J Natl Cancer Inst*. 1982 Apr;68(4):589-96.
- Smith MA, Altekruze SF, Adamson PC, Reaman GH, Seibel NL. Declining childhood and adolescent cancer mortality. *Cancer*. 2014 Aug 15;120(16):2497-506.
- Smith WC, Nakshatri H, Leroy P, Rees J, Chambon P. A retinoic acid response element is present in the mouse cellular retinol binding protein I (mCRBPI) promoter. *EMBO J*. 1991 Aug;10(8):2223-30.
- Wakamatsu Y, Watanabe Y, Nakamura H, Kondoh H. Regulation of the neural crest cell fate by N-myc: promotion of ventral migration and neuronal differentiation. *Development*. 1997 May;124(10):1953-62.
- Zimmerman KA, Yancopoulos GD, Collum RG, Smith RK, Kohl NE, Denis KA, Nau MM, Witte ON, Toran-Allerand D, Gee CE, et al. Differential expression of myc family genes during murine development. *Nature*. 1986 Feb 27-Mar 5;319(6056):780-3.

## **Chapter 2**

- Amatruda TT, III, Sidell N, Ranyard J, Koeffler HP. Retinoic acid treatment of human neuroblastoma cells is associated with decreased N-myc expression. *Biochem. Biophys. Res. Commun.*1985 126:1189-1195.
- Brodeur GM. Neuroblastoma: biological insights into a clinical enigma. *Nat. Rev. Cancer.*2003 3:203-216.
- Cacci E, Ajmone-Cat MA, Anelli T, Biagioni S, Minghetti L. In vitro neuronal and glial differentiation from embryonic or adult neural precursor cells are differently affected by chronic or acute activation of microglia. *Glia.*2008 56:412-425.
- Charron J, Malynn BA, Fisher P, Stewart V, Jeannotte L, Goff SP, Robertson EJ, Alt FW. Embryonic lethality in mice homozygous for a targeted disruption of the N-myc gene. *Genes Dev.*1992 6:2248-2257.
- Chen Y and Stallings RL. Differential patterns of microRNA expression in neuroblastoma are correlated with prognosis, differentiation, and apoptosis. *Cancer Res.*2007 67:976-983.
- Coller HA, Forman JJ, Legesse-Miller A. "Myc'ed messages": myc induces transcription of E2F1 while inhibiting its translation via a microRNA polycistron. *PLoS. Genet.*2007 3:e146.
- Davis A and Bradley A. Mutation of N-myc in mice: what does the phenotype tell us? *Bioessays.*1993 15:273-275.
- De Laurenti V, Raschella G, Barcaroli D, Annicchiarico-Petruzzelli M, Ranalli M, Catani MV, Tanno B, Costanzo A, Levrero M, Melino G. Induction of neuronal differentiation by p73 in a neuroblastoma cell line. *J. Biol. Chem.*2000 275:15226-15231.

- Dweep H, Sticht C, Pandey P, Gretz N. miRWalk--database: prediction of possible miRNA binding sites by "walking" the genes of three genomes. *J. Biomed. Inform.*2011 44:839-847.
- Edsjö A, Nilsson H, Vandesompele J, Karlsson J, Pattyn F, Culp LA, Speleman F, Pålman S. Neuroblastoma cells with overexpressed MYCN retain their capacity to undergo neuronal differentiation. *Lab Invest.*2004 84:406-417.
- Eijkelenboom A and Burgering BM. FOXOs: signalling integrators for homeostasis maintenance. *Nat. Rev. Mol. Cell Biol.*2013 14:83-97.
- Eilers M and Eisenman RN. Myc's broad reach. *Genes Dev.*2008 22:2755-2766.
- Gatti G, Maresca G, Natoli M, Florenzano F, Nicolini A, Felsani A, D'Agnano I. MYC prevents apoptosis and enhances endoreduplication induced by paclitaxel. *PLoS. One.*2009 4:e5442.
- Hill DP and Robertson KA. Characterization of the cholinergic neuronal differentiation of the human neuroblastoma cell line LA-N-5 after treatment with retinoic acid. *Brain Res. Dev. Brain Res.*1997 102:53-67.
- Haug BH, Henriksen JR, Buechner J, Geerts D, Tomte E, Kogner P, Martinsson T, Flaegstad T, Sveinbjornsson B, Einvik C. MYCN-regulated miRNA-92 inhibits secretion of the tumor suppressor DICKKOPF-3 (DKK3) in neuroblastoma. *Carcinogenesis.*2011 32:1005-1012.
- Hui AB, Lo KW, Yin XL, Poon WS, Ng HK. Detection of multiple gene amplifications in glioblastoma multiforme using array-based comparative genomic hybridization. *Lab Invest.*2001 81:717-723.
- Irwin M, Marin MC, Phillips AC, Seelan RS, Smith DI, Liu W, Flores ER, Tsai KY, Jacks T, Vousden KH, Kaelin WG, Jr. Role for the p53 homologue p73 in E2F-1-induced apoptosis. *Nature.*2000 407:645-648.

- Jee MK, Jung JS, Im YB, Jung SJ, Kang SK. Silencing of miR20a is crucial for Ngn1-mediated neuroprotection in injured spinal cord. *Hum. Gene Ther.*2012 23:508-520.
- Kim WR and Sun W. Programmed cell death during postnatal development of the rodent nervous system. *Dev. Growth Differ.*2011 53:225-235.
- Knoepfler PS, Cheng PF, Eisenman RN. N-myc is essential during neurogenesis for the rapid expansion of progenitor cell populations and the inhibition of neuronal differentiation. *Genes Dev.*2002 16:2699-2712.
- Li G, Luna C, Qiu J, Epstein DL, Gonzalez P. Alterations in microRNA expression in stress-induced cellular senescence. *Mech. Ageing Dev.*2009 130:731-741.
- Liu DZ, Ander BP, Tian Y, Stamova B, Jickling GC, Davis RR, Sharp FR. Integrated analysis of mRNA and microRNA expression in mature neurons, neural progenitor cells and neuroblastoma cells. *Gene.*2012 495:120-127.
- Malynn BA, de Alboran IM, O'Hagan RC, Bronson R, Davidson L, DePinho RA, Alt FW. N-myc can functionally replace c-myc in murine development, cellular growth, and differentiation. *Genes Dev.*2000 14:1390-1399.
- Maresca G, Natoli M, Nardella M, Arisi I, Trisciuglio D, Desideri M, Brandi R, D'Aguanno S, Nicotra MR, D'Onofrio M, Urbani A, Natali PG, Del BD, Felsani A, D'Agnano I. LMNA knock-down affects differentiation and progression of human neuroblastoma cells. *PLoS. One.*2012 7:e45513.
- Melotte V, Qu X, Ongenaert M, van CW, de Bruine AP, Baldwin HS, Van EM. The N-myc downstream regulated gene (NDRG) family: diverse functions, multiple applications. *FASEB J.*2010 24:4153-4166.
- Moens CB, Auerbach AB, Conlon RA, Joyner AL, Rossant J. A targeted mutation reveals a role for N-myc in branching morphogenesis in the embryonic mouse lung. *Genes Dev.*1992 6:691-704.

- Moens CB, Stanton BR, Parada LF, Rossant J. Defects in heart and lung development in compound heterozygotes for two different targeted mutations at the N-myc locus. *Development*.1993 119:485-499.
- Munoz J, Vendrell E, Aiza G, Nistal M, Pestana A, Peinado MA, Castresana JS. Determination of genomic damage in neuroblastic tumors by arbitrarily primed PCR: MYCN amplification as a marker for genomic instability in neuroblastomas. *Neuropathology*.2006 26:165-169.
- Murphy DM, Buckley PG, Bryan K, Watters KM, Koster J, Van SP, Molenaar J, Versteeg R, Stallings RL. Dissection of the oncogenic MYCN transcriptional network reveals a large set of clinically relevant cell cycle genes as drivers of neuroblastoma tumorigenesis. *Mol. Carcinog*.2011 50:403-411.
- Nau MM, Brooks BJ, Jr., Carney DN, Gazdar AF, Battey JF, Sausville EA, Minna JD. Human small-cell lung cancers show amplification and expression of the N-myc gene. *Proc. Natl. Acad. Sci. U. S. A*.1986 83:1092-1096.
- O'Donnell KA, Wentzel EA, Zeller KI, Dang CV, Mendell JT. c-Myc-regulated microRNAs modulate E2F1 expression. *Nature*.2005 435:839-843.
- Oppenheim RW. Cell death during development of the nervous system. *Annu. Rev. Neurosci*.1991 14:453-501.
- Påhlman S, Ruusala AI, Abrahamsson L, Mattsson ME, Esscher T. Retinoic acid-induced differentiation of cultured human neuroblastoma cells: a comparison with phorbol ester-induced differentiation. *Cell Differ*.1984 14:135-144.
- Pelengaris S, Khan M, Evan G. c-MYC: more than just a matter of life and death. *Nat. Rev. Cancer*.2002 2:764-776.
- Ribatti D, Raffaghello L, Pastorino F, Nico B, Brignole C, Vacca A, Ponzoni M. In vivo angiogenic activity of neuroblastoma correlates with MYCN oncogene overexpression. *Int. J. Cancer*.2002 102:351-354.



- Sawai S, Shimono A, Hanaoka K, Kondoh H. Embryonic lethality resulting from disruption of both N-myc alleles in mouse zygotes. *New Biol.*1991 3:861-869.
- Sawai S, Shimono A, Wakamatsu Y, Palmes C, Hanaoka K, Kondoh H. Defects of embryonic organogenesis resulting from targeted disruption of the N-myc gene in the mouse. *Development.*1993 117:1445-1455.
- Schulte JH, Horn S, Otto T, Samans B, Heukamp LC, Eilers UC, Krause M, Astrahantseff K, Klein-Hitpass L, Buettner R, Schramm A, Christiansen H, Eilers M, Eggert A, Berwanger B. MYCN regulates oncogenic MicroRNAs in neuroblastoma. *Int. J. Cancer.*2008 122:699-704.
- Senyuk V, Zhang Y, Liu Y, Ming M, Premanand K, Zhou L, Chen P, Chen J, Rowley JD, Nucifora G, Qian Z. Critical role of miR-9 in myelopoiesis and EVI1-induced leukemogenesis. *Proc. Natl. Acad. Sci. U. S. A.*2013 110:5594-5599.
- Sidell N. Retinoic acid-induced growth inhibition and morphologic differentiation of human neuroblastoma cells in vitro. *J. Natl. Cancer Inst.*1982 68:589-596.
- Squire J, Goddard AD, Canton M, Becker A, Phillips RA, Gallie BL. Tumour induction by the retinoblastoma mutation is independent of N-myc expression. *Nature.*1986 322:555-557.
- Stanton BR, Perkins AS, Tessarollo L, Sassoon DA, Parada LF. Loss of N-myc function results in embryonic lethality and failure of the epithelial component of the embryo to develop. *Genes Dev.*1992 6:2235-2247.
- Stallings RL. MicroRNA involvement in the pathogenesis of neuroblastoma: potential for microRNA mediated therapeutics. *Curr. Pharm. Des.*2009 15:456-462.
- Strieder V and Lutz W. E2F proteins regulate MYCN expression in neuroblastomas. *J. Biol. Chem.*2003 278:2983-2989.

- Stiewe T and Putzer BM. Role of the p53-homologue p73 in E2F1-induced apoptosis. *Nat. Genet.*2000 26:464-469.
- Suenaga Y, Kaneko Y, Matsumoto D, Hossain MS, Ozaki T, Nakagawara A. Positive auto-regulation of MYCN in human neuroblastoma. *Biochem. Biophys. Res. Commun.*2009 390:21-26.
- Sundelacruz S, Levin M, Kaplan DL. Role of membrane potential in the regulation of cell proliferation and differentiation. *Stem Cell Rev.*2009 5:231-246.
- Thiele CJ, Deutsch LA, Israel MA. The expression of multiple proto-oncogenes is differentially regulated during retinoic acid induced maturation of human neuroblastoma cell lines. *Oncogene.*1988 3:281-288.
- Westermarck UK, Wilhelm M, Frenzel A, Henriksson MA. The MYCN oncogene and differentiation in neuroblastoma. *Semin. Cancer Biol.*2011 21:256-266.
- Yoo AS, Staahl BT, Chen L, Crabtree GR. MicroRNA-mediated switching of chromatin-remodelling complexes in neural development. *Nature.*2009 460:642-646.
- Zaika A, Irwin M, Sansome C, Moll UM. Oncogenes induce and activate endogenous p73 protein. *J. Biol. Chem.*2001 276:11310-11316.
- Zimmerman KA, Yancopoulos GD, Collum RG, Smith RK, Kohl NE, Denis KA, Nau MM, Witte ON, Toran-Allerand D, Gee CE et al. Differential expression of myc family genes during murine development. *Nature.*1986 319:780-783.

### **Chapter 3**

- Aebi U, Cohn J, Buhle L, Gerace L. The nuclear lamina is a meshwork of intermediate-type filaments. *Nature*. 1986 Oct 9-15;323(6088):560-4.
- Arstikaitis P, Gauthier-Campbell C, Carolina Gutierrez Herrera R, Huang K, Levinson JN, Murphy TH, Kilimann MW, Sala C, Colicos MA, El-Husseini A. Paralemmin-1, a modulator of filopodia induction is required for spine maturation. *Mol Biol Cell*. 2008 May;19(5):2026-38.
- Belyantseva IA, Perrin BJ, Sonnemann KJ, Zhu M, Stepanyan R, McGee J, Frolenkov GI, Walsh EJ, Friderici KH, Friedman TB, Ervasti JM. Gamma-actin is required for cytoskeletal maintenance but not development. *Proc Natl Acad Sci U S A*. 2009 Jun 16;106(24):9703-8.
- Bennett V and Lorenzo DN. Spectrin- and ankyrin-based membrane domains and the evolution of vertebrates. *Curr Top Membr*. 2013;72:1-37.
- Biagioni S, Tata AM, De Jaco A, Augusti-Tocco G. Acetylcholine synthesis and neuron differentiation. *Int J Dev Biol*. 2000;44(6):689-97.
- Bignami F, Bevilacqua P, Biagioni S, De Jaco A, Casamenti F, Felsani A, Augusti-Tocco G. Cellular acetylcholine content and neuronal differentiation. *J Neurochem*. 1997 Oct;69(4):1374-81.
- Bovetti S, Gribaudo S, Puche AC, De Marchis S, Fasolo A. From progenitors to integrated neurons: role of neurotransmitters in adult olfactory neurogenesis. *J Chem Neuroanat*. 2011 Dec;42(4):304-16.
- Brun PJ, Yang KJ, Lee SA, Yuen JJ, Blaner WS. Retinoids: Potent regulators of metabolism. *Biofactors*. 2013 Mar-Apr;39(2):151-63.
- Burke B, Stewart CL. The nuclear lamins: flexibility in function. *Nat Rev Mol Cell Biol*. 2013 Jan;14(1):13-24.

- Causeret F, Jacobs T, Terao M, Heath O, Hoshino M, Nikolic M. Neurabin-I is phosphorylated by Cdk5: implications for neuronal morphogenesis and cortical migration. *Mol Biol Cell*. 2007 Nov;18(11):4327-42.
- Corbeil D, Karbanová J, Fargeas CA, Jászai J. Prominin-1 (CD133): Molecular and Cellular Features Across Species. *Adv Exp Med Biol*. 2013;777:3-24.
- Dahl KN and Kalinowski A. Nucleoskeleton mechanics at a glance. *J Cell Sci*. 2011 Mar 1;124(Pt 5):675-8.
- De Jaco A, Ajmone-Cat MA, Baldelli P, Carbone E, Augusti-Tocco G, Biagioni S. Modulation of acetylcholinesterase and voltage-gated Na(+) channels in choline acetyltransferase- transfected neuroblastoma clones. *J Neurochem*. 2000 Sep;75(3):1123-31.
- Stewart E and Shen K. STORMing towards a clear picture of the cytoskeleton in neurons. *Elife*. 2015 Feb 6;4.
- Grigoriev I, Splinter D, Keijzer N, Wulf PS, Demmers J, Ohtsuka T, Modesti M, Maly IV, Grosveld F, Hoogenraad CC, Akhmanova A. Rab6 regulates transport and targeting of exocytotic carriers. *Dev Cell*. 2007 Aug;13(2):305-14.
- Haque F, Mazzeo D, Patel JT, Smallwood DT, Ellis JA, Shanahan CM, Shackleton S. Mammalian SUN protein interaction networks at the inner nuclear membrane and their role in laminopathy disease processes. *J Biol Chem*. 2010 Jan 29;285(5):3487-98.
- Hall DH and Treinin M. How does morphology relate to function in sensory arbors? *Trends Neurosci*. 2011 Sep;34(9):443-51.
- Hamprecht B. Structural, electrophysiological, biochemical, and pharmacological properties of neuroblastoma-glioma cell hybrids in cell culture. *Int Rev Cytol*. 1977;49:99-170.

- Huang C and Qin D. Role of Lef1 in sustaining self-renewal in mouse embryonic stem cells. *J Genet Genomics*. 2010 Jul;37(7):441-9.
- Huang da W, Sherman BT, Lempicki RA. Systematic and integrative analysis of large gene lists using DAVID bioinformatics resources. *Nat Protoc*. 2009;4(1):44-57.
- Horiuchi Y, Kimura R, Kato N, Fujii T, Seki M, Endo T, Kato T, Kawashima K. Evolutional study on acetylcholine expression. *Life Sci*. 2003 Feb 28;72(15):1745-56.
- Kang HJ, Voleti B, Hajszan T, Rajkowska G, Stockmeier CA, Licznanski P, Lepack A, Majik MS, Jeong LS, Banasr M, Son H, Duman RS. Decreased expression of synapse-related genes and loss of synapses in major depressive disorder. *Nat Med*. 2012 Sep;18(9):1413-7.
- Kapitein LC and Hoogenraad CC. Which way to go? Cytoskeletal organization and polarized transport in neurons. *Mol Cell Neurosci*. 2011 Jan;46(1):9-20.
- Kawauchi T. Cdk5 regulates multiple cellular events in neural development, function and disease. *Dev Growth Differ*. 2014 Jun;56(5):335-48.
- Komuro H and Rakic P. Dynamics of granule cell migration: a confocal microscopic study in acute cerebellar slice preparations. *J Neurosci*. 1995 Feb;15(2):1110-20.
- Lauder JM. Neurotransmitters as growth regulatory signals: role of receptors and second messengers. *Trends Neurosci*. 1993 Jun;16(6):233-40.
- Machnicka B, Czogalla A, Hryniewicz-Jankowska A, Bogusławska DM, Grochowalska R, Heger E, Sikorski AF. Spectrins: a structural platform for stabilization and activation of membrane channels, receptors and transporters. *Biochim Biophys Acta*. 2014 Feb;1838(2):620-34.

- Maresca G, Natoli M, Nardella M, Arisi I, Trisciuglio D, Desideri M, Brandi R, D'Aguanno S, Nicotra MR, D'Onofrio M, Urbani A, Natali PG, Del Bufalo D, Felsani A, D'Agnano I. LMNA knock-down affects differentiation and progression of human neuroblastoma cells. *PLoS One*. 2012;7(9):e45513.
- Mattson MP. Neurotransmitters in the regulation of neuronal cytoarchitecture. *Brain Res*. 1988 Apr-Jun;472(2):179-212.
- Navratil AM, Dozier MG, Whitesell JD, Clay CM, Roberson MS. Role of cortactin in dynamic actin remodeling events in gonadotrope cells. *Endocrinology*. 2014 Feb;155(2):548-57.
- Nelson P, Christian C, Nirenberg M. Synapse formation between clonal neuroblastoma X glioma hybrid cells and striated muscle cells. *Proc Natl Acad Sci U S A*. 1976 Jan;73(1):123-7.
- Nguyen L, Rigo JM, Rocher V, Belachew S, Malgrange B, Rogister B, Leprince P, Moonen G. Neurotransmitters as early signals for central nervous system development. *Cell Tissue Res*. 2001 Aug;305(2):187-202.
- Okumura K, Nakamachi K, Hosoe Y, Nakajima N. Identification of a novel retinoic acid-responsive element within the lamin A/C promoter. *Biochem Biophys Res Commun*. 2000 Mar 5;269(1):197-202.
- Politis PK, Makri G, Thomaidou D, Geissen M, Rohrer H, Matsas R. BM88/CEND1 coordinates cell cycle exit and differentiation of neuronal precursors. *Proc Natl Acad Sci U S A*. 2007 Nov 6;104(45):17861-6.
- Ruediger T and Bolz J. Neurotransmitters and the development of neuronal circuits. *Adv Exp Med Biol*. 2007;621:104-15.
- Saeed AI, Bhagabati NK, Braisted JC, Liang W, Sharov V, Howe EA, Li J, Thiagarajan M, White JA, Quackenbush J. TM4 microarray software suite. *Methods Enzymol*. 2006;411:134-93.

- Salani M, Anelli T, Tocco GA, Lucarini E, Mozzetta C, Poiana G, Tata AM, Biagioni S. Acetylcholine-induced neuronal differentiation: muscarinic receptor activation regulates EGR-1 and REST expression in neuroblastoma cells. *J Neurochem*. 2009 Feb;108(3):821-34.
- Sullivan T, Escalante-Alcalde D, Bhatt H, Anver M, Bhat N, Nagashima K, Stewart CL, Burke B. Loss of A-type lamin expression compromises nuclear envelope integrity leading to muscular dystrophy. *J Cell Biol*. 1999 Nov 29;147(5):913-20.
- Sasaki T, Matsuki N, Ikegaya Y. Effects of axonal topology on the somatic modulation of synaptic outputs. *J Neurosci*. 2012 Feb 22;32(8):2868-76.
- Schlager MA, Kapitein LC, Grigoriev I, Burzynski GM, Wulf PS, Keijzer N, de Graaff E, Fukuda M, Shepherd IT, Akhmanova A, Hoogenraad CC. Pericentrosomal targeting of Rab6 secretory vesicles by Bicaudal-D-related protein 1 (BICDR-1) regulates neurogenesis. *EMBO J*. 2010 May 19;29(10):1637-51.
- Shah K, Lahiri DK. Cdk5 activity in the brain - multiple paths of regulation. *J Cell Sci*. 2014 Jun 1;127(Pt 11):2391-400.
- Smith ER, Zhang XY, Capo-Chichi CD, Chen X, Xu XX. Increased expression of Syne1/nesprin-1 facilitates nuclear envelope structure changes in embryonic stem cell differentiation. *Dev Dyn*. 2011 Oct;240(10):2245-55.
- Street M, Marsh SJ, Stabach PR, Morrow JS, Brown DA, Buckley NJ. Stimulation of G $\alpha$ q-coupled M1 muscarinic receptor causes reversible spectrin redistribution mediated by PLC, PKC and ROCK. *J Cell Sci*. 2006 Apr 15;119(Pt 8):1528-36.
- Susuki K and Rasband MN. Spectrin and ankyrin-based cytoskeletons at polarized domains in myelinated axons. *Exp Biol Med (Maywood)*. 2008 Apr;233(4):394-400.

- Tanabe K, Yamazaki H, Inaguma Y, Asada A, Kimura T, Takahashi J, Taoka M, Ohshima T, Furuichi T, Isobe T, Nagata K, Shirao T, Hisanaga S. Phosphorylation of drebrin by cyclin-dependent kinase 5 and its role in neuronal migration. *PLoS One*. 2014 Mar 17;9(3):e92291.
- Teber I, Köhling R, Speckmann EJ, Barnekow A, Kremerskothen J. Muscarinic acetylcholine receptor stimulation induces expression of the activity-regulated cytoskeleton-associated gene (ARC). *Brain Res Mol Brain Res*. 2004 Feb 5;121(1-2):131-6.
- Tsai LH and Gleeson JG. Nucleokinesis in neuronal migration. *Neuron*. 2005 May 5;46(3):383-8.
- Van Haren J, Draegestein K, Keijzer N, Abrahams JP, Grosveld F, Peeters PJ, Moechars D, Galjart N. Mammalian Navigators are microtubule plus-end tracking proteins that can reorganize the cytoskeleton to induce neurite-like extensions. *Cell Motil Cytoskeleton*. 2009 Oct;66(10):824-38.
- Wanschers B, Van de Vorstenbosch R, Wijers M, Wieringa B, King SM, Fransen J (2008) Rab6 family proteins interact with the dynein light chain protein DYNLRB1. *Cell Motil Cytoskeleton* 65: 183–196
- Weigmann A, Corbeil D, Hellwig A, Huttner WB. Prominin, a novel microvilli-specific polytopic membrane protein of the apical surface of epithelial cells, is targeted to plasmalemmal protrusions of non-epithelial cells. *Proc Natl Acad Sci U S A*. 1997 Nov 11;94(23):12425-30.
- Wessler I, Kirkpatrick CJ. Acetylcholine beyond neurons: the non-neuronal cholinergic system in humans. *Br J Pharmacol*. 2008 Aug;154(8):1558-71.
- Wiche G and Winter L. Plectin isoforms as organizers of intermediate filament cytoarchitecture. *Bioarchitecture*. 2011 Jan;1(1):14-20.
- Wichterle H, Garcia-Verdugo JM, Alvarez-Buylla A. Direct evidence for homotypic, glia-independent neuronal migration. *Neuron*. 1997 May;18(5):779-91.

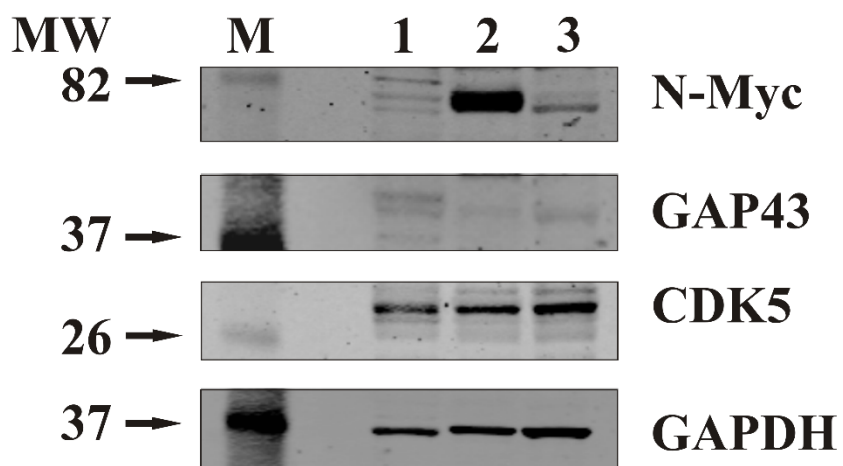


- Wilhelmsen K, Litjens SH, Kuikman I, Tshimbalanga N, Janssen H, van den Bout I, Raymond K, Sonnenberg A. Nesprin-3, a novel outer nuclear membrane protein, associates with the cytoskeletal linker protein plectin. *J Cell Biol.* 2005 Dec 5;171(5):799-810.
- Wilson KL and Foisner R. Lamin-binding Proteins. *Cold Spring Harb Perspect Biol.* 2010 Apr;2(4):a000554.
- Yokoyama T, Copeland NG, Jenkins NA, Montgomery CA, Elder FF, Overbeek PA. Reversal of left-right asymmetry: a situs inversus mutation. *Science.* 1993 Apr 30;260(5108):679-82.
- Zhang Q, Ragnauth C, Greener MJ, Shanahan CM, Roberts RG. The nesprins are giant actin-binding proteins, orthologous to *Drosophila melanogaster* muscle protein MSP-300. *Genomics.* 2002 Nov;80(5):473-81.
- Zhang X, Lei K, Yuan X, Wu X, Zhuang Y, Xu T, Xu R, Han M. SUN1/2 and Syne/Nesprin-1/2 complexes connect centrosome to the nucleus during neurogenesis and neuronal migration in mice. *Neuron.* 2009 Oct 29;64(2):173-87.
- Zhong Z, Chang SA, Kalinowski A, Wilson KL, Dahl KN. Stabilization of the spectrin-like domains of nesprin-1 $\alpha$  by the evolutionarily conserved "adaptive" domain. *Cell Mol Bioeng.* 2010 Jun 1;3(2):139-150.

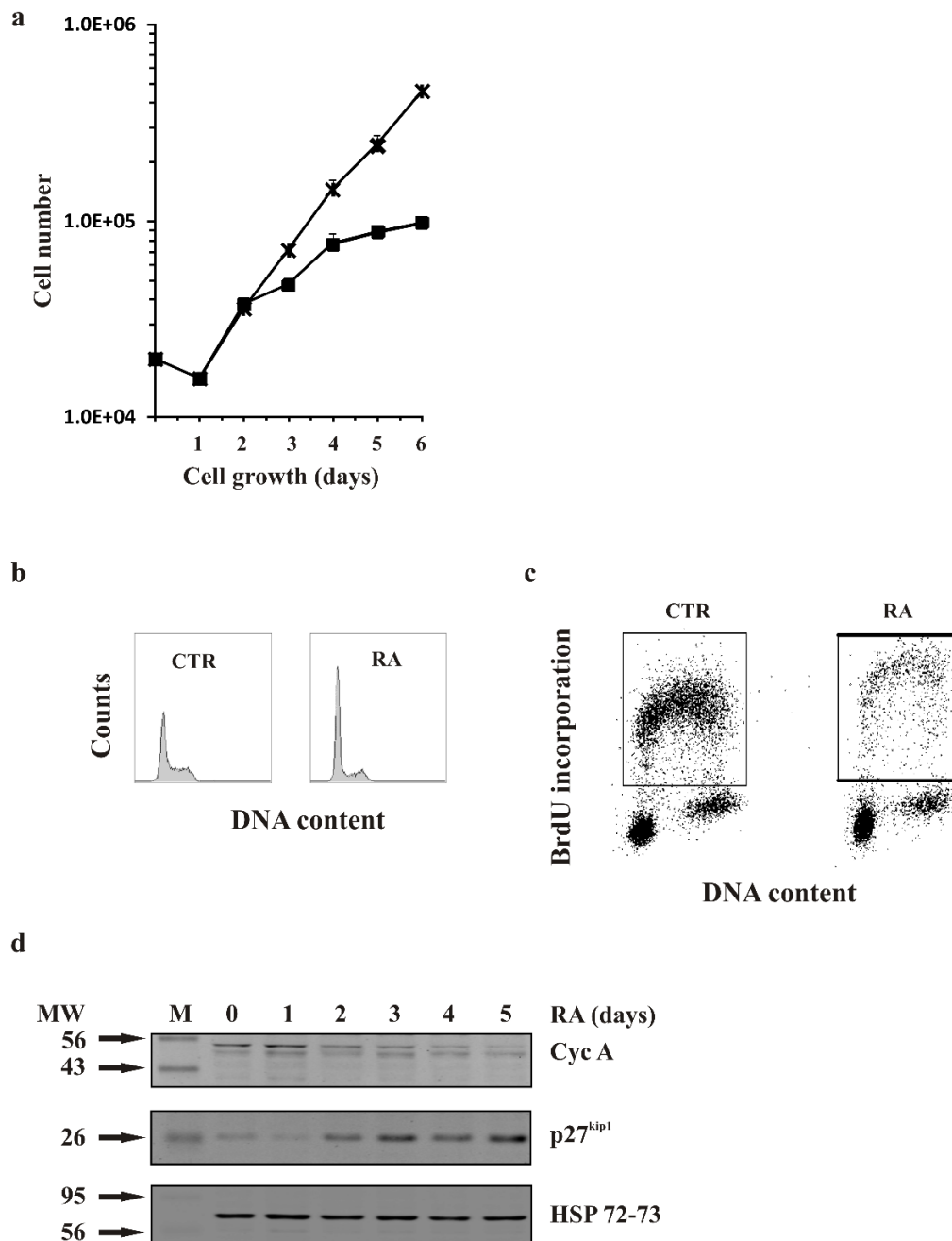
## **Chapter 4**

- Berger-Sweeney J and Hohmann CF. Behavioral consequences of abnormal cortical development: insights into developmental disabilities. *Behav Brain Res.* 1997 Jul;86(2):121-42.
- Blaschke AJ, Staley K, Chun J. Widespread programmed cell death in proliferative and postmitotic regions of the fetal cerebral cortex. *Development.* 1996 Apr;122(4):1165-74.
- Blaschke AJ, Weiner JA, Chun J. Programmed cell death is a universal feature of embryonic and postnatal neuroproliferative regions throughout the central nervous system. *J Comp Neurol.* 1998 Jun 22;396(1):39-50.
- Doherty P, Williams G, Williams EJ. CAMs and axonal growth: a critical evaluation of the role of calcium and the MAPK cascade. *Mol Cell Neurosci.* 2000 Oct;16(4):283-95.
- Jacobs WB, Govoni G, Ho D, Atwal JK, Barnabe-Heider F, Keyes WM, Mills AA, Miller FD, Kaplan DR. p63 is an essential proapoptotic protein during neural development. *Neuron.* 2005 Dec 8;48(5):743-56.
- Kandel E, Schwartz J, Jessell T, Jessell TM, Schwartz JH. *Principles of Neural Science*, Fourth Edition. McGraw-Hill Medical Publishing Division. 2000 Jan.
- Kristiansen M and Ham J. Programmed cell death during neuronal development: the sympathetic neuron model. *Cell Death Differ.* 2014 Jul;21(7):1025-35.
- Lauder JM and Schambra UB. Morphogenetic roles of acetylcholine. *Environ Health Perspect.* 1999 Feb;107 Suppl 1:65-9.
- Lossi L, Castagna C, Merighi A. Neuronal cell death: an overview of its different forms in central and peripheral neurons. *Methods Mol Biol.* 2015;1254:1-18.

- Manent JB and Represa A. Neurotransmitters and brain maturation: early paracrine actions of GABA and glutamate modulate neuronal migration. *Neuroscientist*. 2007 Jun;13(3):268-79.
- Raff MC. Social controls on cell survival and cell death. *Nature*. 1992 Apr 2;356(6368):397-400.
- Rao SM, Jacobson M. *Developmental Neurobiology*, Fourth Edition. Kluwer Academic/Plenum Publishers, New York. 2005.
- Sommer L and Rao M. Neural stem cells and regulation of cell number. *Prog Neurobiol*. 2002 Jan;66(1):1-18.
- Thomaidou D, Mione MC, Cavanagh JF, Parnavelas JG. Apoptosis and its relation to the cell cycle in the developing cerebral cortex. *J Neurosci*. 1997 Feb 1;17(3):1075-85.
- Voyvodic JT. Cell death in cortical development: How much? Why? So what? *Neuron*. 1996 Apr;16(4):693-6.
- Wei MC, Zong WX, Cheng EH, Lindsten T, Panoutsakopoulou V, Ross AJ, Roth KA, MacGregor GR, Thompson CB, Korsmeyer SJ. Proapoptotic BAX and BAK: a requisite gateway to mitochondrial dysfunction and death. *Science*. 2001 Apr 27;292(5517):727-30
- Yeo W, Gautier J. Early neural cell death: dying to become neurons. *Dev Biol*. 2004 Oct 15;274(2):233-44.

**APPENDIX A****Supplementary materials Chapter 2****Supplementary Figure 1**

**Supplementary Figure 1.** Comparative expression of the indicated proteins in embryonic neural progenitors (1), LAN-5 (2) and SK-N-AS (3) cells. GAPDH expression was used to normalise protein loading. The experiment was repeated three times with similar results. M, molecular weight markers; MW, molecular weight.

**Supplementary Figure 2**

**Supplementary Figure 2. Analysis of cell proliferation in differentiating LAN-5 cells** **a)** Growth curves of control (\*) or RA-treated (■) LAN-5 cells. **b)** DNA content histograms in CTR and RA treated cells. **c)** Representative BrdU cytograms in LAN-5 control (CTR) and RA-treated (RA) cells as evaluated by flow cytometry. In the insert are the DNA synthesising cells that are positive for BrdU incorporation; the number represents the fraction of BrdU-positive cells. **d)** Representative blots of the indicated proteins in LAN-5 cells induced to differentiate for 5 days. Untreated control (0). HSP 72-73 expression was used to normalise protein loading. The experiment was repeated three times showing similar results. M, molecular weight markers; MW, molecular weight.

**RT<sup>2</sup> Profiler™ PCR Array Human p53 Signaling Pathway (PAHS-027A)**

Position	Unigene	GeneBank	Symbol	Description	Gene Name
A01	Hs.552567	NM_001160	APAF1	Apoptotic peptidase activating factor 1	APAF-1, CED4
A02	Hs.367437	NM_000051	ATM	Ataxia telangiectasia mutated	AT1, ATA, ATC, ATD, ATDC, ATE, TEL1, TELO1
A03	Hs.271791	NM_001184	ATR	Ataxia telangiectasia and Rad3 related	FCTCS, FRP1, MEC1, SCKL, SCKL1
A04	Hs.194654	NM_001702	BAI1	Brain-specific angiogenesis inhibitor 1	GDAIF
A05	Hs.624291	NM_004324	BAX	BCL2-associated X protein	BCL2L4
A06	Hs.150749	NM_000633	BCL2	B-cell CLL/lymphoma 2	Bcl-2, PPP1R50
A07	Hs.227817	NM_004049	BCL2A1	BCL2-related protein A1	ACC-1, ACC-2, BCL2L5, BFL1, GRS, HBPA1
A08	Hs.591054	NM_001196	BID	BH3 interacting domain death agonist	FP497
A09	Hs.744872	NM_001168	BIRC5	Baculoviral IAP repeat containing 5	API4, EPR-1
A10	Hs.194143	NM_007294	BRCA1	Breast cancer 1, early onset	BRCAI, BRCC1, BROVCA1, IRIS, PNCA4, PPP1R53, PSCP, RNF53
A11	Hs.34012	NM_000059	BRCA2	Breast cancer 2, early onset	BRCC2, BROVCA2, FACD, FAD, FAD1, FANCB, FANCD, FANCD1, GLM3, PNCA2
A12	Hs.519162	NM_006763	BTG2	BTG family, member 2	PC3, TIS21
B01	Hs.368982	NM_032982	CASP2	Caspase 2, apoptosis-related cysteine peptidase	CASP-2, ICH1, NEDD-2, NEDD2, PPP1R57
B02	Hs.329502	NM_001229	CASP9	Caspase 9, apoptosis-related cysteine peptidase	APAF-3, APAF3, ICE-LAP6, MCH6, PPP1R56
B03	Hs.194698	NM_004701	CCNB2	Cyclin B2	HsT17299
B04	Hs.727669	NM_057749	CCNE2	Cyclin E2	CYCE2
B05	Hs.740456	NM_004354	CCNG2	Cyclin G2	-
B06	Hs.292524	NM_001239	CCNH	Cyclin H	CAK, p34, p37
B07	Hs.732435	NM_001786	CDK1	Cyclin-dependent kinase 1	CDC2, CDC28A, P34CDC2
B08	Hs.437705	NM_001789	CDC25A	Cell division cycle 25 homolog A (S. pombe)	CDC25A2
B09	Hs.656	NM_001790	CDC25C	Cell division cycle 25 homolog C (S. pombe)	CDC25, PPP1R60
B10	Hs.95577	NM_000075	CDK4	Cyclin-dependent kinase 4	CMM3, PSK-J3
B11	Hs.732576	NM_000389	CDKN1A	Cyclin-dependent kinase inhibitor 1A (p21, Cip1)	CAP20, CDKN1, CIP1, MDA-6, P21,

					SDI1, WAF1, p21CIP1
B12	Hs.512599	NM_000077	CDKN2A	Cyclin-dependent kinase inhibitor 2A (melanoma, p16, inhibits CDK4)	ARF, CDK4I, CDKN2, CMM2, INK4, INK4A, MLM, MTS-1, MTS1, P14, P14ARF, P16, P16-INK4A, P16INK4, P16INK4A, P19, P19ARF, TP16
C01	Hs.595920	NM_001274	CHEK1	CHK1 checkpoint homolog (S. pombe)	CHK1
C02	Hs.505297	NM_007194	CHEK2	CHK2 checkpoint homolog (S. pombe)	CDS1, CHK2, HuCds1, LFS2, PP1425, RAD53, hCds1
C03	Hs.591016	NM_003805	CRADD	CASP2 and RIPK1 domain containing adaptor with death domain	MRT34, RAIDD
C04	Hs.202672	NM_001379	DNMT1	DNA (cytosine-5-)-methyltransferase 1	ADCADN, AIM, CXXC9, DNMT, HSN1E, MCMT
C05	Hs.654393	NM_005225	E2F1	E2F transcription factor 1	E2F-1, RBAP1, RBBP3, RBP3
C06	Hs.703174	NM_001949	E2F3	E2F transcription factor 3	E2F-3
C07	Hs.708393	NM_001964	EGR1	Early growth response 1	AT225, G0S30, KROX-24, NGFI-A, TIS8, ZIF-268, ZNF225
C08	Hs.643514	NM_004879	EI24	Etoposide induced 2.4 mRNA	EPG4, PIG8, TP53I8
C09	Hs.208124	NM_000125	ESR1	Estrogen receptor 1	ER, ESR, ESRA, ESTRR, Era, NR3A1
C10	Hs.86131	NM_003824	FADD	Fas (TNFRSF6)-associated via death domain	MORT1
C11	Hs.2007	NM_000639	FASLG	Fas ligand (TNF superfamily, member 6)	ALPS1B, APT1LG1, APTL, CD178, CD95-L, CD95L, FASL, TNFSF6
C12	Hs.220950	NM_001455	FOXO3	Forkhead box O3	AF6q21, FKHRL1, FKHRL1P2, FOXO2, FOXO3A
D01	Hs.80409	NM_001924	GADD45A	Growth arrest and DNA-damage-inducible, alpha	DDIT1, GADD45
D02	Hs.661218	NM_002066	GML	Glycosylphosphatidylinositol anchored molecule like protein	LY6DL
D03	Hs.88556	NM_004964	HDAC1	Histone deacetylase 1	GON-10, HD1, RPD3, RPD3L1
D04	Hs.591588	NM_000189	HK2	Hexokinase 2	HKII, HXK2
D05	Hs.93177	NM_002176	IFNB1	Interferon, beta 1, fibroblast	IFB, IFF, IFNB
D06	Hs.714012	NM_000875	IGF1R	Insulin-like growth factor 1	CD221, IGFIR, IGFR,

				receptor	JTK13
D07	Hs.654458	NM_000600	IL6	Interleukin 6 (interferon, beta 2)	BSF2, HGF, HSF, IFNB2, IL-6
D08	Hs.696684	NM_002228	JUN	Jun proto-oncogene	AP-1, AP1, c-Jun
D09	Hs.505033	NM_004985	KRAS	V-Ki-ras2 Kirsten rat sarcoma viral oncogene homolog	C-K-RAS, CFC2, K-RAS2A, K-RAS2B, K-RAS4A, K-RAS4B, KI-RAS, KRAS1, KRAS2, NS, NS3, RASK2
D10	Hs.592290	NM_145886	PIDD	P53-induced death domain protein	LRDD
D11	Hs.632486	NM_021960	MCL1	Myeloid cell leukemia sequence 1 (BCL2-related)	BCL2L3, EAT, MCL1-ES, MCL1L, MCL1S, Mcl-1, TM, bcl2-L-3, mcl1, EAT
D12	Hs.733536	NM_002392	MDM2	Mdm2 p53 binding protein homolog (mouse)	ACTFS, HDMX, hdm2
E01	Hs.497492	NM_002393	MDM4	Mdm4 p53 binding protein homolog (mouse)	HDMX, MDMX, MRP1
E02	Hs.195364	NM_000249	MLH1	MutL homolog 1, colon cancer, nonpolyposis type 2 (E. coli)	COCA2, FCC2, HNPCC, HNPCC2, hMLH1
E03	Hs.597656	NM_000251	MSH2	MutS homolog 2, colon cancer, nonpolyposis type 1 (E. coli)	COCA1, FCC1, HNPCC, HNPCC1, LCFS2
E04	Hs.202453	NM_002467	MYC	V-myc myelocytomatosis viral oncogene homolog (avian)	MRTL, MYCC, bHLHe39, c-Myc
E05	Hs.181768	NM_002478	MYOD1	Myogenic differentiation 1	MYF3, MYOD, PUM, bHLHe1
E06	Hs.113577	NM_000267	NF1	Neurofibromin 1	NFNS, VRNF, WSS
E07	Hs.618430	NM_003998	NFKB1	Nuclear factor of kappa light polypeptide gene enhancer in B-cells 1	EBP-1, KBF1, NF-kB1, NF-kappa-B, NF-kappaB, NFKB-p105, NFKB-p50, NFkappaB, p105, p50
E08	Hs.160953	NM_022112	TP53AIP1	Tumor protein p53 regulated apoptosis inducing protein 1	P53AIP1
E09	Hs.533055	NM_003884	KAT2B	K(lysine) acetyltransferase 2B	CAF, P, P, CAF, PCAF
E10	Hs.20930	NM_020418	PCBP4	Poly(rC) binding protein 4	CBP, LIP4, MCG10
E11	Hs.744934	NM_182649	PCNA	Proliferating cell nuclear antigen	-
E12	Hs.286073	NM_003620	PPM1D	Protein phosphatase, Mg <sup>2+</sup> /Mn <sup>2+</sup> dependent, 1D	PP2C-DELTA, WIP1
F01	Hs.366401	NM_003981	PRC1	Protein regulator of cytokinesis 1	ASE1
F02	Hs.708867	NM_002737	PRKCA	Protein kinase C, alpha	AAG6, PKC-alpha, PKCA, PRKACA
F03	Hs.500466	NM_000314	PTEN	Phosphatase and tensin homolog	10q23del, BZS, CWS1, DEC, GLM2, MHAM, MMAC1, PTEN1, TEP1



F04	Hs.350966	NM_004219	PTTG1	Pituitary tumor-transforming 1	EAP1, HPTTG, PTTG, TUTR1
F05	Hs.408528	NM_000321	RB1	Retinoblastoma 1	OSRC, RB, p105-Rb, pRb, pp110
F06	Hs.502875	NM_021975	RELA	V-rel reticuloendotheliosis viral oncogene homolog A (avian)	NFKB3, p65
F07	Hs.100890	NM_019845	RPRM	Reprimo, TP53 dependent G2 arrest mediator candidate	REPRIMO
F08	Hs.591336	NM_014454	SESN1	Sestrin 1	PA26, SEST1
F09	Hs.469543	NM_031459	SESN2	Sestrin 2	HI95, SES2, SEST2
F10	Hs.731827	NM_003031	SIAH1	Seven in absentia homolog 1 (Drosophila)	SIAH1A
F11	Hs.369779	NM_012238	SIRT1	Sirtuin 1	SIR2L1
F12	Hs.743244	NM_007315	STAT1	Signal transducer and activator of transcription 1, 91kDa	CANDF7, ISGF-3, STAT91
G01	Hs.386390	NM_006354	TADA3	Transcriptional adaptor 3	ADA3, NGG1, STAF54, TADA3L, hADA3
G02	Hs.241570	NM_000594	TNF	Tumor necrosis factor	DIF, TNF-alpha, TNFA, TNFSF2
G03	Hs.521456	NM_003842	TNFRSF10B	Tumor necrosis factor receptor superfamily, member 10b	CD262, DR5, KILLER, KILLER, DR5, TRAIL-R2, TRAILR2, TRICK2, TRICK2A, TRICK2B, TRICKB, ZTNFR9
G04	Hs.213467	NM_003840	TNFRSF10D	Tumor necrosis factor receptor superfamily, member 10d, decoy with truncated death domain	CD264, DCR2, TRAIL-R4, TRAILR4, TRUNDD
G05	Hs.740601	NM_000546	TP53	Tumor protein p53	BCC7, LFS1, P53, TRP53
G06	Hs.523968	NM_005426	TP53BP2	Tumor protein p53 binding protein, 2	53BP2, ASPP2, BBP, P53BP2, PPP1R13A
G07	Hs.192132	NM_005427	TP73	Tumor protein p73	P73
G08	Hs.137569	NM_003722	TP63	Tumor protein p63	AIS, B(p51A), B(p51B), EEC3, KET, LMS, NBP, OFC8, RHS, SHFM4, TP53CP, TP53L, TP73L, p40, p51, p53CP, p63, p73H, p73L
G09	Hs.522506	NM_021138	TRAF2	TNF receptor-associated factor 2	MGC:45012, TRAP, TRAP3
G10	Hs.370854	NM_000368	TSC1	Tuberous sclerosis 1	LAM, TSC
G11	Hs.591980	NM_000378	WT1	Wilms tumor 1	AWT1, EWS-WT1, GUD, NPHS4, WAGR, WIT-2, WT33
G12	Hs.388739	NM_021141	XRCC5	X-ray repair complementing defective repair in Chinese	KARP-1, KARP1, KU80, KUB2, Ku86,

				hamster cells 5 (double-strand-break rejoining)	NFIV
H01	Hs.534255	NM_004048	B2M	Beta-2-microglobulin	-
H02	Hs.412707	NM_000194	HPRT1	Hypoxanthine phosphoribosyltransferase 1	HGPRT, HPRT
H03	Hs.523185	NM_012423	RPL13A	Ribosomal protein L13a	L13A, TSTA1
H04	Hs.544577	NM_002046	GAPDH	Glyceraldehyde-3-phosphate dehydrogenase	G3PD, GAPD
H05	Hs.520640	NM_001101	ACTB	Actin, beta	BRWS1, PS1TP5BP1
H06	N/A	SA_00105	HGDC	Human Genomic DNA Contamination	HIGX1A
H07	N/A	SA_00104	RTC	Reverse Transcription Control	RTC
H08	N/A	SA_00104	RTC	Reverse Transcription Control	RTC
H09	N/A	SA_00104	RTC	Reverse Transcription Control	RTC
H10	N/A	SA_00103	PPC	Positive PCR Control	PPC
H11	N/A	SA_00103	PPC	Positive PCR Control	PPC
H12	N/A	SA_00103	PPC	Positive PCR Control	PPC

## APPENDIX B

## Supplementary materials Chapter 3

David categories genes list Figure 3Common categories 2/4<sub>RA vs CTR</sub> /N18TG2<sub>RA vs CTR</sub> Down**GO:0055114~oxidation reduction**

ID	Gene Name
A_55_P1953301	sorbitol dehydrogenase
A_52_P498193	aldehyde dehydrogenase 1 family, member L2
A_55_P2090214	cytochrome b5 reductase 2
A_51_P291749	peroxisomal trans-2-enoyl-CoA reductase
A_51_P481159	carbonyl reductase 3
A_55_P2095196	RIKEN cDNA 2310005E10 gene
A_55_P2183288	crystallin, zeta (quinone reductase)-like 1
A_51_P128987	aldo-keto reductase family 1, member B8
A_55_P2130388	microtubule associated monooxygenase, calponin and LIM domain containing 1
A_55_P2043622	glyoxylate reductase/hydroxypyruvate reductase
A_51_P251352	solute carrier family 25 (mitochondrial carrier, adenine nucleotide translocator), member 13
A_51_P486618	RIKEN cDNA 2310005E10 gene
A_55_P2028798	NAD(P)H dehydrogenase, quinone 2
A_55_P2024245	5,10-methylenetetrahydrofolate reductase
A_55_P1990919	selenoprotein X 1

**GO:0000786~nucleosome**

ID	Gene Name
A_51_P270949	histone cluster 1, H1b
A_51_P464822	histone cluster 1, H1e
A_52_P420466, A_55_P2084631	histone cluster 1, H2ad; histone cluster 1, H2ae; histone cluster 1, H2ag; histone cluster 1, H2ah; histone cluster 1, H2ai; similar to histone 2a; histone cluster 1, H2an; histone cluster 1, H2ao; histone cluster 1, H2ac; histone cluster 1, H2ab
A_55_P2084666	histone cluster 1, H2af
A_52_P498208	histone cluster 1, H2ak
A_55_P1972018	histone cluster 1, H4k; histone cluster 1, H4m; histone cluster 4, H4; similar to germinal histone H4 gene; histone cluster 1, H4h; histone cluster 1, H4j; histone cluster 1, H4i; histone cluster 1, H4d; histone cluster 1, H4c; histone cluster 1, H4f; histone cluster 1, H4b; histone cluster 1, H4a; histone cluster 2, H4; similar to histone H4

**IPR013091:EGF calcium-binding**

ID	Gene Name
A_55_P2111355	EGF-like domain 7
A_55_P2185332	cysteine-rich with EGF-like domains 1
A_65_P08768	fibulin 1
A_52_P590535	fibulin 2

**GO:0006631~fatty acid metabolic process**

ID	Gene Name
A_51_P284608	CD74 antigen (invariant polypeptide of major histocompatibility complex, class II antigen-associated)
A_55_P2037528	acyl-CoA synthetase family member 3
A_51_P380699	acyl-CoA synthetase long-chain family member 6
A_51_P489153	carnitine O-octanoyltransferase

**Common categories 2/4 <sub>RA vs CTR</sub> /N18TG2 <sub>RA vs CTR</sub> Up****GO:0048598~embryonic morphogenesis**

ID	Gene Name
A_51_P384754	LIM domain binding 1
A_51_P501844	cytochrome P450, family 26, subfamily b, polypeptide 1
A_30_P01019818, A_55_P2024993	homeo box B4
A_55_P2000289	mab-21-like 2 (C. elegans)

**GO:0030528~transcription regulator activity**

ID	Gene Name
A_51_P384754	LIM domain binding 1
A_55_P2091601	collagen, type XI, alpha 2
A_30_P01019818, A_55_P2024993	homeo box B4
A_55_P2001793	myelin transcription factor 1-like
A_55_P2208579	one cut domain, family member 2
A_55_P2083213	purine rich element binding protein B
A_52_P158431	teashirt zinc finger family member 2
A_51_P446583	zinc finger protein 445

**David categories genes list Figure 4****Differential categories 2/4<sub>RA vs CTR</sub> /N18TG2<sub>RA vs CTR</sub> Down in N18****GO:0008092~cytoskeletal protein binding**

ID	Gene Name
A_51_P303906	ARP2 actin-related protein 2 homolog (yeast); predicted gene 6828
A_51_P466288	FERM domain containing 5 FERM, RhoGEF (Arhgef) and pleckstrin domain protein 1 (chondrocyte-derived); similar to FERMRhoGEF
A_52_P330395	(Arhgef) and pleckstrin domain protein 1
A_52_P579531	PDZ and LIM domain 3
A_55_P2002963	coronin, actin binding protein 1A
A_55_P1956667	cytoplasmic FMR1 interacting protein 1
A_55_P2195157	drebrin 1
A_55_P1960097	erythrocyte protein band 4.1-like 3
A_55_P2013948	gelsolin
A_55_P2062793	microfibrillar-associated protein 2
A_55_P1964193	microtubule-associated protein 1B
A_52_P22763	microtubule-associated protein 2
A_55_P1955039	myosin IB
A_52_P367520	nexilin
A_52_P225570, A_55_P2130890	parvin, alpha predicted gene 3787; predicted gene 9844; predicted gene 8034; similar to thymosin, beta 10; thymosin, beta 10
A_55_P2092085	10
A_55_P1968295	protein kinase C and casein kinase substrate in neurons 3
A_55_P2008889	thymosin beta 15b1; thymosin beta 15b2; Tmsb15b1- Tmsb15b2 readthrough transcript
A_55_P2032818	tripartite motif-containing 2
A_52_P315976	tropomyosin 2, beta
A_52_P260555	villin 1

**GO:0051493~regulation of cytoskeleton organization**

ID	Gene Name
A_55_P2167112	KN motif and ankyrin repeat domains 2
A_55_P2002963	coronin, actin binding protein 1A
A_55_P2013948	gelsolin
A_55_P1964193	microtubule-associated protein 1B
A_52_P22763	microtubule-associated protein 2
A_52_P367520	nexilin predicted gene 3787; predicted gene 9844; predicted gene 8034; similar to thymosin, beta 10; thymosin, beta 10
A_55_P2092085	10
A_66_P129873	predicted gene 6477; predicted gene 9118; nucleophosmin 1; similar to Nucleophosmin (NPM)

(Nucleolar phosphoprotein B23) (Numatrin) (Nucleolar protein NO38); predicted gene 7289; predicted gene 5611  
 A\_51\_P140690 stathmin-like 3  
 thymosin beta 15b1; thymosin beta 15b2; Tmsb15b1-  
 A\_55\_P2008889 Tmsb15b2 readthrough transcript  
 A\_52\_P260555 villin 1

### SP\_PIR\_KEYWORDS~neurogenesis

ID	Gene Name
A_51_P176352	N-myc downstream regulated gene 2
A_55_P2031496	RUN and FYVE domain containing 3
A_55_P1956667	cytoplasmic FMR1 interacting protein 1
A_55_P2204804	doublecortin-like kinase 1
A_55_P2195157	drebrin 1
A_55_P2013730	immunoglobulin superfamily containing leucine-rich repeat 2
A_55_P2017710	immunoglobulin superfamily, member 9
A_52_P93910	neuropilin 2
A_30_P01033574, A_30_P01031735, A_30_P01031414, A_30_P01028040, A_30_P01031208, A_30_P01033124, A_30_P01022868	tubulin tyrosine ligase-like family, member 7
A_55_P2102335	zinc finger protein 423; similar to mKIAA0760 protein

### GO:0008360~regulation of cell shape

ID	Gene Name
A_52_P155554	CDC42 effector protein (Rho GTPase binding) 2
A_55_P1962039	annexin A7
A_55_P2002963	coronin, actin binding protein 1A
A_55_P1956667	cytoplasmic FMR1 interacting protein 1
A_55_P2130178	fibronectin 1

### Differential categories 2/4<sub>RA vs CTR</sub> /N18TG2<sub>RA vs CTR</sub> Down in 2/4

#### GO:0000278~mitotic cell cycle

ID	Gene Name
A_51_P314907	DBF4 homolog (S. cerevisiae)
A_51_P393958	F-box protein 5
A_51_P170696	HAUS augmin-like complex, subunit 1
A_51_P312310	Mdm2, transformed 3T3 cell double minute p53 binding protein

A_51_P413539	NIMA (never in mitosis gene a)-related expressed kinase 6
A_52_P139650	RIKEN cDNA 2810433K01 gene
A_55_P2056473	SPC24, NDC80 kinetochore complex component, homolog (S. cerevisiae)
A_55_P1965154	SPC25, NDC80 kinetochore complex component, homolog (S. cerevisiae)
A_52_P509710	ZW10 interactor
A_66_P134542	anillin, actin binding protein
A_55_P1988228	asp (abnormal spindle)-like, microcephaly associated (Drosophila)
A_55_P1980636	aurora kinase A
A_55_P1983769,	baculoviral IAP repeat-containing 5
A_55_P1983773	budding uninhibited by benzimidazoles 1 homolog (S. cerevisiae)
A_51_P123405	budding uninhibited by benzimidazoles 1 homolog, beta (S. cerevisiae)
A_51_P490509	cell division cycle 123 homolog (S. cerevisiae)
A_55_P2008735	cell division cycle 2 homolog A (S. pombe)
A_55_P2048588	cell division cycle 20 homolog (S. cerevisiae)
A_55_P1996946	cell division cycle 25 homolog B (S. pombe)
A_52_P612382	cell division cycle associated 2
A_52_P211223	cell division cycle associated 3
A_52_P628067	cell division cycle associated 5
A_51_P125135	cell division cycle associated 8
A_51_P155142,	cell division cycle associated 8
A_55_P2170681	centromere protein E
A_51_P164014	cyclin A2
A_51_P481920	cyclin F
A_55_P2039324	expressed sequence C79407
A_52_P148212	growth arrest and DNA-damage-inducible 45 alpha
A_51_P296608	inner centromere protein
A_55_P2028054,	kinesin family member 18A
A_55_P1978201	kinesin family member 20B
A_51_P332355	kinetochore associated 1
A_55_P2109717	non-SMC condensin I complex, subunit H
A_51_P408071	non-SMC condensin II complex, subunit G2
A_55_P1967291	nuclear distribution gene E homolog 1 (A nidulans)
A_51_P424810	nucleolar and spindle associated protein 1
A_55_P2165334	pituitary tumor-transforming gene 1
A_51_P240453	polo-like kinase 1 (Drosophila)
A_55_P1987499	polyamine-modulated factor 1
A_51_P344566	polymerase (DNA directed), alpha 1
A_55_P1966528	predicted gene 4799; TAF10 RNA polymerase II, TATA
A_51_P415905	box binding protein (TBP)-associated factor
A_66_P129029,	
A_66_P120260	
A_55_P1952256,	
A_55_P2103706,	
A_55_P2128668,	predicted gene 8416; predicted gene 5593; cyclin B1;
A_55_P2065671	similar to cyclin B1; predicted gene 4870

A_55_P2059686	regulator of chromosome condensation 1
A_52_P76034	regulator of chromosome condensation 2; hypothetical protein LOC100047340
A_51_P300936	retinoblastoma binding protein 8
A_51_P487999	shugoshin-like 1 ( <i>S. pombe</i> )
A_55_P2076048	similar to Nuf2 protein; NUF2, NDC80 kinetochore complex component, homolog ( <i>S. cerevisiae</i> )
A_55_P1975685	similar to nucleoporin 37; nucleoporin 37
A_55_P2133255	similar to spindle assembly checkpoint protein; MAD2
A_51_P513530	mitotic arrest deficient-like 1 (yeast)
A_55_P2068663,	sperm associated antigen 5
A_55_P2043862	stathmin 1; predicted gene 11223; predicted gene 6393
A_55_P2172274	structural maintenance of chromosomes 2
A_55_P2037712	structural maintenance of chromosomes 4
A_55_P2000304	telomeric repeat binding factor 1
A_51_P336721	timeless interacting protein
A_51_P451151,	
A_55_P1996941	ubiquitin-conjugating enzyme E2C; predicted gene 8956

#### **GO:0000779~condensed chromosome, centromeric region**

ID	Gene Name
A_52_P139650	RIKEN cDNA 2810433K01 gene
A_55_P2056473	SPC24, NDC80 kinetochore complex component, homolog ( <i>S. cerevisiae</i> )
A_55_P1965154	SPC25, NDC80 kinetochore complex component, homolog ( <i>S. cerevisiae</i> )
A_52_P509710	ZW10 interactor
A_51_P123405	budding uninhibited by benzimidazoles 1 homolog ( <i>S. cerevisiae</i> )
A_51_P490509	budding uninhibited by benzimidazoles 1 homolog, beta ( <i>S. cerevisiae</i> )
A_66_P121459	centromere protein A
A_51_P164014	centromere protein E
A_52_P304947	centromere protein N
A_55_P2028054,	
A_55_P1978201	inner centromere protein
A_51_P408071	kinetochore associated 1
A_55_P2165334	nuclear distribution gene E homolog 1 ( <i>A. nidulans</i> )
A_66_P118696	nucleoporin 107
A_66_P115378	origin recognition complex, subunit 2-like ( <i>S. cerevisiae</i> )
A_55_P1966528	polyamine-modulated factor 1
A_51_P487999	shugoshin-like 1 ( <i>S. pombe</i> )
A_52_P27020	shugoshin-like 2 ( <i>S. pombe</i> )
A_55_P2076048	similar to Nuf2 protein; NUF2, NDC80 kinetochore complex component, homolog ( <i>S. cerevisiae</i> )
A_55_P1975685	similar to nucleoporin 37; nucleoporin 37
A_55_P2133255	similar to spindle assembly checkpoint protein; MAD2
A_51_P513530	mitotic arrest deficient-like 1 (yeast)
	sperm associated antigen 5



**GO:0005819~spindle**

ID	Gene Name
A_51_P393958	F-box protein 5
A_51_P170696	HAUS augmin-like complex, subunit 1
A_52_P139650	RIKEN cDNA 2810433K01 gene
A_51_P369200	TPX2, microtubule-associated protein homolog (Xenopus laevis) asp (abnormal spindle)-like, microcephaly associated (Drosophila)
A_55_P1988228	aurora kinase A
A_55_P1980636	
A_55_P1983769, A_55_P1983773	baculoviral IAP repeat-containing 5
A_51_P164014	centromere protein E
A_55_P2028054, A_55_P1978201	inner centromere protein
A_51_P332355	kinesin family member 18A
A_55_P2056654	kinesin family member 22
A_51_P408071	kinetochore associated 1
A_55_P2165334	nuclear distribution gene E homolog 1 (A nidulans)
A_51_P240453	nucleolar and spindle associated protein 1 predicted gene 7743; calmodulin 3; calmodulin 2; calmodulin 1; predicted gene 7308
A_55_P2021841	proline/serine-rich coiled-coil 1
A_55_P2429225	protein regulator of cytokinesis 1
A_55_P1988083	regulator of chromosome condensation 2; hypothetical protein LOC100047340
A_52_P76034	similar to spindle assembly checkpoint protein; MAD2
A_55_P2133255	mitotic arrest deficient-like 1 (yeast)
A_51_P513530	sperm associated antigen 5

**SP\_PIR\_KEYWORDS~dna replication**

ID	Gene Name
A_51_P314418	Bloom syndrome homolog (human)
A_51_P314907	DBF4 homolog (S. cerevisiae)
A_51_P168632	DNA primase, p49 subunit
A_51_P337089	GIN5 complex subunit 1 (Psf1 homolog)
A_66_P115378	origin recognition complex, subunit 2-like (S. cerevisiae)
A_55_P2159026, A_55_P2107357	origin recognition complex, subunit 5-like (S. cerevisiae)
A_51_P415905	polymerase (DNA directed), alpha 1
A_55_P2089035	polymerase (DNA directed), epsilon
A_66_P106090	predicted gene 6195; replication protein A3
A_55_P2159801, A_55_P2159807	replication factor C (activator 1) 4 replication factor C (activator 1) 5; similar to replication factor C 5
A_51_P246339	
A_55_P2173982	ribonucleotide reductase M2

**IPR000789:Cyclin-dependent kinase, regulatory subunit**

ID	Gene Name
A_51_P227004, A_30_P01028956	hypothetical protein LOC100045673; predicted gene 6531
A_51_P227004, A_30_P01028956, A_55_P2061495	predicted gene 10124; predicted gene 6340; CDC28 protein kinase 1b similar to Cyclin-dependent kinases regulatory subunit 2 (CKS-2); CDC28 protein kinase regulatory subunit 2; predicted gene 15452
A_55_P1965050	predicted gene 15452

**Differential categories 2/4<sub>RA vs CTR</sub> /N18TG2<sub>RA vs CTR</sub> Up in N18****GO:0031669~cellular response to nutrient levels**

ID	Gene Name
A_51_P338443	angiopoietin-like 4
A_55_P2145942	autophagy-related 16-like 1 (yeast)
A_52_P647919	similar to USF2; upstream transcription factor 2
A_55_P2002557	sterol regulatory element binding transcription factor 1

**GO:0006350~transcription**

ID	Gene Name
A_51_P161554	AT rich interactive domain 3B (BRIGHT-like)
A_55_P1990879	BTG3 associated nuclear protein
A_55_P2062598	E2F transcription factor 7
A_55_P2147842	GATA-like 1
A_55_P2101001	MAD homolog 3 (Drosophila)
A_51_P204442	PHD finger protein 19
A_55_P2018442	TATA box binding protein-like 1
A_55_P2086949	Zfp91-Cntf readthrough transcript; zinc finger protein 91; ciliary neurotrophic factor
A_55_P2168736	avian reticuloendotheliosis viral (v-rel) oncogene related B
A_66_P132855	bromodomain adjacent to zinc finger domain, 1B
A_51_P336385	death inducer-obliterator 1
A_51_P516705	endoplasmic reticulum (ER) to nucleus signalling 1
A_52_P219943	enhancer of polycomb homolog 1 (Drosophila)
A_52_P653902	enhancer of yellow 2 homolog (Drosophila); predicted gene 16373
A_51_P355753	hypermethylated in cancer 1
A_52_P381953	interferon regulatory factor 2 binding protein 1
A_66_P114543	jumonji domain containing 6
A_51_P420400, A_55_P2076871	lymphoid enhancer binding factor 1
A_55_P2147591	mediator complex subunit 27
A_55_P2033521	mediator of RNA polymerase II transcription, subunit 6 homolog (yeast)

A_55_P2176838,	
A_55_P2152437	microphthalmia-associated transcription factor
A_55_P2056120	myelin transcription factor 1-like
A_55_P2086687	nuclear factor I/B
A_51_P223776	nuclear receptor subfamily 1, group D, member 1
A_55_P2022946	paired box gene 6
A_52_P647919	similar to USF2; upstream transcription factor 2
A_55_P2002557	sterol regulatory element binding transcription factor 1
	suppressor of defective silencing 3 homolog (S. cerevisiae)
A_52_P579876	
A_51_P438805,	
A_55_P2006255	thioredoxin interacting protein
A_52_P606679	transcription elongation factor B (SIII), polypeptide 3
A_51_P370341	zinc finger and BTB domain containing 48
A_52_P4846	zinc finger protein 451
A_51_P488730	zinc finger protein 612
A_51_P472621	zinc finger protein 719
A_51_P424561	zinc finger protein 93; predicted gene 11677

#### **mmu03040:Spliceosome**

ID	Gene Name
A_55_P2161535	DEAD (Asp-Glu-Ala-Asp) box polypeptide 23
A_51_P250551	DEAH (Asp-Glu-Ala-His) box polypeptide 38
A_55_P2143119	HLA-B-associated transcript 1A
A_52_P672453	PRP3 pre-mRNA processing factor 3 homolog (yeast)
A_52_P869802	THO complex 3
A_51_P292877	small nuclear ribonucleoprotein 200 (U5)

#### **GO:0051028~mRNA transport**

ID	Gene Name
A_55_P2143119	HLA-B-associated transcript 1A
A_52_P869802	THO complex 3
	enhancer of yellow 2 homolog (Drosophila); predicted gene 16373
A_52_P653902	
A_51_P448447	nucleoporin like 2

#### **Differential categories 2/4<sub>RA vs CTR</sub> /N18TG2<sub>RA vs CTR</sub> Up in 2/4**

#### **GO:0043005~neuron projection**

ID	Gene Name
A_51_P312497	ATPase, Cu <sup>++</sup> transporting, alpha polypeptide
A_55_P2026530	ELKS/RAB6-interacting/CAST family member 2
A_65_P13713,	
A_52_P351925	ankyrin 3, epithelial
A_55_P2075726	catenin (cadherin associated protein), alpha 2
A_55_P2173183	cyclin-dependent kinase 5, regulatory subunit 1 (p35)

A_55_P1995040	dystrophin related protein 2
A_66_P108003	espin
A_55_P2167070	kinesin family member 5A
A_55_P2044119	kinesin light chain 1; similar to Kinesin light chain 1
A_55_P2173011	neurofascin
A_51_P469285	neuropilin 1
A_55_P1990299	oligophrenin 1
A_52_P239536	protein phosphatase 1, regulatory (inhibitor) subunit 9A sema domain, transmembrane domain (TM), and cytoplasmic domain, (semaphorin) 6A
A_55_P2249849	solute carrier family 12, member 5
A_52_P557129	synaptotagmin I
A_55_P2058957	synaptotagmin I
A_51_P182728	syntaxin 1A (brain)

### GO:0045202~synapse

ID	Gene Name
A_55_P2026530	ELKS/RAB6-interacting/CAST family member 2
A_55_P2109326	acetylcholinesterase
A_52_P351925, A_65_P13713	ankyrin 3, epithelial
A_55_P2029711	cadherin 2; similar to N-cadherin
A_52_P222026	cholinergic receptor, nicotinic, beta polypeptide 2 (neuronal)
A_55_P2173183	cyclin-dependent kinase 5, regulatory subunit 1 (p35)
A_52_P89049	discs, large homolog 2 (Drosophila)
A_52_P16232	gamma-aminobutyric acid (GABA) B receptor, 1
A_55_P1982127	glutamate receptor interacting protein 1
A_55_P1960989	neuroligin 2
A_55_P1990299	oligophrenin 1
A_55_P1956567	similar to RAB3C, member RAS oncogene family; RAB3C, member RAS oncogene family
A_55_P2108324, A_52_P197666	similar to neuroligin 3; neuroligin 3
A_51_P389988	solute carrier family 40 (iron-regulated transporter), member 1
A_55_P2187171	synaptic vesicle glycoprotein 2c
A_55_P2058957	synaptotagmin I
A_51_P182728	syntaxin 1A (brain)
A_55_P2047135	unc-13 homolog A (C. elegans)

### GO:0006928~cell motion

ID	Gene Name
A_51_P320852	CD9 antigen
A_52_P337246	ISL1 transcription factor, LIM/homeodomain
A_55_P2372877	LIM homeobox protein 4
A_52_P351925, A_65_P13713	ankyrin 3, epithelial
A_55_P2029711	cadherin 2; similar to N-cadherin
A_55_P2075726	catenin (cadherin associated protein), alpha 2

A_55_P2173183	cyclin-dependent kinase 5, regulatory subunit 1 (p35)
A_66_P135185	ets variant gene 1
A_55_P1967761	forkhead box C1
A_52_P459929	integrin alpha 1
A_55_P2173011	neurofascin
A_51_P469285	neuropilin 1
A_66_P114782, A_55_P2074281	nuclear receptor subfamily 2, group F, member 1
A_66_P105791	protein kinase C, alpha
A_55_P2249849	sema domain, transmembrane domain (TM), and cytoplasmic domain, (semaphorin) 6A
A_55_P2128283	similar to COUP-TFI; nuclear receptor subfamily 2, group F, member 2
A_55_P1958394	slit homolog 2 (Drosophila)
A_51_P106591	trinucleotide repeat containing 4

### **David categories genes list Figure 5**

#### **Common categories 2/4<sub>RA vs CTR</sub> Down**

##### **GO:0007049~cell cycle**

ID	Gene Name
A_55_P2000833	E2F transcription factor 8
A_30_P01021891	KH domain containing, RNA binding, signal transduction associated 1
A_51_P501018	NIMA (never in mitosis gene a)-related expressed kinase 2
A_52_P529570	NSL1, MIND kinetochore complex component, homolog (S. cerevisiae)
A_55_P2134804	RIKEN cDNA 2810452K22 gene; similar to cyclin-dependent kinase 2-interacting protein
A_52_P131672	RNA binding motif protein 7
A_30_P01018424, A_30_P01023090, A_30_P01021217, A_55_P1977583	annexin A11; predicted gene 2260; predicted gene 2274
A_51_P388325	calmegin
A_55_P2139112	cell division cycle 26; predicted gene 9174
A_52_P211223	cell division cycle associated 2
A_51_P331462	cell growth regulator with ring finger domain 1
A_52_P445622	chromatin modifying protein 1B; RIKEN cDNA 2610002M06 gene
A_51_P195034	establishment of cohesion 1 homolog 2 (S. cerevisiae)
A_51_P332355	kinesin family member 18A
A_51_P100174	meiosis-specific nuclear structural protein 1
A_55_P2129319	meiotic recombination 11 homolog A (S. cerevisiae)

A_55_P2017826	myeloblastosis oncogene
A_51_P205106	myeloid leukemia factor 1
A_65_P03031	non-SMC condensin II complex, subunit D3
A_55_P1980543	predicted gene 14176; similar to Chain A, Crystal Structure Of Human Rangap1-Ubc9; ubiquitin-conjugating enzyme E2I; predicted gene 5931
A_51_P286665	retinoblastoma-like 1 (p107)
A_55_P1976694	septin 11
A_55_P2017160	similar to Dual specificity protein phosphatase CDC14A (CDC14 cell division cycle 14 homolog A); CDC14 cell division cycle 14 homolog A ( <i>S. cerevisiae</i> )
A_55_P2082837	similar to Spindlin 1; spindlin 1; spindlin family, member 3
A_55_P2040295,	similar to tyrosine phosphatase; predicted gene 8783;
A_52_P516034	predicted gene 15801; predicted gene 5951; protein tyrosine phosphatase 4a1; similar to killer cell lectin-like receptor subfamily A member 2
A_51_P352264,	sirtuin 7 (silent mating type information regulation 2,
A_55_P2047748	homolog) 7 ( <i>S. cerevisiae</i> )
A_55_P2000623,	
A_52_P491861	stromal antigen 1
A_55_P2051405	tet oncogene family member 2
A_52_P179729	thioredoxin-like 4A

#### GO:0000279~M phase

ID	Gene Name
A_51_P501018	NIMA (never in mitosis gene a)-related expressed kinase 2
A_52_P529570	NSL1, MIND kinetochore complex component, homolog ( <i>S. cerevisiae</i> )
A_52_P131672	RNA binding motif protein 7
A_51_P388325	calmegin
A_55_P2139112	cell division cycle 26; predicted gene 9174
A_52_P211223	cell division cycle associated 2
A_51_P332355	kinesin family member 18A
A_51_P100174	meiosis-specific nuclear structural protein 1
A_55_P2129319	meiotic recombination 11 homolog A ( <i>S. cerevisiae</i> )
A_65_P03031	non-SMC condensin II complex, subunit D3
A_55_P1980543	predicted gene 14176; similar to Chain A, Crystal Structure Of Human Rangap1-Ubc9; ubiquitin-conjugating enzyme E2I; predicted gene 5931
A_55_P2082837	similar to Spindlin 1; spindlin 1; spindlin family, member 3
A_51_P352264,	sirtuin 7 (silent mating type information regulation 2,
A_55_P2047748	homolog) 7 ( <i>S. cerevisiae</i> )
A_55_P2000623,	
A_52_P491861	stromal antigen 1
A_52_P179729	thioredoxin-like 4A

**mmu04120:Ubiquitin mediated proteolysis**

ID	Gene Name
A_55_P2139112	cell division cycle 26; predicted gene 9174
A_55_P1970027	itchy, E3 ubiquitin protein ligase
A_55_P1980543	predicted gene 14176; similar to Chain A, Crystal Structure Of Human Rangap1-Ubc9; ubiquitin-conjugating enzyme E2I; predicted gene 5931
A_55_P2138150	protein inhibitor of activated STAT 2
A_55_P1972182	seven in absentia 1B
A_55_P1990608, A_55_P1990609	ubiquitin-conjugating enzyme E2, J1
A_55_P2138257	ubiquitin-conjugating enzyme E2D 2; predicted gene 9762
A_30_P01026871	ubiquitin-conjugating enzyme E2D 3 (UBC4/5 homolog, yeast); similar to UBE2D3; predicted gene 4596; predicted gene 15361
A_52_P665386	ubiquitin-conjugating enzyme E2M (UBC12 homolog, yeast)
A_52_P154501	ubiquitin-conjugating enzyme E2Q (putative) 2

**Common categories 2/4<sub>RA vs CTR</sub> Up****GO:0045202~synapse**

ID	Gene Name
A_55_P1956557	RAB3A, member RAS oncogene family
A_55_P2143219, A_55_P2143233	RAS, guanyl releasing protein 2
A_55_P2055463	SNAP-associated protein
A_51_P282594	SV2 related protein
A_55_P2067632	Usher syndrome 1C homolog (human)
A_55_P2052799	calcium/calmodulin-dependent serine protein kinase (MAGUK family)
A_55_P2156583	cyclin-dependent kinase 5, regulatory subunit 1 (p35)
A_55_P1962771	cytoplasmic FMR1 interacting protein 2
A_55_P2164070	glutamate receptor interacting protein 1
A_55_P2096867	growth associated protein 43
A_55_P1985433	neuregulin 1
A_55_P1954067, A_55_P1954061	neurexin II
A_51_P182572	phosphatase and actin regulator 1
A_55_P1978795	praja 2, RING-H2 motif containing
A_55_P1962219	proline rich membrane anchor 1
A_55_P2031979	sarcospan
A_51_P217336	secretory carrier membrane protein 1
A_52_P409731	secretory carrier membrane protein 5
A_52_P393607	seizure related gene 6
A_55_P1956567	similar to RAB3C, member RAS oncogene family;

A_55_P1981200	RAB3C, member RAS oncogene family similar to metabotropic glutamate receptor type 1; glutamate receptor, metabotropic 1
A_51_P389988	solute carrier family 40 (iron-regulated transporter), member 1
A_52_P62444	synapsin II
A_55_P1965219	synaptotagmin VI
A_55_P2179448,	
A_55_P1956267	synaptotagmin XI; similar to synaptotagmin XI
A_55_P1984815	syntaphilin
A_55_P2071834	talin 2

### GO:0031175~neuron projection development

ID	Gene Name
A_51_P189943	Down syndrome cell adhesion molecule
A_55_P1967010	G protein-regulated inducer of neurite outgrowth 1
A_55_P1956557	RAB3A, member RAS oncogene family
A_55_P2075726	catenin (cadherin associated protein), alpha 2
A_55_P2156583	cyclin-dependent kinase 5, regulatory subunit 1 (p35)
A_55_P2148748,	
A_55_P2204804	doublecortin-like kinase 1
A_51_P144319	ephrin A5
A_55_P2096867	growth associated protein 43
A_51_P239673	hypoxanthine guanine phosphoribosyl transferase 1
A_52_P360330	microtubule-associated protein 1B
A_52_P22763	microtubule-associated protein 2
A_52_P236448	nerve growth factor receptor (TNFR superfamily, member 16)
A_55_P2173011	neurofascin
A_66_P128909	numb-like
A_52_P526396	predicted gene 3086; atlastin GTPase 1; similar to Spg3a protein
A_51_P380013	predicted gene 3655; B-cell leukemia/lymphoma 2
A_52_P94401	reticulon 4 receptor-like 1
A_55_P1958379	slit homolog 1 (Drosophila)
A_51_P140690	stathmin-like 3
A_55_P2077188	syntaxin binding protein 1
A_52_P24308	ubiquitin carboxy-terminal hydrolase L1

### GO:0007010~cytoskeleton organization

ID	Gene Name
A_55_P2096395	CDC42 binding protein kinase alpha
A_55_P2067632	Usher syndrome 1C homolog (human)
A_55_P2024808	c-abl oncogene 1, receptor tyrosine kinase
A_55_P2195157	drebrin 1
A_55_P2055638,	
A_55_P2013948	gelsolin
A_55_P2065621	hook homolog 2 (Drosophila)
A_55_P2017373	internexin neuronal intermediate filament protein, alpha



A_55_P2177658	microtubule associated serine/threonine kinase 1
A_52_P360330	microtubule-associated protein 1B
A_52_P22763	microtubule-associated protein 2
A_55_P2023692,	neuralized homolog 1A (Drosophila); similar to
A_55_P2016618	neuralized 1
A_52_P201551	neuron navigator 1
A_55_P1979397	paralemmin
A_55_P1968895	peripherin
A_51_P380013	predicted gene 3655; B-cell leukemia/lymphoma 2
A_55_P2092085	predicted gene 3787; predicted gene 9844; predicted gene 8034; similar to thymosin, beta 10; thymosin, beta 10
A_55_P2128526	profilin 2
A_52_P284889	protein kinase C, zeta
A_51_P140690	stathmin-like 3
A_55_P2085295	subacute ozone induced inflammation; RIKEN cDNA 2610204M08 gene
A_55_P2071834	talin 2
A_55_P2004797	transforming, acidic coiled-coil containing protein 2
A_51_P246924	tubulin polymerization-promoting protein family member 3

#### **GO:0008092~cytoskeletal protein binding**

ID	Gene Name
A_66_P122173	MKL/myocardin-like 2
A_52_P529360	RAB11 family interacting protein 5 (class I)
A_55_P2069470	RIKEN cDNA 1110017D15 gene
A_55_P2075627	adenomatosis polyposis coli 2
A_51_P200667	calmin
A_55_P2156583	cyclin-dependent kinase 5, regulatory subunit 1 (p35)
A_55_P2195157	drebrin 1
A_55_P2055638,	
A_55_P2013948	gelsolin
A_55_P1992655,	
A_55_P2009792	histone deacetylase 6
A_55_P2065621	hook homolog 2 (Drosophila)
A_52_P360330	microtubule-associated protein 1B
A_52_P22763	microtubule-associated protein 2
A_52_P652316	microtubule-associated protein, RP/EB family, member 2
A_55_P2087404	microtubule-associated protein, RP/EB family, member 3
A_55_P2074836	mitogen-activated protein kinase 8 interacting protein 1
A_52_P370392	mitogen-activated protein kinase 8 interacting protein 2
A_55_P2090070	myosin, heavy polypeptide 14
A_51_P198645	parvin, beta; similar to parvin, beta
A_51_P182572	phosphatase and actin regulator 1
A_55_P2139027	plectin 1
A_55_P2092085	predicted gene 3787; predicted gene 9844; predicted gene 8034; similar to thymosin, beta 10; thymosin, beta 10

A_55_P2128526	profilin 2
A_55_P2110713	similar to Annexin A2 (Annexin II) (Lipocortin II) (Calpactin I heavy chain) (Chromobindin-8) (p36) (Protein I) (Placental anticoagulant protein IV) (PAP-IV); annexin A2
A_55_P2072985	spectrin alpha 2
A_51_P489138	spectrin beta 1
A_55_P2085295	subacute ozone induced inflammation; RIKEN cDNA 2610204M08 gene
A_52_P282741	syndecan 3
A_55_P2071834	talin 2
A_55_P2032818	tripartite motif-containing 2
A_52_P315976, A_55_P2121408	tropomyosin 2, beta
A_51_P246924	tubulin polymerization-promoting protein family member 3

### GO:0006887~exocytosis

ID	Gene Name
A_55_P2081123	P140 gene
A_55_P1956557	RAB3A, member RAS oncogene family
A_52_P432919	RAB3D, member RAS oncogene family
A_55_P2055463	SNAP-associated protein
A_52_P180842	exocyst complex component 3
A_55_P1997415	exocyst complex component 6B
A_51_P190254, A_52_P201206	secernin 1
A_51_P217336	secretory carrier membrane protein 1
A_52_P409731	secretory carrier membrane protein 5
A_55_P1965219	synaptotagmin VI
A_55_P2077188	syntaxin binding protein 1

### SP\_PIR\_KEYWORDS~microtubule

ID	Gene Name
A_55_P2041723	Mid1 interacting protein 1 (gastrulation specific G12-like (zebrafish))
A_55_P2075627	adenomatous polyposis coli 2
A_55_P1975385	dynactin 1
A_52_P678895	dynein light chain Tctex-type 3
A_55_P2113673	echinoderm microtubule associated protein like 1; similar to echinoderm microtubule associated protein like 1
A_55_P1989921	echinoderm microtubule associated protein like 2
A_51_P181851	echinoderm microtubule associated protein like 3
A_55_P2065621	hook homolog 2 (Drosophila)
A_52_P282500	kinesin family member 21B
A_51_P107020	kinesin family member 5A
A_55_P2060349	leucine zipper, putative tumor suppressor 2
A_52_P360330	microtubule-associated protein 1B
A_52_P22763	microtubule-associated protein 2
A_52_P652316	microtubule-associated protein, RP/EB family, member

	2
A_55_P2087404	microtubule-associated protein, RP/EB family, member 3
A_52_P201551	neuron navigator 1
A_55_P2013645	similar to Tubulin, gamma 2; tubulin, gamma 2
A_51_P246924	tubulin polymerization-promoting protein family member 3
A_55_P2041828	tubulin, beta 3; tubulin, beta 3, pseudogene 1
A_51_P421140	tubulin, beta 6

### **GO:0008021~synaptic vesicle**

ID	Gene Name
A_55_P1956557	RAB3A, member RAS oncogene family
A_51_P282594	SV2 related protein
A_51_P217336	secretory carrier membrane protein 1
A_52_P409731	secretory carrier membrane protein 5
A_55_P1956567	similar to RAB3C, member RAS oncogene family; RAB3C, member RAS oncogene family
A_51_P389988	solute carrier family 40 (iron-regulated transporter), member 1
A_52_P62444	synapsin II
A_55_P1965219	synaptotagmin VI
A_55_P2179448, A_55_P1956267	synaptotagmin XI; similar to synaptotagmin XI

## **David categories genes list Figure 6**

### **Differential categories 2/4<sub>RA vs CTR</sub> Down in CTR**

#### **GO:0002009~morphogenesis of an epithelium**

ID	Gene Name
A_52_P87843	aldehyde dehydrogenase family 1, subfamily A3
A_51_P417701	apoptotic peptidase activating factor 1
A_52_P106259	epidermal growth factor receptor
A_55_P2053933	forkhead box A1; similar to Hepatocyte nuclear factor 3-alpha (HNF-3A) (Forkhead box protein A1)
A_52_P128134	forkhead box D1
A_52_P634090	jagged 1
A_55_P2127804	mitogen-activated protein kinase kinase kinase 7; predicted gene 8188
A_52_P472319, A_55_P2151822	plexin D1
A_55_P1990495	signal transducer and activator of transcription 5A

**mghPathway:Growth Hormone Signaling Pathway**

ID	Gene Name
A_52_P175242	insulin receptor substrate 1
A_55_P2121662, A_52_P243249	mitogen-activated protein kinase 3
A_55_P1990495	signal transducer and activator of transcription 5A
A_51_P279606	suppressor of cytokine signaling 1

**mmu04010:MAPK signaling pathway**

ID	Gene Name
A_55_P2158990	Jun oncogene
A_65_P12152	RAS p21 protein activator 2
A_66_P116252	dual specificity phosphatase 16
A_66_P119155	dual specificity phosphatase 3 (vaccinia virus phosphatase VH1-related)
A_52_P106259	epidermal growth factor receptor
A_51_P440985	fibroblast growth factor 15
A_52_P64364	inhibitor of kappaB kinase beta
A_55_P2121662, A_52_P243249	mitogen-activated protein kinase 3
A_55_P2127804	mitogen-activated protein kinase kinase kinase 7; predicted gene 8188
A_55_P1967978	nuclear factor of activated T-cells, cytoplasmic, calcineurin-dependent 2
A_55_P2162807	phospholipase A2, group IIE
A_52_P558859	related RAS viral (r-ras) oncogene homolog 2
A_55_P1968068	transformation related protein 53
A_51_P317640, A_65_P10913	transforming growth factor, beta 2

**GO:0030335~positive regulation of cell migration**

ID	Gene Name
A_55_P2059352	collagen, type XVIII, alpha 1
A_52_P175242	insulin receptor substrate 1
A_52_P558859	related RAS viral (r-ras) oncogene homolog 2
A_51_P452629	toll-like receptor 2

**Differential categories 2/4<sub>RA vs CTR</sub> Up in CTR****GO:0031967~organelle envelope**

ID	Gene Name
A_52_P153189	ADP-ribosylation factor-like 2 binding protein
A_51_P354744	COX15 homolog, cytochrome c oxidase assembly protein (yeast)
A_55_P2116889	HCLS1 associated X-1; silica-induced gene 111
A_52_P139747	NADH dehydrogenase (ubiquinone) 1 alpha subcomplex, 1
A_51_P201904	NADH dehydrogenase (ubiquinone) 1 beta subcomplex, 5
A_51_P140211	NADH dehydrogenase (ubiquinone) flavoprotein 3
A_52_P112178	SLIT-ROBO Rho GTPase activating protein 2
A_55_P2017590	endo/exonuclease (5'-3'), endonuclease G-like fractured callus expressed transcript 1; dynein heavy chain domain 1
A_55_P2087157	heterogeneous nuclear ribonucleoprotein L-like; glutathione peroxidase 4
A_51_P462448	lamin A
A_52_P137765	nuclear RNA export factor 1 homolog ( <i>S. cerevisiae</i> )
A_66_P127567	nucleoporin like 2
A_51_P448447	predicted gene 6917; similar to chromobox homolog 3; predicted gene 5792; predicted gene 7469; predicted gene 6901; predicted gene 7721; predicted gene 5196; complement component 7; chromobox homolog 3 ( <i>Drosophila</i> HP1 gamma)
A_55_P2017038	predicted gene 7684; membrane-associated ring finger (C3HC4) 5
A_51_P405668	presenilin associated, rhomboid-like
A_55_P2130877,	prohibitin; predicted gene 4773; RIKEN cDNA 1700071K01 gene
A_52_P247943	proline dehydrogenase
A_51_P165934	protein phosphatase 2 (formerly 2A), regulatory subunit B (PR 52), beta isoform
A_51_P220278	retinol saturase (all trans retinol 13,14 reductase)
A_51_P319070	similar to cytochrome b5 outer mitochondrial membrane precursor; cytochrome b5 type B
A_55_P1963712	solute carrier family 25, member 39
A_51_P121455	solute carrier family 25, member 44
A_51_P488768	succinate-CoA ligase, GDP-forming, alpha subunit
A_51_P491227	synaptic nuclear envelope 1
A_55_P2026295	

**GO:0044430~cytoskeletal part**

ID	Gene Name
A_52_P153189	ADP-ribosylation factor-like 2 binding protein
A_51_P509760	ARP1 actin-related protein 1 homolog A, centractin alpha (yeast)

A_55_P2065389,	
A_30_P01027099,	
A_66_P106654,	
A_30_P01032420,	calmodulin regulated spectrin-associated protein 1;
A_55_P2065385,	similar to calmodulin regulated spectrin-associated
A_30_P01024942	protein 1
A_66_P132777	centrosomal protein 68
A_55_P2128929	coiled-coil and C2 domain containing 2A
A_55_P2000148	dynein, axonemal, intermediate chain 1
A_55_P2107667	enabled homolog (Drosophila)
A_51_P114062	frequenin homolog (Drosophila)
A_55_P2039881	glycoprotein Ib, beta polypeptide
A_55_P2116664	hook homolog 2 (Drosophila)
A_55_P2047788	katanin p60 subunit A-like 1
A_55_P2016024	kinesin family member 3C
A_52_P137765	lamin A
A_51_P438149	microtubule-associated protein, RP/EB family, member 2
A_55_P2059357	myosin VIIA
A_55_P2154054	myosin XVIII A
A_66_P104309	myosin, light polypeptide 2, regulatory, cardiac, slow
A_55_P2107045	myosin, light polypeptide 4
A_55_P1952990	myosin, light polypeptide 6B
A_55_P2059695	neuron navigator 1
A_55_P2131785	non-protein coding RNA 153
A_55_P1977653	palladin, cytoskeletal associated protein
A_55_P1985025	par-3 (partitioning defective 3) homolog (C. elegans)
A_55_P2039881	similar to CDCrel-1AI; septin 5
A_55_P2106414,	similar to UCH37-interacting protein 1; HAUS augmin-
A_55_P2083093	like complex, subunit 7
A_55_P2099790,	similar to neurofilament protein; neurofilament, heavy
A_55_P2053181	polypeptide
A_52_P291971	staufen (RNA binding protein) homolog 2 (Drosophila)
A_55_P2052696	synemin, intermediate filament protein
A_52_P122673	testis specific gene A14
A_51_P199608	tubulin tyrosine ligase-like 1
A_51_P514256	tubulin, beta 2a, pseudogene 2; tubulin, beta 2B

**Differential categories 2/4<sub>RA vs CTR</sub> Down in RA****SP\_PIR\_KEYWORDS~cell cycle**

ID	Gene Name
A_55_P2177755	CDK2 (cyclin-dependent kinase 2)-associated protein 1; predicted gene 12184
A_51_P314907	DBF4 homolog ( <i>S. cerevisiae</i> )
A_52_P533146	DNA-damage inducible transcript 3
A_55_P2317665	E2F transcription factor 1
A_51_P368009	E2F transcription factor 2
A_52_P270164,	
A_30_P01026205	E2F transcription factor 6
A_55_P2062598	E2F transcription factor 7
A_51_P393958	F-box protein 5
A_52_P556462	Fanconi anemia, complementation group D2
A_55_P2025790	Fanconi anemia, complementation group I
A_55_P1994751,	KH domain containing, RNA binding, signal
A_30_P01021155	transduction associated 1
A_51_P418317	MIS12 homolog (yeast)
	NDC80 homolog, kinetochore complex component ( <i>S. cerevisiae</i> )
A_51_P191649	
A_55_P1997097	RIKEN cDNA 2310022M17 gene; predicted gene 7843
A_55_P2140383,	
A_52_P330540	RIKEN cDNA 2610039C10 gene
A_52_P139650	RIKEN cDNA 2810433K01 gene
A_55_P1993019,	
A_66_P128631,	RIKEN cDNA 2810452K22 gene; similar to cyclin-
A_55_P2134800	dependent kinase 2-interacting protein
A_51_P369252	RIKEN cDNA 4632434I11 gene
A_55_P2133652	RIKEN cDNA 4922501C03 gene
A_52_P655265	RIKEN cDNA 6720463M24 gene
	Ras association (RalGDS/AF-6) domain family member
A_55_P2092909	1
A_52_P178904	SEH1-like ( <i>S. cerevisiae</i> )
	SET domain containing (lysine methyltransferase) 8;
A_51_P201971	predicted gene 8590
	SPC24, NDC80 kinetochore complex component,
A_55_P2056473	homolog ( <i>S. cerevisiae</i> )
	SPC25, NDC80 kinetochore complex component,
A_55_P1965154	homolog ( <i>S. cerevisiae</i> )
A_55_P1990373,	
A_55_P2123673	TMF1-regulated nuclear protein 1
A_66_P136186	WEE 1 homolog 1 ( <i>S. pombe</i> )
	ZW10 homolog ( <i>Drosophila</i> ), centromere/kinetochore
A_51_P137007	protein
A_52_P509710	ZW10 interactor
A_55_P2040743	Zwilch, kinetochore associated, homolog ( <i>Drosophila</i> )
A_55_P2034230	anaphase promoting complex subunit 4
A_66_P134542	anillin, actin binding protein
A_55_P2120254	arginine vasopressin-induced 1

A_55_P1988228	asp (abnormal spindle)-like, microcephaly associated (Drosophila)
A_55_P1980636	aurora kinase A
A_55_P1983768, A_55_P1983769, A_55_P1983773	baculoviral IAP repeat-containing 5
A_51_P123405	budding uninhibited by benzimidazoles 1 homolog (S. cerevisiae)
A_51_P490509	budding uninhibited by benzimidazoles 1 homolog, beta (S. cerevisiae)
A_51_P392546	cDNA sequence BC023882
A_51_P442964	cancer susceptibility candidate 5
A_51_P517096	caspase 8 associated protein 2
A_55_P2008735	cell division cycle 123 homolog (S. cerevisiae)
A_55_P2048588	cell division cycle 2 homolog A (S. pombe)
A_55_P2022658	cell division cycle 2-like 1
A_55_P1996946	cell division cycle 20 homolog (S. cerevisiae)
A_52_P612382	cell division cycle 25 homolog B (S. pombe)
A_66_P131979	cell division cycle 6 homolog (S. cerevisiae); predicted gene 9430; similar to cell division cycle 6 homolog
A_52_P628067	cell division cycle associated 3
A_51_P125135	cell division cycle associated 5
A_51_P155142, A_55_P2170681	cell division cycle associated 8
A_51_P164014	centromere protein E
A_51_P196973	chromatin assembly factor 1, subunit A (p150)
A_51_P133612	chromatin licensing and DNA replication factor 1
A_52_P476075	claspin homolog (Xenopus laevis)
A_52_P75348	coiled-coil domain containing 99
A_51_P481920	cyclin A2
A_55_P2039324	cyclin F
A_55_P1967592	cyclin K; similar to cyclin K
A_55_P1962274	cyclin T1
A_51_P363947	cyclin-dependent kinase inhibitor 1A (P21)
A_55_P2022251	cyclin-dependent kinase inhibitor 2D (p19, inhibits CDK4)
A_52_P162099	cytoskeleton associated protein 2
A_55_P2050439, A_52_P411003	discs, large (Drosophila) homolog-associated protein 5
A_52_P148212	expressed sequence C79407
A_55_P2128646	geminin
A_51_P151586	germ cell-specific gene 2
A_55_P2162537	inhibitor of growth family, member 4
A_55_P2028054, A_55_P1978201	inner centromere protein
A_52_P642801	large tumor suppressor
A_55_P1989916	lin-54 homolog (C. elegans)
A_52_P330984	lin-9 homolog (C. elegans)
A_55_P1953087	minichromosome maintenance deficient 3 (S. cerevisiae)
A_55_P2009091	mitotic arrest deficient 1-like 1



A_51_P315634	neural precursor cell expressed, developmentally down-regulated gene 1
A_51_P202074	non-SMC condensin I complex, subunit D2
A_55_P1967291	non-SMC condensin I complex, subunit H
A_55_P2154228	non-SMC condensin II complex, subunit D3
A_51_P424810	non-SMC condensin II complex, subunit G2
	nuclear distribution gene C homolog ( <i>Aspergillus</i> ), pseudogene 1; nuclear distribution gene C homolog ( <i>Aspergillus</i> )
A_55_P2068849	
A_55_P2165334	nuclear distribution gene E homolog 1 ( <i>A. nidulans</i> )
A_51_P240453	nucleolar and spindle associated protein 1
	par-6 (partitioning defective 6,) homolog alpha ( <i>C. elegans</i> )
A_51_P456366	
A_55_P1987499	pituitary tumor-transforming gene 1
	platelet-activating factor acetylhydrolase, isoform 1b, subunit 1
A_55_P1992769	
A_51_P344566	polo-like kinase 1 ( <i>Drosophila</i> )
A_55_P1966528	polyamine-modulated factor 1
	predicted gene 14292; Wilms' tumour 1-associating protein
A_55_P2008452	
	predicted gene 2180; CTF8, chromosome transmission fidelity factor 8 homolog ( <i>S. cerevisiae</i> )
A_55_P1967880	
A_55_P1957168	predicted gene 2296; ubiquitin-conjugating enzyme E2S
A_51_P237512	predicted gene 6597; RIKEN cDNA 1110001A07 gene
	predicted gene 7390; transcription factor Dp 1; similar to Transcription factor Dp-1 (E2F dimerization partner 1) (DRTF1-polypeptide 1)
A_52_P103550	
A_55_P2103706,	
A_55_P2128668,	predicted gene 8416; predicted gene 5593; cyclin B1; similar to cyclin B1; predicted gene 4870
A_55_P1952256	predicted gene 8545; microtubule-associated protein, RP/EB family, member 1; similar to Microtubule-associated protein RP/EB family member 1 (APC-binding protein EB1) (End-binding protein 1) (EB1)
A_55_P2473316	protein phosphatase 1G (formerly 2C), magnesium-dependent, gamma isoform
A_51_P484832	
A_55_P1988083	protein regulator of cytokinesis 1
A_51_P189746	proviral integration site 3
	regulator of chromosome condensation 2; hypothetical protein LOC100047340
A_52_P76034	
A_55_P2166399	serine/threonine kinase 11
A_51_P487999	shugoshin-like 1 ( <i>S. pombe</i> )
A_52_P27020	shugoshin-like 2 ( <i>S. pombe</i> )
A_51_P238448	similar to Cyclin D3; cyclin D3
	similar to Cyclin-dependent kinases regulatory subunit 2 (CKS-2); CDC28 protein kinase regulatory subunit 2; predicted gene 15452
A_55_P1965050	
A_55_P1987028,	similar to Kifc1 protein; kinesin family member C1;
A_30_P01019819	predicted gene 4137
A_55_P2100209,	similar to Kinesin-like protein KIF2C (Mitotic centromere-associated kinesin) (MCAK); kinesin family
A_66_P125209	

	member 2C
A_55_P2076048	similar to Nuf2 protein; NUF2, NDC80 kinetochore complex component, homolog ( <i>S. cerevisiae</i> )
A_55_P2024302	similar to Spindlin 1; spindlin 1; spindlin family, member 3
A_55_P1975685	similar to nucleoporin 37; nucleoporin 37
A_51_P348652	spastin
A_51_P513530	sperm associated antigen 5
A_51_P123047	structural maintenance of chromosomes 1A
A_55_P2172274	structural maintenance of chromosomes 2
A_55_P2037712	structural maintenance of chromosomes 4
A_55_P2000304	telomeric repeat binding factor 1
A_55_P2081303	tet oncogene family member 2
A_55_P2006255,	
A_51_P438805	thioredoxin interacting protein
A_52_P424826	thioredoxin-like 4B
A_51_P336721	timeless interacting protein
A_55_P2073709	transcription factor Dp 2
A_52_P117420	transforming, acidic coiled-coil containing protein 1
A_55_P2126109,	
A_55_P1961059	ubiquitin specific peptidase 16
A_51_P451151,	
A_55_P1996941	ubiquitin-conjugating enzyme E2C; predicted gene 8956 vomeronasal 2, receptor 53; predicted gene 8146; gene model 398, (NCBI); vomeronasal 2, receptor 54; HAUS
A_55_P1973178,	augmin-like complex, subunit 5
A_55_P1959313	zinc finger, C3HC type 1
A_55_P2129286	

### GO:0005694~chromosome

ID	Gene Name
A_51_P330213	ASF1 anti-silencing function 1 homolog B ( <i>S. cerevisiae</i> )
A_55_P2055419	AT rich interactive domain 4A (RBP1-like)
A_51_P314418	Bloom syndrome homolog (human)
A_51_P195573	DNA methyltransferase (cytosine-5) 1
A_51_P338998	DNA primase, p58 subunit
A_52_P270164,	
A_30_P01026205	E2F transcription factor 6
A_52_P556462	Fanconi anemia, complementation group D2
A_55_P2025790	Fanconi anemia, complementation group I
A_55_P2099526	H2A histone family, member V
A_55_P2077746	M-phase phosphoprotein 8
A_51_P418317	MIS12 homolog (yeast)
	NDC80 homolog, kinetochore complex component ( <i>S. cerevisiae</i> )
A_51_P191649	RAD51 homolog ( <i>S. cerevisiae</i> )
A_51_P148105	RAN GTPase activating protein 1
A_52_P252737	RIKEN cDNA 2310022M17 gene; predicted gene 7843
A_55_P1997097	RIKEN cDNA 2610028A01 gene
A_51_P192089	RIKEN cDNA 2610036L11 gene
A_52_P609024	

A_55_P2140383, A_52_P330540 A_52_P139650 A_52_P178904	RIKEN cDNA 2610039C10 gene RIKEN cDNA 2810433K01 gene SEH1-like ( <i>S. cerevisiae</i> ) SET domain containing (lysine methyltransferase) 8;
A_51_P201971	predicted gene 8590
A_55_P2056473	SPC24, NDC80 kinetochore complex component, homolog ( <i>S. cerevisiae</i> )
A_55_P1965154 A_52_P639551, A_55_P2087865	SPC25, NDC80 kinetochore complex component, homolog ( <i>S. cerevisiae</i> )
A_51_P137007 A_52_P509710 A_55_P2040743 A_51_P253803, A_55_P2073377 A_51_P270519 A_55_P1983768, A_55_P1983769, A_55_P1983773 A_51_P314019 A_66_P132855	Terf1 (TRF1)-interacting nuclear factor 2 ZW10 homolog ( <i>Drosophila</i> ), centromere/kinetochore protein ZW10 interactor Zwilch, kinetochore associated, homolog ( <i>Drosophila</i> )
A_51_P123405	antigen identified by monoclonal antibody Ki 67 apoptosis-inducing, TAF9-like domain 1
A_51_P490509 A_51_P155142, A_55_P2170681 A_66_P121459 A_51_P164014 A_55_P2106150, A_55_P2077263 A_52_P304947 A_51_P228171 A_51_P133582	baculoviral IAP repeat-containing 5 barrier to autointegration factor 1 bromodomain adjacent to zinc finger domain, 1B budding uninhibited by benzimidazoles 1 homolog ( <i>S. cerevisiae</i> ) budding uninhibited by benzimidazoles 1 homolog, beta ( <i>S. cerevisiae</i> ) cell division cycle associated 8 centromere protein A centromere protein E
A_52_P504743 A_52_P476075 A_52_P75348 A_52_P148212	centromere protein K centromere protein N centromere protein P chromobox homolog 4 ( <i>Drosophila</i> Pc class) chromodomain protein, Y chromosome-like; predicted gene 7584 claspin homolog ( <i>Xenopus laevis</i> ) coiled-coil domain containing 99 expressed sequence C79407
A_55_P2020461, A_55_P2162136, A_55_P2026214, A_55_P2028491	high mobility group nucleosomal binding domain 4; predicted gene 7931; predicted gene 10282; predicted gene 3338; high mobility group nucleosomal binding domain 2; predicted gene 6594; predicted gene 6750; predicted gene 10182; predicted gene 6724; predicted gene 4248; predicted gene 9525; predicted gene 15296; similar to Hmgn2 protein; predicted gene 7125; hypothetical protein LOC638323; predicted gene 6651; predicted gene 5899; predicted gene 14008; predicted

	gene 16494; similar to high mobility group nucleosomal binding domain 2
A_55_P2099961, A_66_P100853, A_55_P2084656, A_55_P2084631 A_55_P2084666	histone cluster 1, H2ad; histone cluster 1, H2ae; histone cluster 1, H2ag; histone cluster 1, H2ah; histone cluster 1, H2ai; similar to histone 2a; histone cluster 1, H2an; histone cluster 1, H2ao; histone cluster 1, H2ac; histone cluster 1, H2ab
A_55_P2177154 A_55_P2177154 A_55_P2177154 A_55_P2177154 A_55_P2177154	histone cluster 1, H2af histone cluster 1, H2bg; histone cluster 1, H2be; histone cluster 2, H2bb; histone cluster 1, H2bc histone cluster 1, H2bh histone cluster 1, H2bk histone cluster 1, H2bm histone cluster 1, H2bp
A_55_P2106569, A_55_P1988754, A_51_P505521, A_55_P2091147, A_55_P2158701, A_55_P2091145	histone cluster 1, H4k; histone cluster 1, H4m; histone cluster 4, H4; similar to germinal histone H4 gene; histone cluster 1, H4h; histone cluster 1, H4j; histone cluster 1, H4i; histone cluster 1, H4d; histone cluster 1, H4c; histone cluster 1, H4f; histone cluster 1, H4b; histone cluster 1, H4a; histone cluster 2, H4; similar to histone H4
A_55_P2131438 A_55_P2028054, A_55_P1978201 A_55_P1989916 A_55_P2036526 A_55_P2009091 A_55_P1988373	histone cluster 2, H3b; histone cluster 1, H3f; histone cluster 1, H3e; histone cluster 2, H3c1; histone cluster 1, H3d; histone cluster 1, H3c; histone cluster 1, H3b; histone cluster 2, H3c2; histone cluster 2, H2aa1; histone cluster 2, H2aa2
A_52_P522023 A_51_P202074 A_55_P2154228 A_55_P2165334 A_66_P115378 A_55_P1965554 A_55_P1966528 A_51_P415905	inner centromere protein lin-54 homolog ( <i>C. elegans</i> ) methyl-CpG binding domain protein 2 mitotic arrest deficient 1-like 1 myeloid leukemia factor 1 interacting protein neural regeneration protein; alkB, alkylation repair homolog 1 ( <i>E. coli</i> ) non-SMC condensin I complex, subunit D2 non-SMC condensin II complex, subunit D3 nuclear distribution gene E homolog 1 ( <i>A. nidulans</i> ) origin recognition complex, subunit 2-like ( <i>S. cerevisiae</i> ) origin recognition complex, subunit 3-like ( <i>S. cerevisiae</i> ) polyamine-modulated factor 1 polymerase (DNA directed), alpha 1
A_55_P1989102, A_55_P2171158 A_55_P1982451	predicted gene 11663; predicted gene 2992; predicted gene 7862; high mobility group nucleosomal binding domain 1; similar to high mobility group nucleosomal binding domain 1 predicted gene 11914; nucleosome binding protein 1 predicted gene 13121; predicted gene 3160; high-mobility group (nonhistone chromosomal) protein 1-like 1; predicted gene 6090; predicted gene 3851; predicted gene 8967; predicted gene 7782; predicted gene 4587;
A_55_P2018283	predicted gene 4689; predicted gene 3307; predicted

gene 13932; predicted gene 15059; predicted gene 3565; predicted gene 15447; predicted gene 12587; predicted gene 9012; predicted gene 6115; predicted gene 9480; high mobility group box 1; predicted gene 8423; predicted gene 5853; predicted gene 8288; predicted gene 7888; predicted gene 8594; predicted gene 15387; predicted gene 5473; predicted gene 8807; similar to high mobility group box 1; similar to 2810416G20Rik protein; predicted gene 8390; predicted gene, OTTMUSG00000005439; predicted gene 5842; predicted gene 5527; predicted gene 8563; predicted gene 2710; predicted gene 12331; predicted gene 5937; predicted gene 5504; similar to high-mobility group box 1; predicted gene 10361; predicted gene 2607; predicted gene 7422; predicted gene 10075; predicted gene 12568; predicted gene 6589; predicted gene 4383; predicted gene 8031; similar to High mobility group protein 1 (HMG-1) (High mobility group protein B1) (Amphoterin) (Heparin-binding protein p30); predicted gene 7468; predicted gene 8554  
 predicted gene 3353; predicted gene 13142; predicted gene 13169; similar to protein phosphatase 2, regulatory subunit B (B56), alpha isoform; predicted gene 13244; predicted gene 13233; protein phosphatase 2, regulatory subunit B (B56), alpha isoform  
 A\_55\_P1975772 predicted gene 3507; integrin beta 3 binding protein (beta3-endonexin); similar to integrin beta 3 binding protein  
 A\_55\_P2098539  
 A\_51\_P237512 predicted gene 6597; RIKEN cDNA 1110001A07 gene  
 A\_55\_P2288117 protein phosphatase 2 (formerly 2A), catalytic subunit, alpha isoform  
 A\_52\_P76034 regulator of chromosome condensation 2; hypothetical  
 A\_51\_P254912 protein LOC100047340  
 A\_55\_P2159801, replication factor C (activator 1) 2  
 A\_55\_P2159807 replication factor C (activator 1) 4  
 A\_51\_P246339 replication factor C (activator 1) 5; similar to replication  
 A\_51\_P234308 factor C 5  
 A\_51\_P236013 replication protein A2  
 A\_51\_P487999 ring finger protein 40  
 A\_52\_P27020 shugoshin-like 1 (*S. pombe*)  
 A\_55\_P2082203, shugoshin-like 2 (*S. pombe*)  
 A\_30\_P01024929, similar to Bromodomain adjacent to zinc finger domain  
 A\_30\_P01029783 protein 1A (Cbp146); bromodomain adjacent to zinc  
 finger domain 1A  
 similar to Hist1h2bj protein; histone cluster 1, H2bl;  
 predicted gene, OTTMUSG000000013203; histone cluster  
 1, H2bj; histone cluster 1, H2bf; H2b histone family  
 member; histone cluster 1, H2bn  
 A\_55\_P2177154 similar to Nuf2 protein; NUF2, NDC80 kinetochore  
 complex component, homolog (*S. cerevisiae*)  
 A\_55\_P2076048

A_55_P2023094	similar to PES1 protein; predicted gene 5472; pescadillo
A_55_P1975685	homolog 1, containing BRCT domain (zebrafish)
A_55_P2072468	similar to nucleoporin 37; nucleoporin 37
A_51_P513530	sirtuin 6 (silent mating type information regulation 2,
A_55_P1967138	homolog) 6 ( <i>S. cerevisiae</i> )
A_51_P123047	sperm associated antigen 5
A_55_P2172274	stimulated by retinoic acid 13
A_55_P2037712	structural maintenance of chromosomes 1A
A_52_P579876	structural maintenance of chromosomes 2
A_51_P214796	structural maintenance of chromosomes 4
A_55_P2000304	suppressor of defective silencing 3 homolog ( <i>S.</i>
A_52_P387564	<i>cerevisiae</i> )
A_51_P336721	suppressor of zeste 12 homolog ( <i>Drosophila</i> )
A_55_P1995205	telomeric repeat binding factor 1
	thymopoietin
	timeless interacting protein
	topoisomerase (DNA) II alpha

### SP\_PIR\_KEYWORDS~translocation

ID	Gene Name
A_55_P2034570	DEAD (Asp-Glu-Ala-Asp) box polypeptide 19a
A_55_P1979305,	
A_51_P328133	GLE1 RNA export mediator (yeast)
A_52_P178904	SEH1-like ( <i>S. cerevisiae</i> )
A_55_P2045066	eukaryotic translation initiation factor 5A
A_55_P1959056	nuclear pore membrane protein 121
A_51_P411297	nucleoporin 50
A_52_P237669,	
A_55_P2127020	nucleoporin 54
A_55_P1968276	predicted gene 12906; predicted gene 7250; translocase
A_65_P06453,	of outer mitochondrial membrane 22 homolog (yeast)
A_55_P2050799	predicted gene 4353; nucleoporin 35
A_55_P1952744	predicted gene 9797; translocase of inner mitochondrial
A_55_P2180491	membrane 8 homolog a1 (yeast); similar to small zinc
A_55_P1975685	finger-like protein
A_52_P520408	ribosome binding protein 1
A_55_P1957003,	similar to nucleoporin 37; nucleoporin 37
A_55_P1957004	stress-associated endoplasmic reticulum protein 1
A_52_P338180	translocase of inner mitochondrial membrane 10
A_51_P421984	homolog (yeast)
A_55_P2127692	translocase of inner mitochondrial membrane 13
A_51_P421804	homolog (yeast)
A_51_P499169	translocase of inner mitochondrial membrane 22
A_51_P407606	homolog (yeast)
	translocase of inner mitochondrial membrane 50
	homolog (yeast)
	translocase of inner mitochondrial membrane 9 homolog
	(yeast)
	translocating chain-associating membrane protein 1
	transmembrane protein 48

## Differential categories 2/4 RA vs CTR Up in RA

### GO:0031175~neuron projection development

ID	Gene Name
A_51_P312497	ATPase, Cu <sup>++</sup> transporting, alpha polypeptide
A_55_P2100555	L1 cell adhesion molecule
A_55_P2105673, A_55_P2372877	LIM homeobox protein 4
A_51_P200561	RIKEN cDNA 4930506M07 gene
A_52_P489778	actin-binding LIM protein 1
A_51_P344249	amyloid beta (A4) precursor protein-binding, family B, member 1
A_52_P351925, A_65_P13713	ankyrin 3, epithelial
A_55_P2142393	calcium channel, voltage-dependent, P/Q type, alpha 1A subunit
A_55_P2173183	cyclin-dependent kinase 5, regulatory subunit 1 (p35)
A_55_P1956667	cytoplasmic FMR1 interacting protein 1
A_66_P135185	ets variant gene 1
A_55_P2057777	fibroblast growth factor receptor 1
A_55_P2017710	immunoglobulin superfamily, member 9
A_55_P2048937	kinesin family member 5C
A_55_P2059307	microtubule-associated protein 2
A_55_P2088525	myosin, heavy polypeptide 10, non-muscle
A_51_P469285	neuropilin 1
A_52_P663600	p21 protein (Cdc42/Rac)-activated kinase 1
A_52_P539632	plexin A3
A_52_P239536	protein phosphatase 1, regulatory (inhibitor) subunit 9A sema domain, immunoglobulin domain (Ig), TM domain, and short cytoplasmic domain
A_52_P243391	
A_51_P227777	topoisomerase (DNA) II beta

### GO:0045202~synapse

ID	Gene Name
A_55_P2100555	L1 cell adhesion molecule
A_52_P588539	SNAP-associated protein
A_55_P2109326	acetylcholinesterase
A_51_P344249	amyloid beta (A4) precursor protein-binding, family B, member 1
A_52_P351925, A_65_P13713	ankyrin 3, epithelial
A_52_P442169	bassoon
A_55_P2000133, A_55_P2029711	cadherin 2; similar to N-cadherin
A_52_P428745	calcium/calmodulin-dependent protein kinase II, delta
A_55_P2180744	calsyntenin 3
A_55_P2173183	cyclin-dependent kinase 5, regulatory subunit 1 (p35)
A_55_P1956667	cytoplasmic FMR1 interacting protein 1

A_52_P89049	discs, large homolog 2 ( <i>Drosophila</i> )
A_52_P16232	gamma-aminobutyric acid (GABA) B receptor, 1
A_55_P1982131	glutamate receptor interacting protein 1
A_55_P1961400	glutamate receptor, ionotropic, delta 2 (Grid2)
A_55_P2017710	interacting protein 1
A_55_P2008066	immunoglobulin superfamily, member 9
A_52_P320971	inositol 1,4,5-triphosphate receptor 1
A_55_P2088525	metallothionein 3
A_55_P1960989	myosin, heavy polypeptide 10, non-muscle
A_55_P2068233,	neuroligin 2
A_52_P605517	phosphatase and actin regulator 1
A_52_P420712	praja 2, RING-H2 motif containing
A_52_P393314	purinergic receptor P2X, ligand-gated ion channel, 7
A_55_P1978028	seizure related gene 6
A_52_P243391	sema domain, immunoglobulin domain (Ig), TM domain,
A_55_P2178137	and short cytoplasmic domain
A_55_P2108324,	septin 3
A_52_P197666	similar to neuroligin 3; neuroligin 3
A_51_P346491	synapsin II
A_52_P202142	synaptic vesicle glycoprotein 2 a
A_55_P2187171	synaptic vesicle glycoprotein 2c
A_52_P239320	synaptogyrin 1
A_52_P389347	synaptosomal-associated protein 29
A_55_P2058957	synaptotagmin I

### **GO:0005938~cell cortex**

ID	Gene Name
A_55_P1966274	PDZ domain containing 4
A_51_P347862	actinin, alpha 1
A_55_P1988623	adducin 3 (gamma)
A_55_P2002963	coronin, actin binding protein 1A
A_55_P2037677	cortactin; predicted gene 8786
A_55_P2037101	exocyst complex component 2
A_52_P219661	exocyst complex component 6
A_55_P2001920	filamin, alpha
A_55_P2008061	inositol 1,4,5-triphosphate receptor 2
A_55_P2178044	inositol polyphosphate phosphatase-like 1
A_51_P124568	membrane protein, palmitoylated
A_55_P2088525	myosin, heavy polypeptide 10, non-muscle
A_51_P352968	myristoylated alanine rich protein kinase C substrate
A_52_P239536	protein phosphatase 1, regulatory (inhibitor) subunit 9A
A_55_P2178137	septin 3
A_51_P213691	sodium channel, nonvoltage-gated 1 alpha
A_52_P467690,	
A_55_P2081223,	
A_51_P428086	spectrin beta 2

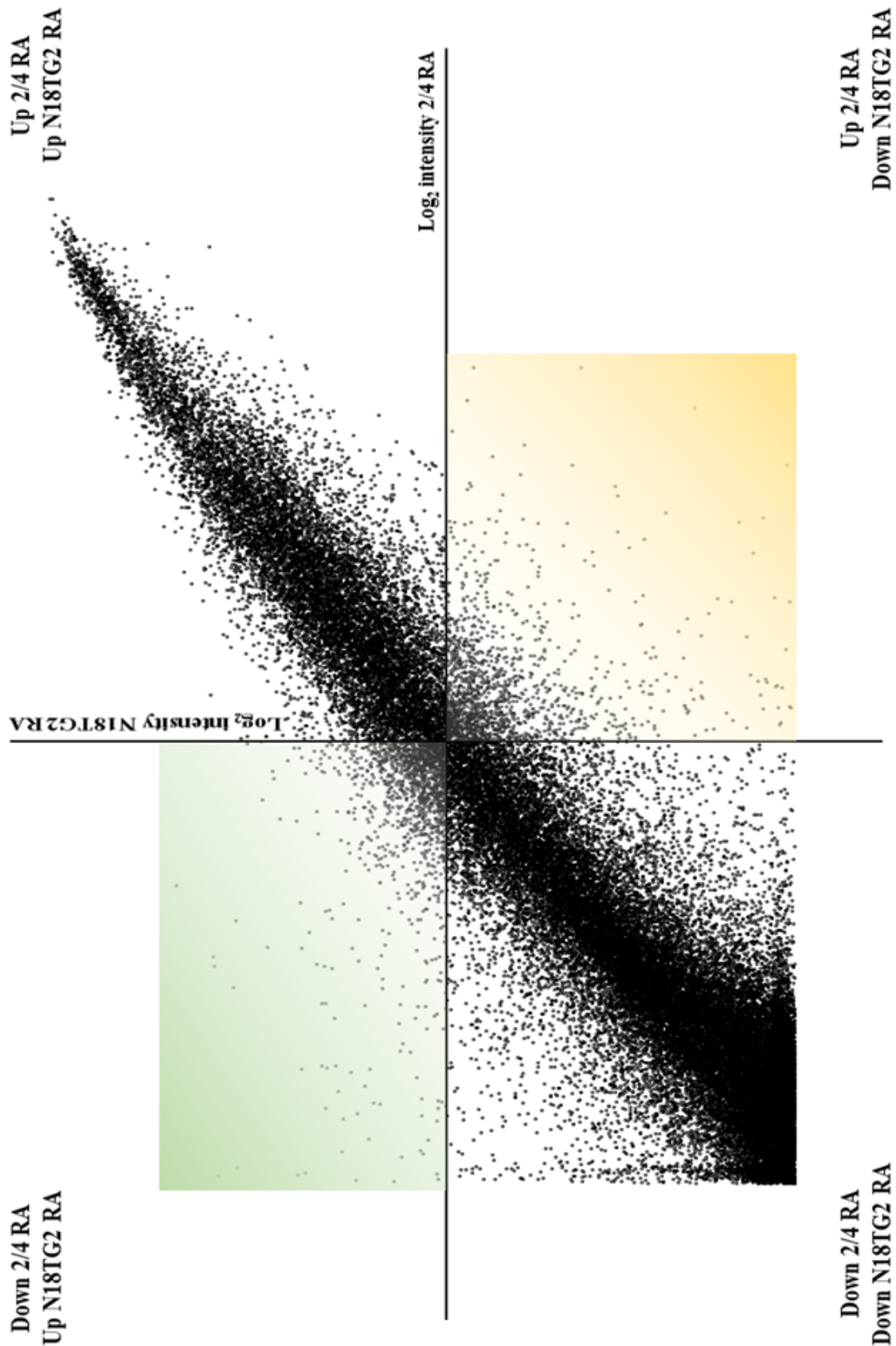


**GO:0030427~site of polarized growth**

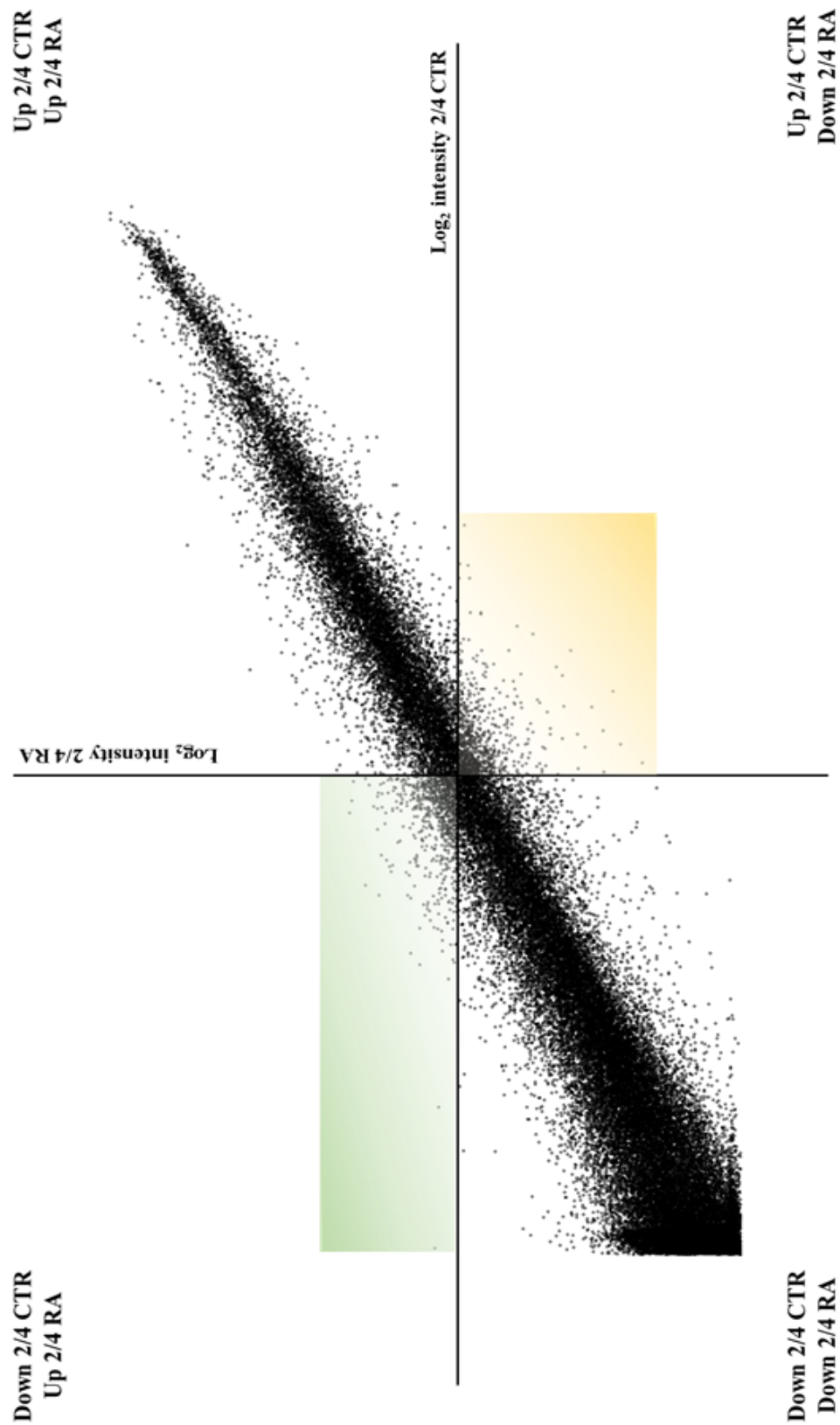
ID	Gene Name
A_51_P200561	RIKEN cDNA 4930506M07 gene
A_51_P344249	amyloid beta (A4) precursor protein-binding, family B, member 1
A_55_P2173183	cyclin-dependent kinase 5, regulatory subunit 1 (p35)
A_55_P2042486	dihydropyrimidinase-like 3
A_55_P2100149,	
A_55_P1954486	microtubule-associated protein tau
A_55_P2088525	myosin, heavy polypeptide 10, non-muscle
A_52_P663600	p21 protein (Cdc42/Rac)-activated kinase 1
A_52_P239536	protein phosphatase 1, regulatory (inhibitor) subunit 9A

**GO:0050770~regulation of axonogenesis**

ID	Gene Name
A_55_P2142393	calcium channel, voltage-dependent, P/Q type, alpha 1A subunit
A_55_P2100149,	
A_55_P1954486	microtubule-associated protein tau
A_51_P469285	neuropilin 1
A_55_P2056533,	neurotrophic tyrosine kinase, receptor, type 3; similar to
A_66_P118329	neurotrophic tyrosine kinase, receptor, type 3
A_52_P539632	plexin A3
A_55_P1967266	plexin B2
A_52_P243391	sema domain, immunoglobulin domain (Ig), TM domain, and short cytoplasmic domain



**Supplementary Figure 1. Divergence of expression pattern in N18TG2 and 2/4 cells after RA treatment**  
 Correlation plot between Log<sub>2</sub> intensity fluorescence values of 2/4 and N18TG2 cells in RA-treated conditions. The values reported were fished out comparing transcripts modulation during RA stimulus for each cell line. Uniquely genes with a minimum fold change of 2.0 were considered.



**Supplementary Figure 2. Correlation of expression pattern in 2/4 cells** Correlation plot between Log<sub>2</sub> intensity fluorescence values of 2/4 cells in untreated (CTR) and RA-treated conditions. The values reported were fished out comparing transcripts modulation after RA treatment in 2/4 cells, specifically. Uniquely genes with a minimum fold change of 2.0 were considered.